

# **Physicochemical Changes of Cellulose Subjected to Oxidative Conditions**

By Ivan J. De Souza

A thesis submitted to the Faculty of Graduate Studies and Research in partial fulfillment of the requirements for the degree of Master of Science

Department of Chemistry  
McGill University  
Montréal, Québec, Canada

December 1999

©Ivan J. De Souza, 1999



**National Library  
of Canada**

**Acquisitions and  
Bibliographic Services**

**395 Wellington Street  
Ottawa ON K1A 0N4  
Canada**

**Bibliothèque nationale  
du Canada**

**Acquisitions et  
services bibliographiques**

**395, rue Wellington  
Ottawa ON K1A 0N4  
Canada**

*Your file Votre référence*

*Our file Notre référence*

**The author has granted a non-exclusive licence allowing the National Library of Canada to reproduce, loan, distribute or sell copies of this thesis in microform, paper or electronic formats.**

**The author retains ownership of the copyright in this thesis. Neither the thesis nor substantial extracts from it may be printed or otherwise reproduced without the author's permission.**

**L'auteur a accordé une licence non exclusive permettant à la Bibliothèque nationale du Canada de reproduire, prêter, distribuer ou vendre des copies de cette thèse sous la forme de microfiche/film, de reproduction sur papier ou sur format électronique.**

**L'auteur conserve la propriété du droit d'auteur qui protège cette thèse. Ni la thèse ni des extraits substantiels de celle-ci ne doivent être imprimés ou autrement reproduits sans son autorisation.**

**0-612-64340-9**

**Canada**

Dedicated to  
*my wife Lin-Pei*

## Abstract

---

This study focuses on understanding the physicochemical properties of cellulose as it undergoes the oxygen delignification process. Cellulose contributes to fibre strength but is degraded by oxygen attack. Four different types of cellulose, namely a fully bleached softwood pulp (Q-90), hemicellulose reduced pulp derived from Q-90, cotton cellulose and microcrystalline cellulose (Avicel), were subjected to pressurised oxygen and nitrogen treatments in a kettle reactor. The changes in relative degree of crystallinity, viscosity and carboxylic acid content as a function of time were used to evaluate cellulose degradation. X-ray diffraction, Fourier transform infrared (FTIR) spectroscopy and  $^{13}\text{C}$  solid state nuclear magnetic resonance (NMR) spectroscopy determined the relative degree of crystallinity. Viscosity and conductometric titration measurements followed the changes in the degree of polymerisation and carboxylic acid content respectively.

A plot of relative degree of crystallinity as a function of oxidation time showed reproducible and consistent results for all celluloses with all applied techniques. The relationship showed a common trend wherein three phases were apparent: an initial increase in relative degree of crystallinity was followed by a decrease and then another gradual increase. The change from a decrease in relative degree of crystallinity to an increase occurred at fifteen minutes for Q-90 and hemicellulose reduced pulp, and at thirty minutes for cotton cellulose. No change in the relative degree of crystallinity with time was evident for Avicel. These trends were rationalised using the concept of the fringed micelle model.

## Résumé

---

L'objectif de cette étude est la compréhension des propriétés physico-chimiques de la cellulose soumise à un procédé de delignification par l'oxygène. La cellulose contribue à la force des fibres, mais elle se dégrade du fait de l'attaque de l'oxygène. Quatre types de cellulose, à savoir: de la pâte de bois mou complètement blanchie (Q-90), de la pâte réduite en hemicellulose dérivée de la Q-90, de la cellulose de coton ainsi que de la cellulose microcristalline (Avicel), ont été traités à l'oxygène et l'azote sous pression dans un réacteur-bouilloire. Les changements du degré relatif de cristallinité, de la viscosité ainsi que du taux d'acide carboxylique en fonction du temps ont été employés pour évaluer la dégradation de la cellulose. La diffraction de rayons-X, la spectroscopie infra-rouge à transformée de Fourier (SIRTF) ainsi que la résonance magnétique nucléaire (RMN)  $^{13}\text{C}$  en phase solide ont servi à déterminer le degré relatif de cristallinité. Des mesures de la viscosité ainsi que des titrages conductométriques ont servi à déterminer respectivement le degré de polymérisation et le taux d'acide carboxylique.

Un graphique du degré relatif de cristallinité en fonction du temps d'oxydation indique l'obtention de résultats reproductibles et consistants pour toutes les celluloses avec toutes les techniques appliquées. La courbe indique une tendance commune à trois étapes: une augmentation de la cristallinité apparente, une diminution, suivie d'une augmentation progressive. Le point d'inflexion entre la diminution et l'augmentation du degré relatif de cristallinité se situe à 15 minutes pour la Q-90 et la pâte réduite en hemicellulose, et à 30 minutes pour la cellulose de coton. Aucun changement de degré relatif de cristallinité n'a été observé pour l'Avicel. Ces tendances ont été rationalisées en employant le modèle de la micelle frangée.

## Acknowledgements

---

I sincerely thank my thesis supervisor, Professor Dimitris Argyropoulos for his enthusiastic support, encouragement, and understanding throughout my time at McGill University. His experience and extensive contacts have contributed greatly to my work.

I extend my gratitude to Dr. Jean Bouchard at the Pulp and Paper Research Institute of Canada (PAPRICAN) for sharing his command of cellulose chemistry with me. His group at PAPRICAN is also thanked for instructions on the use of the kettle reactor, obtaining viscosity measurements and provision of the cellulose samples.

I am very appreciative of the time offered by Dr. Richard Berry of PAPRICAN and Professors Robert H. Marchessault and R. St. J. Manley, both of McGill University who provided insightful discussions and recommendations for my thesis.

Dr. Cyril Heitner and Mr. Michael Hellstern of PAPRICAN are also thanked for providing the facility to use the conductometric titrator and their patient instruction on the instrument's operation. Dr. Fred Morin of McGill University was extremely helpful in obtaining solid state nuclear magnetic resonance spectroscopic measurements. Ms Glenna Keating of McGill University provided helpful instruction in the use of the x-ray diffractor. Mr. Jik Ing and his chemical analysis team at PAPRICAN are greatly appreciated for providing metal ion analysis data.

My wife, Lin-Pei, is thanked for the love, support and patience she offered me while completing my thesis. Her ability to motivate me at all times is greatly appreciated. I sincerely thank her for providing the hand drawn figures found within this thesis and for her effort in editing my work. My family members are also thanked for their love, support and encouragement.

I am grateful to my friends and colleagues who have made my experience at McGill enjoyable and worthwhile.

## Table of Contents

---

	<i>Page</i>
<b>Abstract</b> .....	<b>i</b>
<b>Résumé</b> .....	<b>ii</b>
<b>Acknowledgements</b> .....	<b>iii</b>
<b>Table of Contents</b> .....	<b>iv</b>
<b>List of Tables</b> .....	<b>x</b>
<b>List of Figures</b> .....	<b>xi</b>
 <b>Chapter 1 - Introduction</b>	
1.1 Oxygen Delignification.....	1
1.1.1 History & Definition .....	1
1.1.2 Other Types of Delignification.....	2
Chlorine Containing Bleaching Agents .....	3
Oxygen Containing Bleaching Agents.....	4
Biological Systems.....	6
1.1.3 Benefits of Oxygen Delignification.....	6
1.1.4 Disadvantages and Limitations of Oxygen Delignification .....	7
Selectivity.....	8
Temperature .....	9
Mass Transfer and Solubility Considerations .....	9
Incoming Kappa Number Variation.....	10
Transition Metals .....	10

1.2 Chemistry of Oxygen Delignification.....	11
1.2.1 Chemistry of Oxygen .....	11
1.2.2 Lignin .....	13
Lignin Reactions .....	14
1.2.3 Carbohydrates.....	17
Carbohydrate Reactions .....	22
1.2.4 Hemicellulose.....	25
Galactoglucomannans .....	27
Arabinoglucuronoxylan .....	28
Arabinogalactan .....	28
1.3 Methods of Crystallinity Determination .....	28
1.3.1 Water Retention Value (WRV).....	29
1.3.2 Near Infrared (NIR).....	29
1.3.3 X-ray Diffraction .....	30
Fundamentals of the Technique .....	30
Lignin, Hemicellulose and Cellulose Considerations .....	32
Obtaining Measurements with X-ray Diffraction .....	34
1.3.4 Fourier Transform Infrared (FTIR) Spectroscopy.....	35
Fundamentals of the Technique .....	35
Obtaining Measurements with FTIR Spectroscopy .....	36
1.3.5 CP/MAS Solid State Nuclear Magnetic Resonance Spectroscopy .....	37
Fundamentals of the Technique .....	37
Proton Spin Relaxation Time ( $T_{1H}$ ) .....	39
Obtaining Measurements with Solid State NMR Spectroscopy .....	40
1.3.6 Comparison of Techniques (X-ray, FTIR and Solid State NMR).....	41
1.4 Method to Monitor Cellulose Degradation.....	42
1.4.1 Viscosity.....	42
1.4.2 Conductometric Titration.....	43
<b>Chapter 2 - Scope and Aim of Thesis .....</b>	<b>45</b>



## **Chapter 3 - Experimental**

<b>3.1 Oxidation of Pulp</b> .....	<b>47</b>
<b>3.1.1 Q-90, Cotton and Hemicellulose reduced Pulp</b> .....	<b>47</b>
Q-90 .....	47
Cotton.....	48
Hemicellulose Reduced Pulp .....	48
<b>3.1.2 Avicel</b> .....	<b>48</b>
<b>3.2 Crystallinity Determination</b> .....	<b>49</b>
<b>3.2.1 X-ray Diffraction</b> .....	<b>49</b>
Preparation of the Sample Mount .....	49
Q-90, Cotton and Hemicellulose reduced Pulp.....	49
Avicel .....	49
Instrument and Conditions .....	50
Calculation of Crystallinity .....	50
<b>3.2.2 FTIR</b> .....	<b>50</b>
Preparation of the Sample Mount .....	50
Q-90 and Cotton.....	50
Hemicellulose Reduced Pulp .....	51
Avicel .....	51
Instrument and Conditions .....	51
Calculation of Crystallinity .....	51
<b>3.2.3 Solid State NMR</b> .....	<b>52</b>
Sample Preparation to Remove Metal Ions.....	52
Sample Conditioning in the Dessicator.....	52
Instrument and Conditions for <sup>13</sup> CP MAS NMR and Proton T <sub>1</sub> Measurements ....	52
Deconvolution for the Calculation of Crystallinity .....	53
<b>3.3 Viscosity</b> .....	<b>53</b>
<b>3.3.1 Q-90 / Cotton / Hemicellulose reduced Pulp / Avicel</b> .....	<b>53</b>
<b>3.4 Conductometric Titration</b> .....	<b>54</b>

3.4.1 Sample Preparation .....	54
3.4.2 Instrument Criteria and Conditions .....	54
3.4.3 Calculations .....	55

## **Chapter 4 - Results & Discussion – Part I**

### **Evaluation of Techniques**

4.1 Relative Degree of Crystallinity .....	56
4.2 Q-90 .....	59
4.2.1 X-ray Diffraction .....	59
4.2.2 FTIR Spectroscopy .....	61
4.2.3 <sup>13</sup> C Solid State NMR Spectroscopy .....	63
Deconvolution of NMR Signals .....	64
Proton Spin-Lattice Relaxation Time .....	67
4.3 Reproducibility of the Methodology .....	68
4.3.1 X-ray Diffraction .....	69
4.3.2 FTIR Spectroscopy .....	70
4.3.3 <sup>13</sup> C Solid State NMR Spectroscopy .....	71
Deconvolution of NMR Signals .....	71
Proton Spin-Lattice Relaxation Time .....	72
4.3.4 Summary of Q-90 Reproducibility Measurements .....	73

## **Chapter 5 - Results & Discussion – Part II**

### **Relative Degree of Crystallinity for Various Celluloses**

5.1 Hemicellulose Reduced Pulp .....	75
5.1.1 X-ray Diffraction .....	78
5.1.2 FTIR Spectroscopy .....	79
5.1.3 <sup>13</sup> C Solid State NMR Spectroscopy .....	80
Deconvolution of NMR Signals .....	80
Proton Spin-Lattice Relaxation Time .....	81
5.1.4 Summary of Hemicellulose Reduced Results .....	82

5.2 Cotton Cellulose .....	83
5.2.1 X-ray Diffraction .....	84
5.2.2 FTIR Spectroscopy .....	86
5.2.3 <sup>13</sup> C Solid State NMR Spectroscopy .....	86
Deconvolution of NMR Signals .....	87
Proton Spin-Lattice Relaxation Time .....	87
5.2.4 Summary of Cotton Cellulose Results .....	88
5.3 Avicel .....	88
5.3.1 X-ray Diffraction .....	89
5.3.2 FTIR Spectroscopy .....	89
5.3.3 <sup>13</sup> C Solid State NMR Spectroscopy .....	90
Deconvolution of NMR Signals .....	91
Proton Spin-Lattice Relaxation Time .....	92
5.3.4 Summary of Avicel Results .....	92
5.4 Comparison of Techniques by Sample .....	92
5.4.1 Q-90 .....	93
5.4.2 Cotton .....	94
5.5 Comparison of Samples by Analytical Technique .....	95
5.5.1 X-ray Diffraction .....	95
5.5.2 FTIR Spectroscopy .....	97
5.5.3 <sup>13</sup> C Solid State NMR Spectroscopy .....	98
5.6 Proposed Theory Based on Data .....	100
5.6.1 Explanation for the Differences Between Q-90 and Cotton Cellulose .....	106

## **Chapter 6 - Results & Discussion – Part III**

### **Cellulose Depolymerisation and Oxidation**

6.1 Viscosity and Chain Scission .....	107
6.1.1 Q-90 Pulp .....	108
6.1.2 Hemicellulose Reduced Pulp .....	109
6.1.3 Cotton Cellulose .....	110

6.1.4 Avicel .....	111
6.1.5 Degree of Polymerisation.....	112
6.2 Conductometric Titration .....	112
6.2.1 Q-90 Pulp .....	113
6.2.2 Hemicellulose reduced Pulp.....	114
6.2.3 Cotton Cellulose.....	115
6.2.4 Avicel .....	116
6.3 Comparison of Viscosity and Conductometric Titration Measurements.....	117
6.3.1 Carboxylic Acid Content & Degree of Polymerisation.....	117
6.3.2 Chain Scission & Carboxylic Acid Content.....	118
6.4 Summary.....	118
<b>Chapter 7 - Conclusions .....</b>	<b>120</b>
<b>Chapter 8 - Recommendations for Future Work.....</b>	<b>123</b>
<b>Chapter 9 - References .....</b>	<b>125</b>
<b>Appendix I - Schematic of the Kettle Reactor .....</b>	<b>139</b>
<b>Appendix II - Metal Ion Analysis Results.....</b>	<b>140</b>

## List of Tables

---

	<i>Page</i>
<b>Table 5.1</b> Carbohydrate analysis for Q-90 and hemicellulose reduced pulp obtained by two methods. ....	77
<b>Table 6.1</b> Degree of polymerisation data for the cellulose samples used.....	112
<b>Table 6.2</b> Slope values for the various cellulose samples calculated from a plot of the chain scission number versus carboxylic acid content. ....	118

## List of Figures

---

	<i>Page</i>
<b>Figure 1.1</b> Oxygen species involved in the reduction of oxygen to water. ....	9
<b>Figure 1.2</b> Mass transfer associated with oxygen delignification. ....	10
<b>Figure 1.3</b> The three monomer repeat units of lignin.....	13
<b>Figure 1.4</b> Reactions between oxygen and phenolic structures in lignin. ....	15
<b>Figure 1.5</b> Reactions of hydroperoxide intermediates leading to oxygen delignification. ....	16
<b>Figure 1.6</b> Reactions of hydroperoxide intermediates to form muconic acids and ortho- and para-quinones. ....	17
<b>Figure 1.7</b> Central part of the molecular chain of cellulose. ....	18
<b>Figure 1.8</b> Schematic illustration of the structural continuity from the cellulose molecule to the microfibril.....	19
<b>Figure 1.9</b> Projection of the 020 plane in cellulose I showing the hydrogen bonding network and the numbering of the atoms. ....	21
<b>Figure 1.10</b> Oxidation and cleavage of the cellulose chain.....	23
<b>Figure 1.11</b> Carbohydrate reactions which do not produce chain cleavage.....	24
<b>Figure 1.12</b> Formulas of the sugar components for hemicellulose. ....	26
<b>Figure 1.13</b> Principal structure of galactoglucomannan.....	27
<b>Figure 1.14</b> Principal structure of arabinoglucuronoxylan.....	28
<b>Figure 1.15</b> Diagrammatic sketch of reflection of x-rays. ....	31
<b>Figure 1.16</b> Monoclinic unit cell of cellulose I . ....	33
<b>Figure 1.17</b> Lattice planes of the space unit of cellulose I. ....	34
<b>Figure 4.1</b> Schematic representation of the fringed micelle model.....	57
<b>Figure 4.2</b> X-ray diffraction data for Q-90 showing the relative degree of crystallinity as a function of oxidation time. ....	60
<b>Figure 4.3</b> FTIR spectroscopy data for Q-90 showing the relative degree of crystallinity as a function of oxidation time. ....	62

<b>Figure 4.4</b> Solid state NMR data for Q-90 showing the relative degree of crystallinity calculated from the C4 carbon contribution as a function of oxidation time. ....	65
<b>Figure 4.5</b> Solid state NMR data for Q-90 showing the relative degree of crystallinity calculated from the C6 carbon contribution as a function of oxidation time. ....	65
<b>Figure 4.6</b> Solid state NMR data for Q-90 showing the relative degree of crystallinity calculated from the total C4 and C6 contributions as a function of oxidation time...	66
<b>Figure 4.7</b> Proton spin-lattice relaxation times for Q-90 as a function of oxidation time. ....	68
<b>Figure 4.8</b> X-ray diffraction data for the Q-90 reproducibility measurements of the relative degree of crystallinity as a function of oxidation time. ....	69
<b>Figure 4.9</b> FTIR data for the Q-90 reproducibility measurements showing the relative degree of crystallinity as a function of oxidation time. ....	71
<b>Figure 4.10</b> Solid state NMR data for the Q-90 reproducibility measurements showing the relative degree of crystallinity (calculated from the total C4 and C6 contributions) as a function of oxidation time. ....	72
<b>Figure 4.11</b> Proton spin-lattice relaxation times for the Q-90 reproducibility samples as a function of oxidation time. ....	73
<b>Figure 5.1</b> X-ray diffraction data for hemicellulose reduced pulp showing the relative degree of crystallinity as a function of oxidation time. ....	78
<b>Figure 5.2</b> A comparison of the x-ray diffraction data for Q-90 and hemicellulose reduced pulp showing the relative degree of crystallinity as a function of oxidation time. ....	79
<b>Figure 5.3</b> FTIR data for hemicellulose reduced pulp showing the relative degree of crystallinity as a function of oxidation time. ....	80
<b>Figure 5.4</b> Solid state NMR data for hemicellulose reduced pulp showing the relative degree of crystallinity calculated from the total contribution of the C4 and C6 carbons as a function of oxidation time. ....	81
<b>Figure 5.5</b> Proton spin-lattice relaxation times for hemicellulose reduced pulp as a function of oxidation time. ....	82

<b>Figure 5.6</b> X-ray diffraction data for cotton cellulose showing the relative degree of crystallinity as a function of oxidation time. ....	85
<b>Figure 5.7</b> FTIR data for cotton cellulose showing the relative degree of crystallinity as a function of time. ....	86
<b>Figure 5.8</b> Solid state NMR data for cotton cellulose showing the relative degree of crystallinity (calculated from the total contribution of the C4 and C6 carbons) as a function of oxidation time. ....	87
<b>Figure 5.9</b> X-ray diffraction and FTIR data for Avicel showing the relative degree of crystallinity as a function of oxidation time. ....	90
<b>Figure 5.10</b> Solid state NMR data for Avicel showing the relative degree of crystallinity (from the C4, C6 and total C4 and C6 carbons) as a function of oxidation time. ....	91
<b>Figure 5.11</b> Comparison of Q-90 samples using three analytical techniques. ....	93
<b>Figure 5.12</b> Comparison of cotton cellulose samples using three analytical techniques. ....	95
<b>Figure 5.13</b> Cellulose sample comparison by x-ray diffraction. ....	96
<b>Figure 5.14</b> Cellulose sample comparison by FTIR spectroscopy. ....	98
<b>Figure 5.15</b> Cellulose sample comparison by solid state NMR taking into account the total C4 and C6 carbon atom contribution. ....	99
<b>Figure 5.16a</b> Schematic representation of cellulose by the fringed micelle model showing two possible points of attack by oxygen. ....	100
<b>Figure 5.16b</b> Attack on the amorphous domain. ....	101
<b>Figure 5.16c</b> Chain “peeling” attack at the reducing end groups after cleavage in the amorphous domain. ....	102
<b>Figure 5.16d</b> Attack on the crystalline domain. ....	102
<b>Figure 5.16e</b> Attack at two positions on exposed crystalline material of cellulose. ....	103
<b>Figure 5.16f</b> Amorphous regions developing from oxygen attacking the outer portions of the crystalline domain. ....	104
<b>Figure 6.1</b> Q-90 data for the viscosity and chain scission number as a function of oxidation time. ....	109



<b>Figure 6.2</b> Hemicellulose reduced pulp data for viscosity and chain scission number as a function of oxidation time.....	110
<b>Figure 6.3</b> Cotton cellulose data for viscosity and chain scission number as a function of oxidation time.....	111
<b>Figure 6.4</b> Conductometric titration data for Q-90 showing the carboxylic acid content as a function of oxidation time.....	113
<b>Figure 6.5</b> Conductometric titration data for hemicellulose reduced pulp showing the carboxylic acid content as a function of oxidation time.....	115
<b>Figure 6.6</b> Conductometric titration data for cotton cellulose showing the carboxylic acid content as a function of oxidation time.....	116
<b>Figure 6.7</b> Q-90 data showing the relationship of carboxylic acid content as a function of the degree of polymerisation.....	117

# Chapter 1

## Introduction

---

### 1.1 Oxygen Delignification

The treatment of pulp to increase its overall brightness is either termed delignification or bleaching.<sup>1</sup> Higher brightness will increase a pulp's optical quality. Mechanical and chemical pulps in addition to recycled waste paper are all bleached to achieve higher brightness. The brightness of pulp is improved by dissolving and decolourising its coloured components. During the delignification process, physical properties such as strength from the carbohydrate component of pulp need to be preserved as much as possible. The lignin component of pulp imparts colour and is eliminated through delignification. Delignification removes the lignin from dissolved pulps while leaving cellulose in place for making paper.<sup>2</sup> The more lignin that is removed the brighter the paper will be and so the process of delignification is synonymous with bleaching.

Delignification is a multi-step process wherein two types of chemicals are used: 1) oxidants which degrade and decolourise lignin, and 2) alkali which degrade lignin by hydrolysis and cause lignin dissolution.<sup>3</sup> Since a large amount of oxidising chemicals are used, they are chosen based on their selectivity toward degrading the lignin component of pulp instead of its carbohydrate component. Oxidants are also chosen for economic reasons because the cost of the chemical influences the overall cost of the bleaching process.<sup>4</sup> Although there are many processes to delignify pulp oxygen delignification is one of the most environmentally benign process.<sup>5</sup>

#### 1.1.1 History & Definition

Bleaching can be dated back to the ancient Gauls.<sup>3</sup> The Gauls observed that vegetable fibres moistened with an alkaline solution and subjected to sunlight remained brighter than the same fibres without exposure to the solution. The alkaline solution was obtained from vegetable ash. In the eighteenth century, this method of bleaching was

perfected by the Dutch. With the discovery of chlorine by a Swedish chemist, Karl Wilhelm Scheele in 1774, manufacturing bleaching chemicals for brightening fabrics and paper began.<sup>6</sup> Chlorine was observed to have very powerful bleaching action. In the mid-1950's Soviet researchers began an investigation into the use of molecular oxygen with alkali bleach to refine dissolved pulps.<sup>7</sup> The conditions were similar as in alkaline agents used earlier in history except that oxygen was supplied in during the treatment. Since the early days of discovery of oxygen as a bleaching and delignification agent, the practice of oxygen delignification developed significantly. Currently oxygen is combined with other techniques to delignify and brighten paper.<sup>8</sup>

Oxygen delignification uses both alkali and oxygen on unbleached pulp to remove a large portion of lignin from the pulp. Delignification generally proceeds to a point where the rate of removal of lignin becomes low. At that time the degradation and removal of the carbohydrate component begins to increase dramatically. The oxygen delignification process is then stopped and other more selective processes are used to remove the remaining lignin.<sup>9</sup> So that further degradation of the cellulose does not sacrifice the strength of the paper. This later stage is usually carried out in the bleach plant with the use of other chemicals like hydrogen peroxide, ozone, chlorine dioxide and in some cases, molecular chlorine.

This process is normally effective for removing about 30-50% of the lignin from the pulp and is carried out under pressure with an appreciable amount of heat.<sup>10</sup> Oxygen delignification is used on pulp that has been made by chemical pulping rather than mechanical pulping. Mechanical pulps retain lignin in the pulp to produce a larger quantity of paper, while chemical pulps have most of the lignin removed to create the strongest possible paper. The most common chemical pulp is from the Kraft process, however, pulp from the sulphite process is also quite commonly used.

### **1.1.2 Other Types of Delignification**

In addition to oxygen, there are a number of other viable delignification and bleaching chemicals such as chlorine, hypochlorite, chlorine dioxide, hydrogen peroxide, peroxyacids, ozone, and biological systems.<sup>11,12</sup> In order to better understand why oxygen

is one of the most beneficial chemicals to use. it is important to understand briefly the other types of delignification chemicals.

### ***Chlorine Containing Bleaching Agents***

Molecular chlorine has been used in the past due to its selectivity to attack the lignin in the pulp and not the cellulose.<sup>13</sup> Chlorine is relatively inexpensive compared to other chemicals. Chlorine may also be used to control variations in pulp lignin content which allows more expensive chemicals to be used with higher effectiveness.<sup>3</sup> The most important considerations in using molecular chlorine are economics, pulp quality and environmental impact.<sup>7</sup> Since environmental concerns have become more prevalent in recent times, the use of chlorine has declined. The drawback to using chlorine is that there are large amounts of adsorbable chlorinated organics produced from the reaction of the molecular chlorine with lignin in the pulp. Effluents from the chlorination stage contain solids that are only partially biodegradable and in most cases are toxic.<sup>12</sup> The amount of chlorinated organics produced is no longer environmentally acceptable and as such this is not the chemical of choice at present.

Sodium hypochlorite is prepared by introducing chlorine gas into an aqueous solution of sodium hydroxide. In the process of hypochlorite bleaching, heavy metals present from the pulp can decompose the hypochlorite solution into chloride and oxygen.<sup>14</sup> When the hypochlorite is reduced to chloride, two oxidation equivalents are consumed. In principle, hypochlorite can be used in a single stage bleaching sequence or as the first step in a multi-step sequence.<sup>15</sup> It is usually used after chlorination and extraction. Since hypochlorite has a severe degrading effect on cellulose at neutral pH's, it is always used under alkaline conditions with the application of additional sodium hydroxide added to the mixture.<sup>1</sup> Hypochlorite is also used in the purification of dissolved pulps which serve two purposes, that of bleaching and viscosity control.<sup>16</sup> Very careful control of the bleaching conditions is required to give pulp a uniform viscosity and reactivity. Hypochlorite stages, however, are in the process of being phased out of commercial bleach plants for environmental reasons including the perceived hazard of hypochlorite as a chlorine compound and the documented role of these compounds in the formation of chloroform during pulp bleaching.<sup>17</sup>

Under certain circumstances, chlorine dioxide can be considered an unstable compound since it has unpaired electrons that render it very reactive.<sup>18</sup> It is also very toxic and corrosive. It had not been used earlier as a bleaching agent because of these effects. Despite the nature of this gas, developments in bleaching technology progressed to enable chlorine dioxide bleaching to become a fairly safe operation.<sup>19</sup> Chlorine dioxide is moderately soluble in water and as such is generally produced on site at the bleach plant. The German organic chemist, Eric Schmidt was first to use chlorine dioxide for the dissolution of lignin in wood.<sup>20</sup> Commercial bleaching of pulp with chlorine dioxide began in both Sweden and Canada. The use of chlorine dioxide was slow to develop in the first few years after being introduced but later gained widespread use and began to grow quickly. Today chlorine dioxide is used in combination with other oxidising bleaching chemicals and alkali in various multi-stage bleach sequences. The combination of chlorine dioxide with chlorine in a single stage has also proven to be beneficial in that higher pulp brightness is obtained in a shorter reaction time and under less severe conditions.<sup>21</sup> However, with growing environmental concerns regarding the use of chlorine in the bleach plant, there is a movement away from using this chemical combination.

The pulp and paper industry faces a great deal of pressure from bleaching practices that use chlorine containing chemicals.<sup>22</sup> Strict regulations have been set in many countries including Canada to control the amount of adsorbable chlorinated organic compounds that are released into the environment.<sup>23</sup> These regulations have been adopted because of the growing knowledge that some chlorinated phenols released during bleaching are extremely toxic to aquatic life.<sup>24</sup> As a consequence, there is a rapid replacement of chlorine with other chemicals. With the move toward totally chlorine free pulp mills and bleaching plants and closed systems other chemicals are now being looked at more closely to evaluate their effectiveness.

### ***Oxygen Containing Bleaching Agents***

Oxygen has long been used for a variety of industrial applications. Its bleaching effect on cotton has been known since historical times.<sup>25</sup> However, oxygen was not introduced for pulp delignification purposes until the 1970's.<sup>26</sup> The reasons still limiting

the use of oxygen are associated with the difficulties of directing its action more specifically toward lignin without degrading carbohydrates.<sup>27</sup>

Alkaline hydrogen peroxide is widely used in the pulp industry to bleach lignin rich pulps to high levels of brightness. The bleaching effect of hydrogen peroxide has been attributed to its ability to react with various coloured carbonyl containing structures in lignin. The advantages of peroxide lie in its ease of handling and application, its versatility, and the relatively non-toxic and innocuous nature of its reaction products.<sup>28</sup> However, peroxide is susceptible to decomposition and must also be applied under alkaline conditions to achieve optimum results.<sup>29</sup> Other drawbacks are the high price of peroxide and the additives required for stabilisation. Hydrogen peroxide is not an efficient delignifying agent but works well as a brightening agent.<sup>30</sup>

The peroxyacids of interest to the pulp industry at the present time are peracetic acid (also known as peroxyacetic acid), peroxymonosulphuric acid and peroxyformic acid.<sup>7</sup> These chemicals are formed when hydrogen peroxide is reacted with the corresponding acid. The equilibrium mixture contains the peroxyacid and water as well as the acid and hydrogen peroxide. Peroxyacids can delignify and bleach pulp to higher brightness.<sup>31</sup> They are generally used under acidic or slightly basic conditions. More research is certainly needed on peroxyacids since carbohydrates are heavily degraded in these conditions.

Ozone is a powerful oxidising agent that reacts readily with most organic materials including lignocellulosic materials.<sup>32</sup> Its oxidising potential is exceeded by only a few compounds such as fluorine, atomic oxygen and perhydroxyl radicals.<sup>33</sup> Ozone is used in commercial oxidation processes to bleach textiles, waxes and starches and to disinfect air and water.<sup>34</sup> Although ozone is highly reactive, its application is restricted because it is generated in low concentrations and diluted with a carrier gas such as oxygen or air. The main drawback of ozone is its low solubility in water. This limits its reactivity in aqueous systems where ozone must transfer from the gas phase into water to react. The mass transfer of ozone into the liquid phase can be improved by increasing the concentration of ozone in the carrier gas and by compressing the gas mixture.<sup>35</sup> Interest in ozone as a delignifying agent started in the 1990's as a replacement for chlorine. This

interest has been accelerated by the progression towards minimising discharges of chlorinated compounds and by market demands for pulps to be produced free of all chlorine containing compounds. Further investigation into the use of ozone in delignifying pulps is still needed since unwanted reactions with cellulose occur and lead to deterioration in pulp quality.<sup>36</sup> A highly selective ozone treatment remains elusive despite intense efforts directed toward understanding the mechanisms of ozone-carbohydrate reactions and the conditions required to minimise these reactions.

### ***Biological Systems***

The traditional effective approach of using chlorine containing chemicals as delignification agents has been challenged by environmental groups.<sup>7</sup> In response to these pressures, alternative technologies have been developed to partially or completely replace these chemicals. Enzymatic processes have been developed as one of these technologies.<sup>37</sup> Environmental and regulatory concerns have favoured the investigation of enzymes as delignification agents because they are readily biodegradable and do not contribute to organochlorine formation.<sup>7</sup> Enzymes are catalysts of highly specific reactions, and as such are not consumed in the process. Enzymes consist mainly of carbon, oxygen, hydrogen and nitrogen and are classified as protein molecules made by living organisms. Enzymes can break down specific portions of lignin while virtually leaving the cellulose intact.<sup>7</sup> Using enzymes as delignification agents is very new and there is still a lot of preliminary experimentation required before it can be a viable technique for delignification of dissolved pulps.<sup>37</sup>

#### **1.1.3 Benefits of Oxygen Delignification**

The primary benefit of oxygen delignification over other types of delignification processes is that it is environmentally favourable. The chemicals that are added to the pulp for the delignification and the materials that will be removed from the pulp once delignified are all recoverable using the Kraft chemical recovery system.<sup>38</sup> As stated before the majority of pulp that is delignified using oxygen is Kraft pulp, which has a recovery system already in place. The Kraft recovery system is equipped with Brown stock washers that can recycle the oxygen stage effluent. This in essence minimises the

potential environmental impact on the plant that bleaches the pulp in its final stage (after oxygen delignification). The minimisation is proportional to the extent of delignification.

The driving force of using oxygen in a delignification stage has been environmental. Environmental benefits are seen through a reduction of the chlorinated by-products and environmental parameters that affect the bleaching plant.<sup>38</sup> Some of these parameters are the biological oxygen demand (BOD), chemical oxygen demand (COD), levels of organochlorines (measured as adsorbable organic halogens - AOX), and the colour of the effluent water.

Another benefit of using oxygen to delignify pulp is that it can be used in conjunction with other bleaching technologies to reduce the overall cost of the operation.<sup>39</sup> One beneficial aspect is installing an oxygen pre-delignification stage in a chlorine compound based bleach plant. The result is that there will be a decreased need for oxidising chemicals in the delignifying part of the bleaching sequence. The lower cost results from the decreased requirement for delignifying oxidising chemicals (chlorine, chlorine dioxide or ozone) because oxygen is less expensive. Further cost savings result from a decrease in the other oxidising chemicals needed for the final bleaching sequences.

Energy related benefits also arise from using oxygen in delignification. Material recovered from the pulp after the oxygen stage can be burned to provide heat that is necessary to operate an oxygen delignification stage.<sup>7</sup> The lower refining energy requirement coupled with the fact that the manufacturing of oxygen requires only about one eighth of the energy required to make a chemical equivalent amount of chlorine gives oxygen a tremendous advantage over other oxidising chemicals that are still being and have been traditionally used.

#### **1.1.4 Disadvantages and Limitations of Oxygen Delignification**

Two major disadvantages of oxygen delignification are poor selectivity and the slow mass transfer of oxygen. There is a tendency of either oxygen bleaching or delignification to be non-selective at higher degrees of delignification.<sup>8</sup> This is so because the oxygen begins to attack the cellulose and lignin in the pulp. Viscosity and kappa number measurements are used to measure the selectivity. Viscosity is an index of



the degree of carbohydrate polymerisation,<sup>40</sup> and the kappa number is an index of lignin content in the fibre.<sup>40</sup> It is possible to completely remove lignin from pulp fibres while maintaining a specific degree of carbohydrate polymerisation in the fibres. The viscosity should be maintained above some critical value for the pulp to have adequate strength properties. For oxygen delignification, it is difficult to reduce the kappa number to zero while maintaining pulp viscosity above critical values. The degradation of carbohydrates by intermediate products and reactive free radicals contributes to poor selectivity.

Other disadvantages associated with oxygen delignification are that there is a large capital cost for the start up of the process, may be an increased demand exerted on the mill recovery system, increased steam costs, higher maintenance costs and an increase in the overall process complexity.<sup>39</sup>

### ***Selectivity***

One way of defining selectivity is as the amount of lignin removed from pulp (measured as the reduction in kappa number) for a given amount of carbohydrate degradation (measured as the decrease in viscosity). Oxygen is not a selective bleaching chemical compared to chlorine or chlorine dioxide since these chemicals can remove about 90% of the lignin in pulp.<sup>41</sup> Usually oxygen can remove only about 50% of the lignin before degradation of the carbohydrates become extensive.<sup>10</sup> Selectivity is affected by the choice of process conditions and variables and by the presence of pulp contaminants.

These variables are related to the varied reactivity of oxygen containing species present and their reactivity with lignin and carbohydrate structures. Hydroxyl radicals are among the least reactive radical species present. Selectivity can also be improved by a nitrogen dioxide pretreatment that is still in the developmental stages.<sup>42</sup> Lignin removal in the oxygen stage can be as high as 80%.<sup>43</sup> Other pretreatments shown to favourably affect oxygen selectivity include chlorine, chlorine dioxide and acidic hydrogen peroxide.<sup>44</sup>

In order to obtain an effective degree of delignification, cellulose is inevitably attacked and degraded. This eventually leads to a reduced pulp strength and a severe viscosity loss. Why does this occur? It is important to note that in the process of oxygen

delignification, oxygen is reduced to water through four, one electron transfers by the following sequence:<sup>1</sup>

oxygen → peroxy radicals → hydrogen peroxide → hydroxyl radicals → water

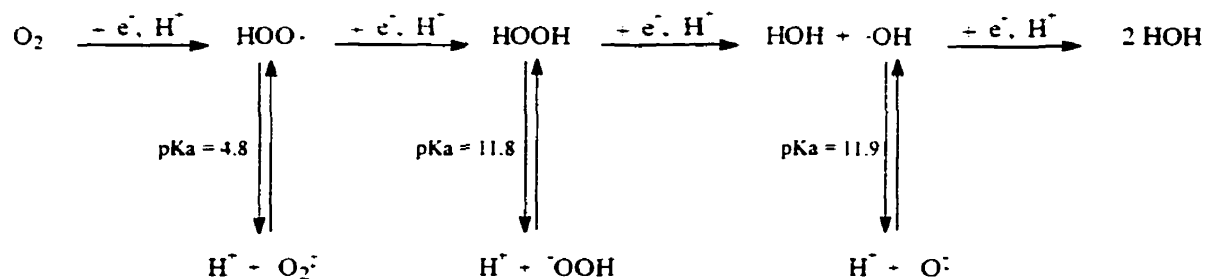


**Figure 1.1** Oxygen species involved in the reduction of oxygen to water.<sup>1</sup>

The hydroxyl radicals that are formed ( $\cdot\text{OH}$ ) react with the lignin and the carbohydrate component.<sup>45</sup> When these radicals react with the carbohydrates there is random chain cleavage and the average degree of polymerisation of the carbohydrates decreases dramatically.<sup>46</sup> As the average degree of polymerisation is decreased, the pulp strength and viscosity are consequently reduced.

### **Temperature**

Oxygen by itself is not very reactive. In order for oxygen to react, high temperatures and ionisation of functional groups within the substrate are needed to allow the release of electrons.<sup>25</sup> The oxygen delignification process therefore uses strongly alkaline media and relatively high temperatures. As the temperature is increased beyond 120 °C there is a sharp increase in the carbohydrate degradation.<sup>3</sup> For this reason temperatures below 120 °C are used.

### **Mass Transfer and Solubility Considerations**

Mass transfer problems are caused by the heterogeneous reaction system (gas-liquid-solid) and the low solubility of oxygen in water.<sup>47</sup> Mass transfer plays a role in limiting the efficiency of the oxygen delignification process. In order for oxidation of lignin to take place, oxygen must be transferred from the gaseous to the liquid state. The

dissolved oxygen in the liquid must then be able to react with solid lignin (ie: a liquid to solid transfer must occur).

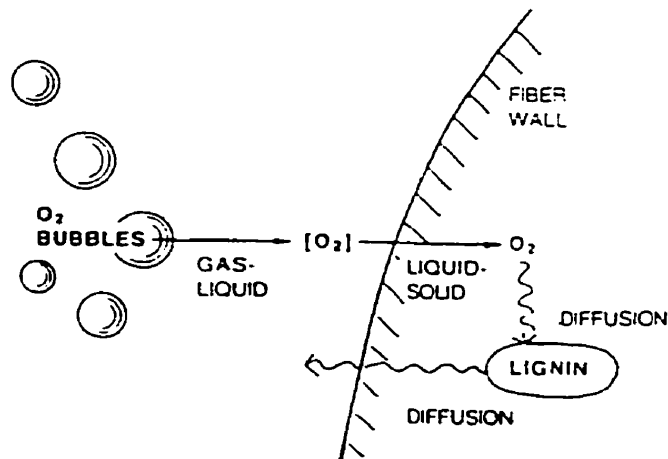


**Figure 1.2** Mass transfer associated with oxygen delignification.<sup>47</sup>

Oxygen is slow to diffuse in aqueous liquid media due to its low solubility compared to other chemicals. Molecular chlorine for instance is one hundred times more soluble in water than oxygen.<sup>47</sup>

#### ***Incoming Kappa Number Variation***

There is a limitation imposed by the incoming kappa number variation.<sup>48</sup> If there is too much variation in the kappa number, the mill will tend to ease up on the oxygen stage performance and put more of a demand on the bleaching chemicals in subsequent stages. This ensures a better quality product but at the expense of the oxygen delignification process not being fully utilised.

#### ***Transition Metals***

Wood with a high content of transition metal ions increases the degradation of the carbohydrate component. Transition metal ions are known to have a harmful effect on cellulose during oxygen delignification and bleaching.<sup>49</sup> Trace quantities of transition metals act as catalysts for the decomposition of the peroxide that is generated. The decomposition forms hydroxyl radicals that are thought to be the main source of the degradation on cellulose. It is important then to control or remove the transition metals

present in the wood. This is amongst the most important factors governing selectivity in oxygen delignification. Transition metals can catalyse the generation of harmful radical species.<sup>49</sup> Most pulps contain appreciable amounts of iron, copper, and manganese all of which have this catalytic effect. One approach to deal with transition metals is to remove them by an acid wash before the pulp encounters oxygen.<sup>50</sup> Another way is to add compounds to the pulp to inhibit carbohydrate degradation. These compounds are called viscosity protectors.<sup>51</sup>

The protector of greatest commercial importance is the magnesium ion. Since its discovery in 1963 by Robert and co-workers, its effectiveness has provided a great insight into the development of oxygen delignification.<sup>52</sup> Magnesium salts inhibit the degradation of carbohydrates.<sup>53</sup> All commercial oxygen delignification plants add a magnesium salt to the alkaline liquor to ensure good selectivity although the protective effect of magnesium depends on the ratio between magnesium and other metals.<sup>54</sup> The magnesium ion is believed to function by precipitating as magnesium hydroxide that surrounds the transition metal ions making them unavailable for catalysis of the peroxide decomposition or by forming complexes with them.<sup>55</sup>

Other reagents which protect additives for oxygen delignification include sodium silicate, potassium iodide, EDTA, formaldehyde and glucitol.<sup>1</sup> All these reagents have the potential ability to either stabilise the peroxide formed during delignification or to decompose it without harming the carbohydrate component.

## **1.2 Chemistry of Oxygen Delignification**

### **1.2.1 Chemistry of Oxygen**

Oxygen in its lowest energy configuration is in the triplet state<sup>56</sup> where it contains two electrons that are unpaired due to their parallel spin.<sup>57</sup> Thus each of these electrons possesses an affinity for other electrons of opposite spin and so oxygen can be considered a free radical. Like other radicals albeit with less reactivity, oxygen has a tendency to react with compatible substrates at regions of high electron density. The result is the initial step in a four step process in which oxygen is reduced to water and the substrate is oxidised.<sup>1</sup> Figure 1.1 presented earlier illustrates this process.

The product of the first step is a negatively charged ion called a superoxide anion  $O_2^-$  which combines with a hydrogen ion to form the hydroperoxy radical  $HOO\bullet$ . Since the radical is a weak acid (possessing a pKa of 4.8), the anion remains uncombined under the alkaline conditions of the oxygen delignification. Both the superoxide anion and the hydroperoxy radicals have higher oxidation potentials than the original oxygen molecule. Thus each can acquire another electron to form the respective peroxide dianion,  $O_2^{2-}$  and the hydroperoxy anion,  $HOO^-$ . The dianion in reality is not sufficiently stable to form in great quantities. The hydroperoxide anion is the dissociated form of hydrogen peroxide. Hydrogen peroxide is a weak acid with a pKa of 11.8 and so both it and its anion are present in great quantities under oxygen delignification conditions.

The third step occurs when hydrogen peroxide accepts an electron to form a hydroxide ion and a hydroxyl radical,  $HO\bullet$ . The hydroxyl radical is also a weak acid with a pKa of 11.9 and so exists in equilibrium with its anion,  $O^-$ . Finally the hydroxyl radical can acquire another electron to form a hydroxide ion in water. The occurrence of hydroxyl radicals in this process is of great significance since they are extremely reactive and are indiscriminate attacking cellulose as well as lignin.<sup>58</sup>

Molecular oxygen is a unique oxidising agent since in its electronically stable form two of the electrons are unpaired. It has a strong tendency to react with organic substances which initiates radical chain reactions. The oxidation proceeds via several intermediates, for example by peroxides, organic radicals and the hydroxyl radical.<sup>59</sup> Unlike oxygen these intermediates are non-selective oxidative agents and in pulp delignification, it is necessary to control their formation in order to try to avoid severe degradation of cellulose.

Oxygen delignification can thus be considered as consisting of two simultaneous general reactions, a desirable delignification reaction and an undesirable and closely related carbohydrate degradation reaction. This latter degradation reaction limits the degree of delignification during the oxygen delignification process. A better understanding of these reactions leads to gaining a greater amount of delignification compared to carbohydrate degradation.

### 1.2.2 Lignin

Lignin is a polymer made up of phenylpropane units. Many aspects in the chemistry of lignin still remain unclear, for example, the specific structural features of lignins located in various morphological regions of wood. Almost all of the properties of lignin are undesirable for paper making applications.<sup>60</sup> The highest qualities of paper are usually made from pulps that have the most amount of lignin removed. Lignin along with acids from some pulping processes causes paper to become brittle. Lignin is also oxidised photochemically to form coloured compounds which give rise to yellowing and discolouration of the end product.<sup>6</sup> Newsprint is the best example of this, but all paper that contains a high degree of lignin will display similar results.

Lignin comprises about 17-33% of the dry weight of wood.<sup>61</sup> It is a complex aromatic polymer which appears to function both as a strengthening agent in the composite wood structure and also as a component which assists in the resistance of the wood towards attack by micro-organisms.<sup>9</sup> It is not presently possible to give a complete structure for the chemical composition of lignin, but all lignins appear to be made up of polymers of *p*-coumaryl alcohol, coniferyl alcohol and sinapyl alcohol.<sup>60</sup>

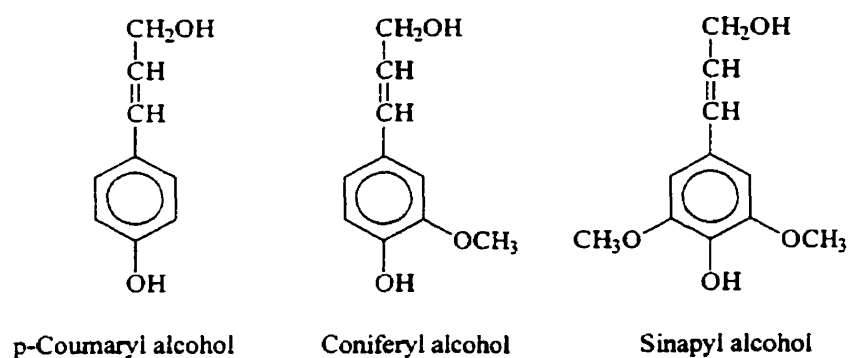


**Figure 1.3** The three monomer repeat units of lignin.<sup>60</sup>

The amount of each of these three monomers in a given lignin sample differs depending on the source of the lignin. Lignin that is derived from softwood consists only from coniferyl alcohol, while if lignin is derived from hardwood it is a combination of coniferyl and sinapyl alcohol.<sup>60</sup> Lignin from grasses has all three alcohols present.<sup>60</sup>

Structural studies of lignin have proven to be very difficult and have been complicated by the fact that there are many bonding patterns present in the polymer. The type of bonds can either be carbon-carbon or carbon-oxygen-carbon (ether) and they may involve both the aromatic rings and the carbon atoms in the side chain. Nevertheless, the principal structural elements in lignin have been largely clarified as a result of detailed studies of isolated lignin preparations. Using specific techniques based on oxidation, reduction or hydrolysis under acidic and alkaline conditions a better but not full understanding of the structure of lignin can be gained.<sup>6</sup>

### ***Lignin Reactions***

Numerous studies using lignin related model compounds have revealed that phenolic and enolic structures constitute the main sites of oxidative attack in alkaline media.<sup>62</sup> Phenolic groups in residual lignin of pulp play an important part in the chemistry of oxygen delignification. Phenolate ions are present under alkaline conditions of the delignification process.<sup>63</sup> It is these phenolate ions that react with oxygen to give phenoxy radicals. A one electron transfer from a high electron density location to the oxygen molecules occurs. Thus the peroxy radical formed may then react either with a phenolate anion or with a resonance stabilised phenoxy radical to form peroxy compounds. These can then rearrange to hydroxy derivatives. It might also happen that these phenoxy radicals undergo further reactions with superoxide radicals that are also present under alkaline conditions, to produce hydroperoxide intermediates. The figure below shows how oxygen can react with the phenolic structures of lignin.

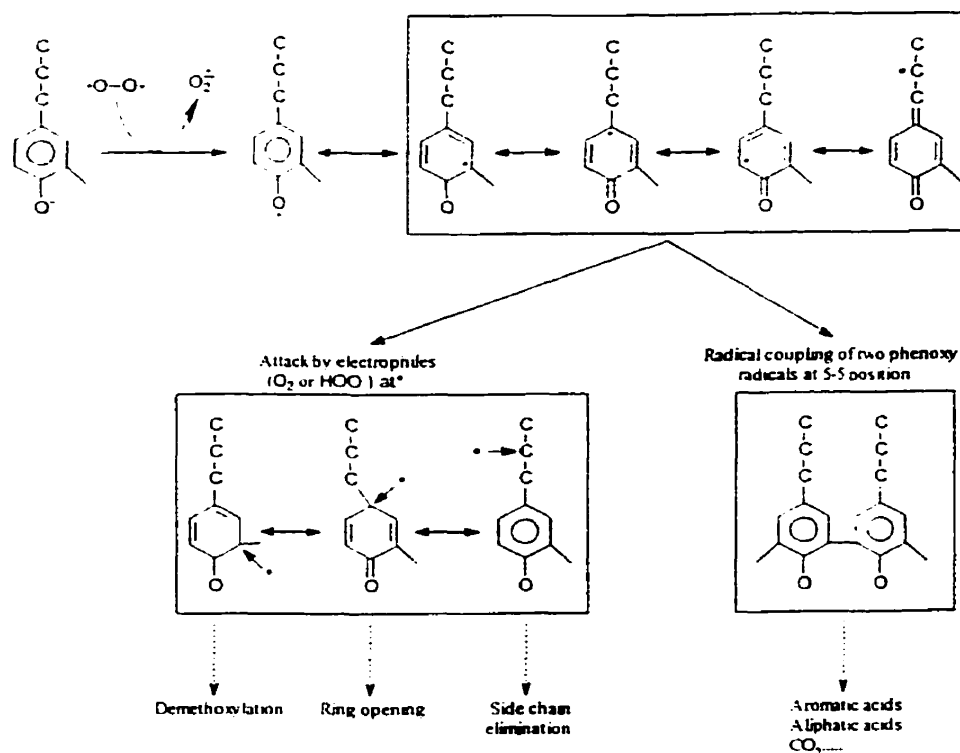


**Figure 1.4** Reactions between oxygen and phenolic structures in lignin.<sup>64</sup>

Two possible pathways that are presented above show 1) a lignin condensed structure forming<sup>64</sup> and 2) opening of the phenolic ring.<sup>65</sup>

The phenoxy radicals formed at an early stage of the process are in principle capable of undergoing coupling reactions to form new carbon-carbon bonds between lignin units. These condensation reactions are undesirable because they increase the molecular size of the lignin and in turn decrease its solubility.<sup>1</sup> Furthermore, the condensed units are resistant to further reaction. Due to the restricted mobility of the phenoxy radicals in lignin it is unlikely that these reactions will occur extensively during oxygen bleaching, but there is still evidence of their occurrence.

In an alkaline environment as found in the oxygen delignification process, the hydroperoxide intermediate exists due to the corresponding anion which can then undergo an intramolecular nucleophilic reaction at an adjacent site. This may be the carbonyl



carbon of the quinone methide, a ring carbon conjugated with it or an adjacent side chain carbon, depending on the location of the hydroperoxy function.<sup>66</sup>

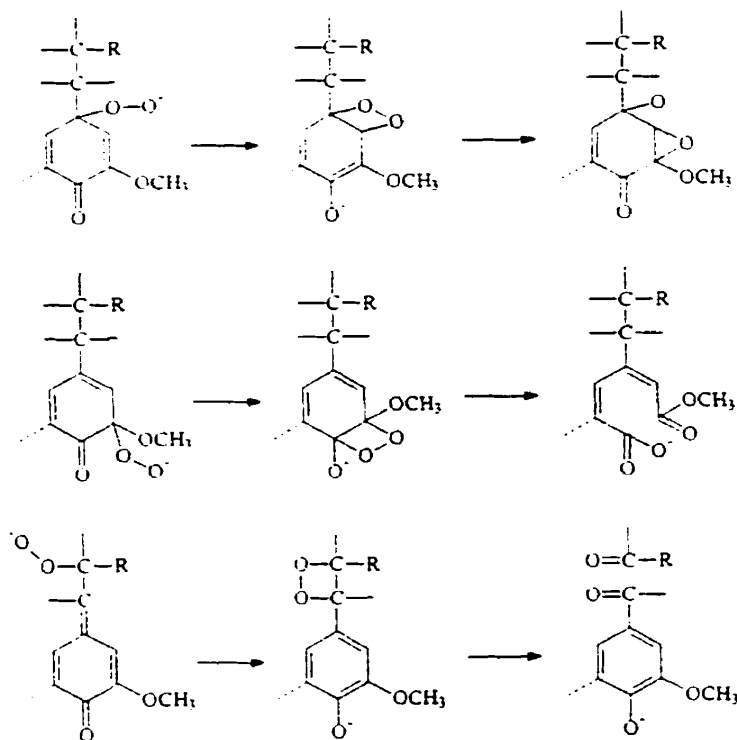


**Figure 1.5** Reactions of hydroperoxide intermediates leading to oxygen delignification.<sup>66</sup>

These reactions eventually lead to the formation of oxirane, muconic acid and carbonyl structures.<sup>67</sup> When forming a carbonyl structure, there is a bond cleavage between two adjoining lignin monomeric units. This leads to the fragmentation of the lignin. The formation of the other structures corresponds to the introduction of hydrophilic groups that give the lignin a polar character that is more easily solubilised in an alkaline environment. Both types of these reactions enhance the solubility of the lignin. Similar reactions involving unionised hydroperoxides are present and include the conversion to ortho- and para-quinones.<sup>68</sup> The resulting quinones are susceptible to nucleophilic attack by the hydrogen peroxide anion.

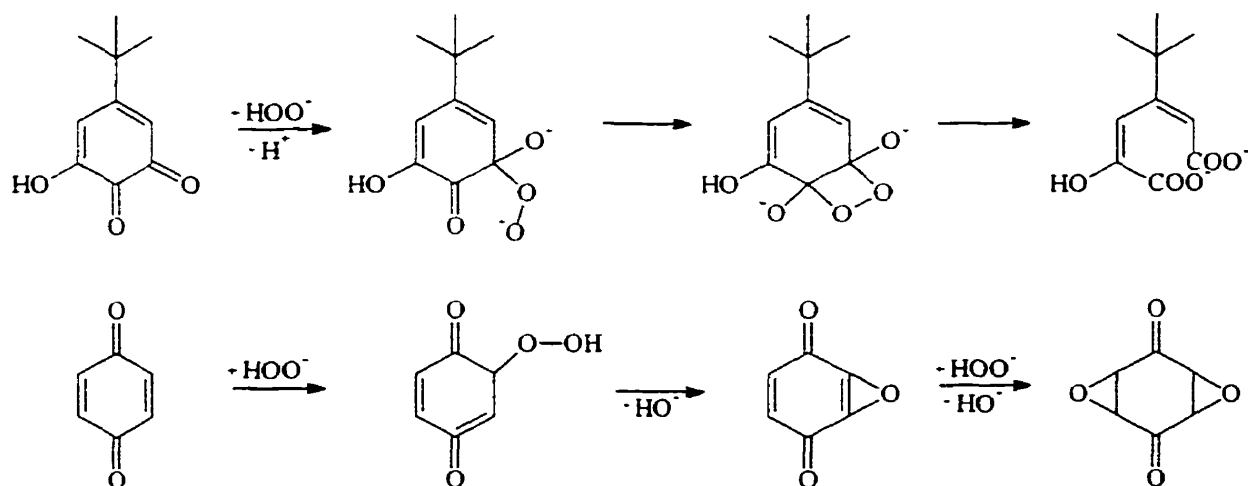


**Figure 1.6** Reactions of hydroperoxide intermediates to form muconic acids and ortho- and para-quinones.<sup>67,68</sup>

These reactions lead to the opening of the aromatic ring of the quinone and the formation of muconic acid and other acidic structures that ionise and impart solubility to the lignin. Thus hydrogen peroxide is present as a result of oxygen reduction and decomposition or hydrolysis of organic hydroperoxide intermediates.

Structures such as catechols, stilbenes and enol ethers are also known to be present in moderate amounts in kraft lignin. During oxygen delignification they are considered very reactive.<sup>1</sup> These structures show that additional phenolic hydroxyl groups and unsaturation on the side chain are both structural features that enhance reactivity. A methoxyl substituent in the aromatic ring also increases the reaction rate.<sup>69</sup> Alternatively a carbonyl group in the  $\alpha$ -position of the side chain decreases the reaction rate.<sup>69</sup>

### 1.2.3 Carbohydrates

Cellulose is the basis of many products like paper, films and fibres and is predominantly isolated from wood by large scale pulping processes. Cellulose is never found pure in nature, however, the cotton fibre is probably the purest natural source.<sup>70</sup> This is so because it seldom contains more than about 5% of other substances.<sup>6</sup> However, in wood cellulose is the main constituent but other substances such as lignin and hemicellulose are present. Approximately 40-45% of the dry substance in most wood

species is cellulose which is located primarily in the secondary cell wall.<sup>61</sup> The separation of cellulose from the other substances in wood requires intensive chemical treatment. The chemical formula for cellulose is  $(C_6H_{10}O_5)_n$ , where  $n$  is the number of repeating units, also known as the degree of polymerisation. The value of  $n$  varies with different sources of cellulose and the treatment to isolate the cellulose. Wood cellulose does not have a particularly high molecular weight and the highest molecular weight celluloses are generally obtained from non-woody sources such as flax and cotton.<sup>60</sup>

The chemical structure of cellulose is understood in detail, however, its supermolecular state including its crystalline and fibrillar structure is still not in agreement with all chemists.<sup>48</sup> Cellulose is a homopolysaccharide comprised of  $\beta$ -D-glucopyranose units which are linked together by (1 $\rightarrow$ 4)-glycosidic bonds.

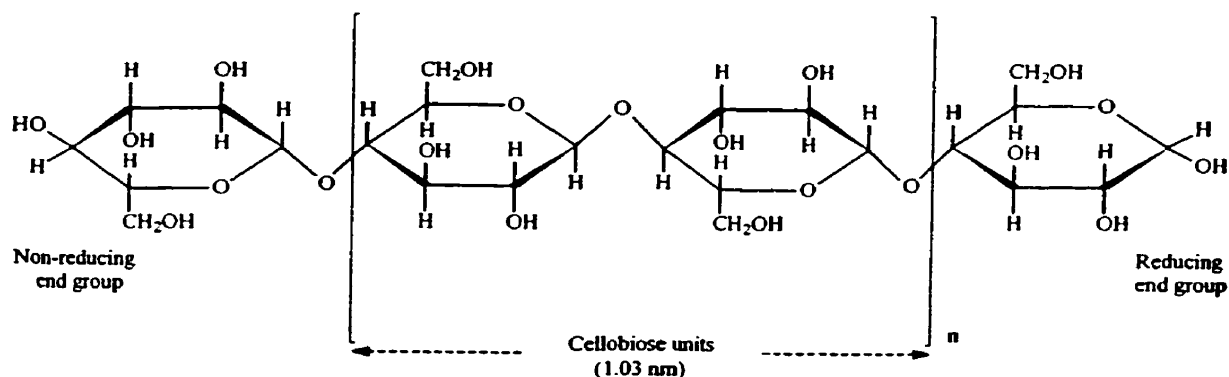


**Figure 1.7** Central part of the molecular chain of cellulose.<sup>61</sup>

Two adjacent glucose units are linked by the elimination of one molecule of water between their hydroxylic groups at carbon 1 and carbon 4. The crystallographic repeating unit of a cellulose chain is a cellobiose unit with a length of 1.03 nm.<sup>71</sup> Cellulose molecules are completely linear and have a strong tendency to form intramolecular and intermolecular hydrogen bonds.<sup>48</sup> Bundles of cellulose molecules are aggregated together to form microfibrils where highly ordered crystalline regions alternate with less ordered amorphous regions. Microfibrils build up fibrils and finally cellulose fibres.<sup>71</sup>

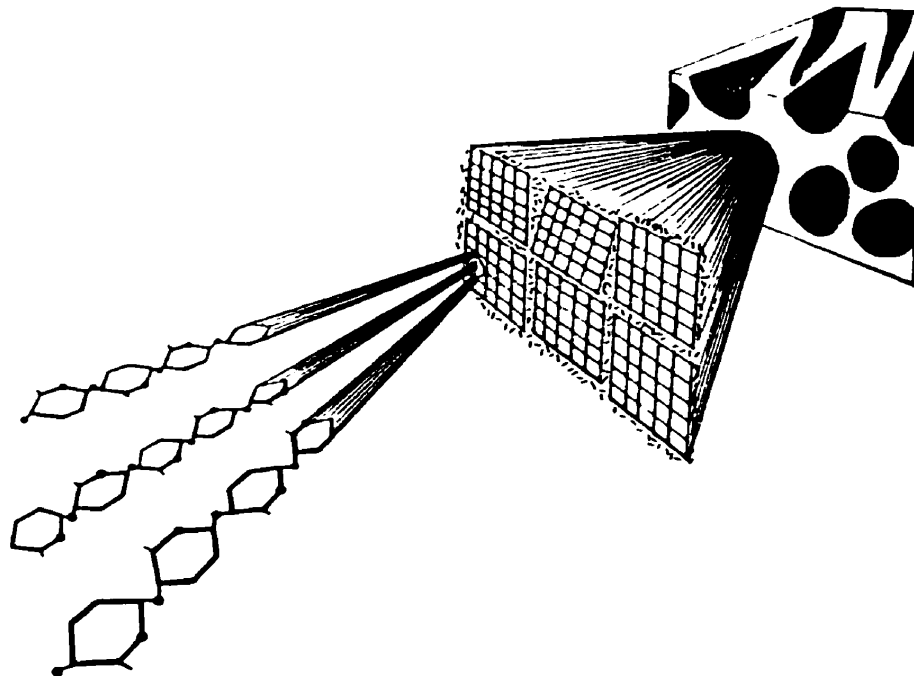


**Figure 1.8** Schematic illustration of the structural continuity from the cellulose molecule to the microfibril.<sup>71</sup>

As a consequence of its fibrous structure, paracrystalline nature and strong hydrogen bonds, cellulose has a high tensile strength and is insoluble in most solvents.<sup>72</sup>

Despite the presence of hydrogen bonds at both ends of the cellulose chain each OH-group displays different behaviour. The C1-OH is an aldehyde hydrate group deriving from the ring formation by an intramolecular hemiacetal linkage. This is why the OH-group at the C1 end has reducing properties, while the OH-group at the C4 end of the cellulose chain is an alcoholic hydroxyl and therefore non-reducing.

The cellulose chain is elongated and the glucose units are arranged in one plane. There are three reasons for this arrangement. The first one is the  $\beta$ -glycosidic linkage. Only the  $\beta$ -position of the hydroxylic group at C1 allows an elongation of the molecular chain.<sup>73</sup> An  $\alpha$ -OH and an  $\alpha$ -glycosidic linkage lead to a helical molecular chain as it occurs with amylose in starch. The second reason comes from the conformation of the pyranose ring. Bent hexagonal rings such as cyclohexane, pyran and pyranose may occur

in various conformations such as the well known chair and boat forms. The most stable form is the one lowest in energy which is the chair form. At normal temperatures bent hexagonal rings take the most stable form so that the glycopyranose units of the cellulose have the chair conformation.<sup>1</sup> The third reason is seen in connection with ring conformation. There can be two chair forms if OH-groups are considered. These hydroxylic groups may have a position above and below the ring (axial conformation) or in the plane of the ring (equatorial conformation). When the OH-groups are in the equatorial conformation the lowest energy is achieved and thus this is the most stable conformation.<sup>1</sup>

The stabilisation of long molecular chains in ordered systems, like that of the formation of supermolecular structures, originates in the presence of functional groups which are able to interact with each other. The functional groups of the cellulose chains are the hydroxyl groups, three of them being linked to each glucose unit. The surfaces of cellulose chains can thus be considered as being studded with OH-groups. These OH-groups are not only responsible for the supermolecular structure but also for the chemical and physical behaviour of the cellulose.

The OH-groups of cellulose molecules are able to form two types of hydrogen bonds depending on their site at the glucose units.

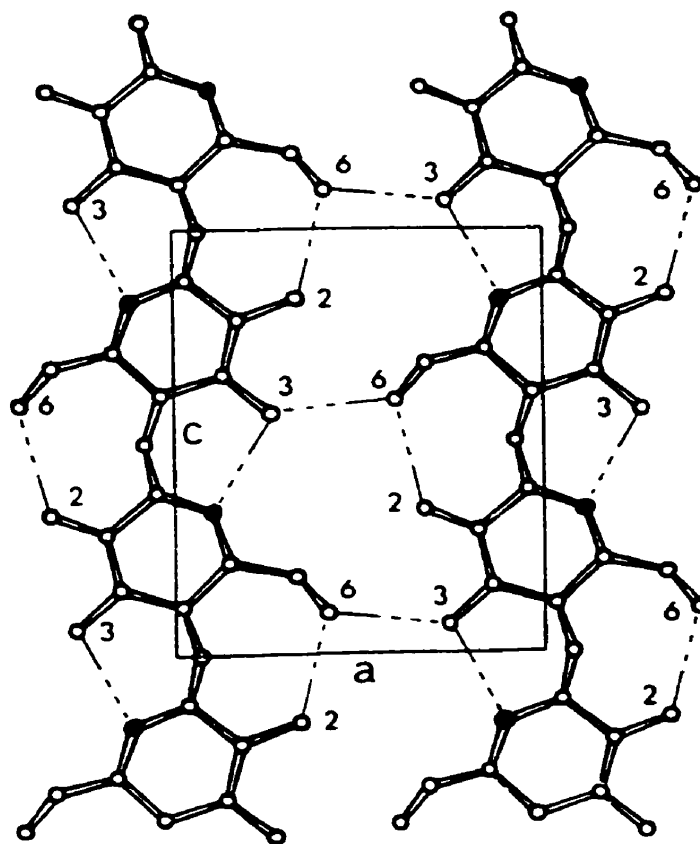


**Figure 1.9** Projection of the 020 plane in cellulose I showing the hydrogen bonding network and the numbering of the atoms.<sup>48</sup>

There are hydrogen bonds between OH-groups of adjacent glucose units in the same cellulose molecule which are known as intramolecular linkages. These linkages give a certain stiffness to a single cellulose chain.<sup>9</sup> There are also hydrogen bonds between OH-groups of adjacent cellulose molecules which are known as intermolecular linkages. These linkages are responsible for the formation of supermolecular structures.<sup>48</sup> The primary structures formed by hydrogen bonds are the fibrils which make up the wall layers and finally the whole cell wall. As well, the surfaces of isolated wood cells or fibres in the non-dried state are able to form hydrogen bonds with each other. The mechanical properties of a pulp or paper sheet are determined by fibre-fibre bonds which are the result of hydrogen bonds between fibre surfaces.<sup>74</sup>

### ***Carbohydrate Reactions***

Cellulose is highly susceptible to oxidising agents.<sup>75</sup> The extent of degradation depends on the nature of the reagent and on the conditions under which oxidation occurs. The hydroxyl and the terminal reducing ends are the sites most susceptible to attack.<sup>76</sup> Most oxidations are random processes wherein carbonyl and carboxyl groups are introduced at various positions in the anhydro-D-glucose units of cellulose. There are also a variety of secondary reactions that can occur including chain scission. Reactions that degrade cellulose can be divided into two categories. The first being random chain cleavage which may occur at any point along the chainlike molecule. The second is endwise "peeling" in which units on the end of the chain are attacked and successively removed. Although both reactions occur during oxygen delignification, random chain cleavage is sometimes believed to be more significant but this view is not shared by everyone and is a source of debate.<sup>77</sup> Degradation of cellulose and other wood polysaccharides during oxygen delignification is often accompanied by a loss in pulp yield and viscosity. The "peeling" reaction of carbohydrates is generally considered to be the most important source of yield loss in alkaline processes, however, during oxygen delignification the "peeling" reaction is of little significance.<sup>78</sup>

Traces of metals that are unavoidably present in unbleached pulps promote random chain cleavage.<sup>79</sup> Transition metals such as iron, manganese and copper, are particularly important in this respect. They catalyse the formation of reactive oxygen based radicals that randomly attack the cellulose chain and ultimately lead to the breakage of the chain at the point of attack. The associated decrease in the average length of the cellulose chains result in a decrease in pulp viscosity. If the reaction is allowed to proceed far enough, a decrease in pulp strength is evident.

The extensive degradation of cellulose during oxygen delignification appears to be due to oxygen initiated free radical chain reactions whose rates are strongly influenced by the existence of hydrogen peroxide and transition metal ions.<sup>80</sup> These factors in turn are dependent upon the existence of hydrogen peroxide precursors in pulp which interact with oxygen and alkali to yield the harmful peroxide by-products. These precursors can include very reactive functional groups such as carbonyl groups common to both lignin

and cellulose. Less reactive groups such as alcohols are dominant in the cellulosic component of pulp. These groups interact with oxygen to form hydrogen peroxide and additional hydrogen peroxide precursors. Thus complete elimination of cellulose degradation during oxygen delignification seems to be impossible.<sup>81</sup>

It is generally accepted that non-reducing end groups and non-terminal glucose residues of cellulose are quite stable towards oxygen under delignifying conditions although reducing end groups are easily oxidised by oxygen.<sup>41</sup> Two mechanisms for carbohydrate attack predominate. The first deals with reactions between lignin and oxygen to produce active oxygen species which in turn degrade carbohydrates. The oxygen species that are involved are seen in Figure 1.1. The role of transition metal ions is to accelerate the formation of active oxygen species.<sup>82</sup> Another mechanism proposed for the degradation of non-terminal glucose residues is an auto-oxidation type mechanism.<sup>83,84</sup> In this mechanism a reaction, probably a direct reaction between non-terminal glucose residues and oxygen, is assumed to play a role as an initiator of a chain reaction by the production of active species such as organic peroxy radicals or peroxides.<sup>85</sup>

The initial step in the chain cleavage process involves oxidation of a hydroxyl group to a carbonyl group.

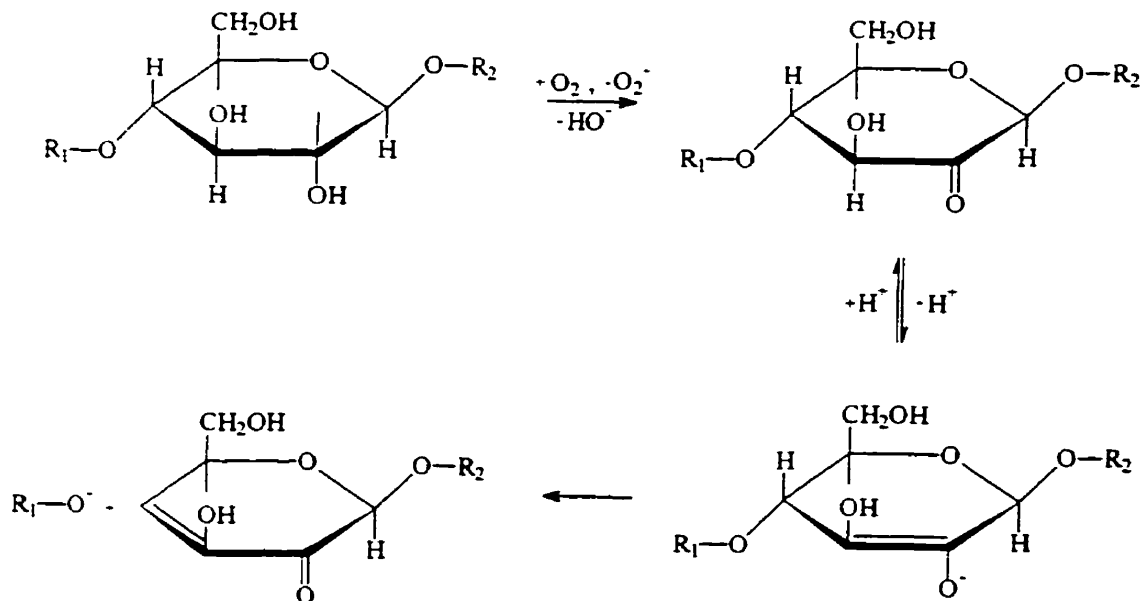


**Figure 1.10** Oxidation and cleavage of the cellulose chain.<sup>78</sup>



The ionised enol form of the resulting carbonyl containing unit then undergoes a beta elimination reaction that breaks the glucosidic linkage joining the affected unit to the rest of the cellulosic chain. The initially formed carbonyl containing unit does not necessarily have to react as described above to break the cellulosic chain. A competing reaction occurs when oxygen attacks its ionised keto form resulting in a cyclic carboxylic acid or an open chain structure containing two carboxylic acid groups.<sup>86</sup>

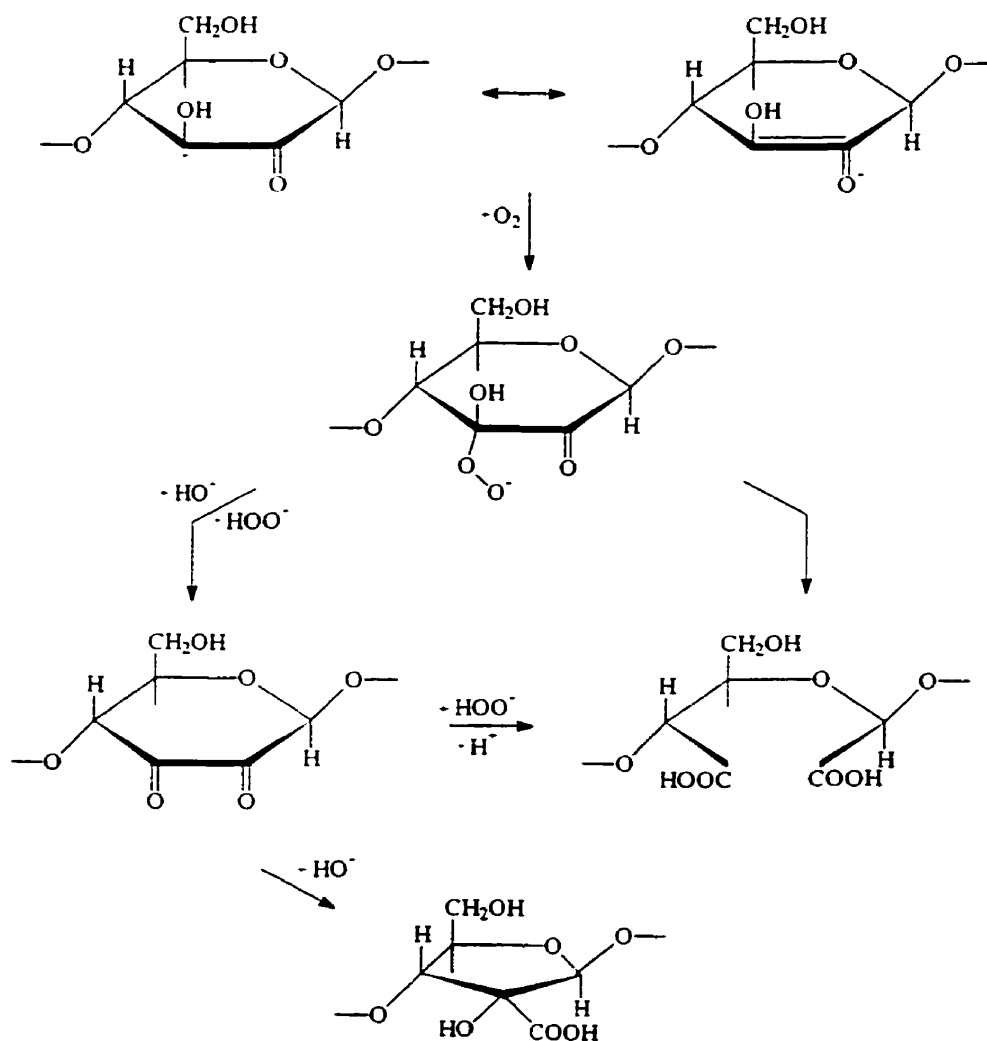


**Figure 1.11** Carbohydrate reactions which do not produce chain cleavage.<sup>78</sup>

In both cases, the cellulosic chain is not broken. The reaction that causes yield loss in alkaline media known as the "peeling" reaction, is usually of less importance in oxygen delignification than random chain cleavage. For an end unit to be susceptible to removal by the "peeling" reaction it must contain a carbonyl group. Due to the fact that the reaction leaves behind a new end unit containing a carbonyl group that is yet another reducing end group, the process is self-propagating. This can in principle continue until all the cellulose is dissolved however it is prevented by a "stopping" reaction that converts the end unit to one that does not contain a carbonyl group.<sup>87</sup> "Peeling" on the other hand, can become important if random chain cleavage is excessive because every chain breakage creates two new chain ends, one of which is a reducing end group.

#### **1.2.4 Hemicellulose**

Hemicelluloses were originally believed to be intermediates in the biosynthesis of cellulose.<sup>6</sup> Today it is known that hemicelluloses belong to a group of heterogeneous polysaccharides which are formed through biosynthetic routes different than that of cellulose.<sup>60</sup> Although considerably less abundant than cellulose, the hemicellulose contribute significantly to the chemical and physical properties of the fibres.<sup>88</sup> The presence of hemicellulose in pulp after treatment to remove lignin is unequivocal.<sup>89</sup> Resistance of the hemicellulose components to removal are probably caused by the existence of some chemical linkages between high molecular weight fractions of cellulose and the hemicellulose. The idea that some chemical linkages are likely to be present between cellulose and the residual hemicellulose in pulp may cause a strong resistance to oxygen delignification.<sup>90</sup>

In contrast to cellulose which is a homopolysaccharide, hemicelluloses are heteropolysaccharides. Like cellulose most hemicelluloses function as supporting material in the cell walls. Hemicelluloses differ from cellulose by: a composition of various sugar units, a much shorter molecular chains, and a branching of molecules which mostly have a degree of polymerisation of 200.<sup>61</sup> The sugar units making up the hemicellulose can be subdivided into groups such as pentoses, hexoses, hexuronic acids and deoxy-hexoses.

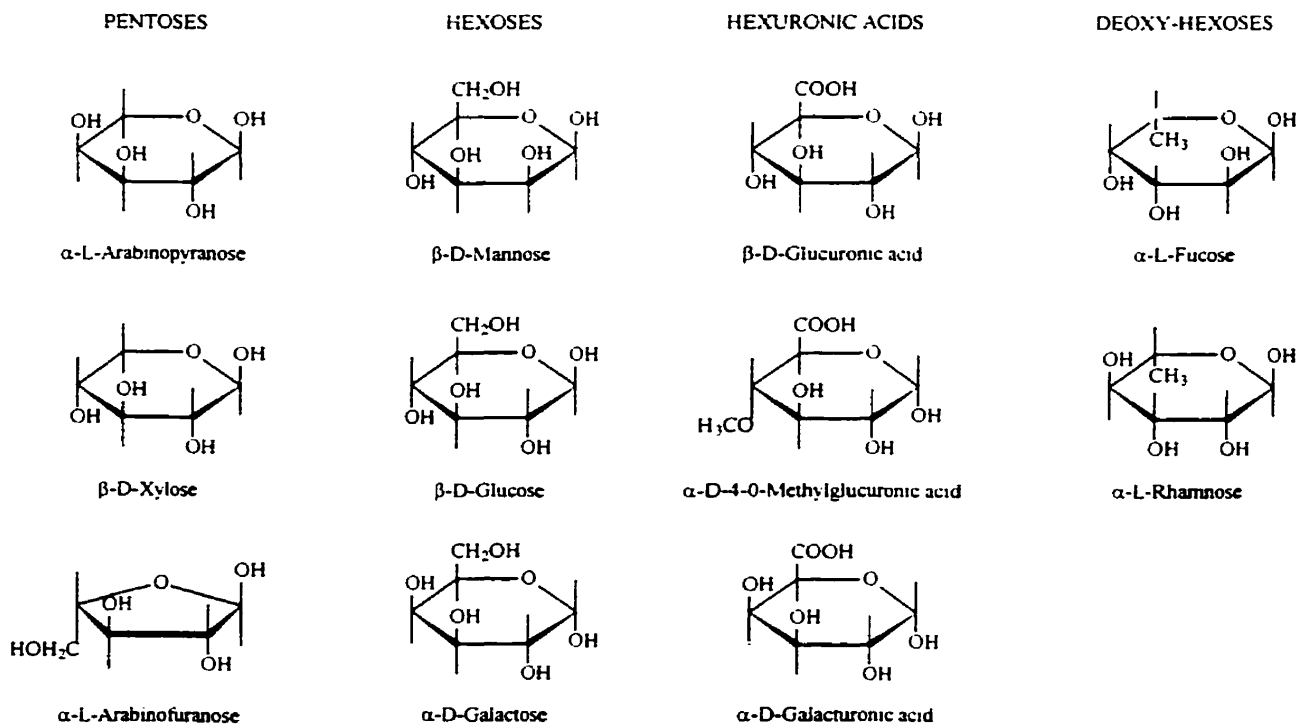


**Figure 1.12** Formulas of the sugar components for hemicellulose.<sup>61</sup>

The main chain of hemicellulose can consist of one unit to create a homopolymer like in xylans, or two or more units to create a heteropolymer like in glucomannans. Some of the units are always or sometimes side groups of a main chain. Most hemicelluloses are relatively easily hydrolysed by acids to their monomeric components consisting of D-glucose, D-mannose, D-galactose, D-xylose, L-arabinose and small amounts of L-rhamnose in addition to D-glucuronic acid, 4-O-methyl-D-glucuronic acid and D-galacturonic acid.

Softwoods and hardwoods differ not only in the percentages of hemicellulose but also in the percentages of the individual hemicelluloses and composition of these hemicelluloses.<sup>1</sup> If only the non-glucosidic sugar units in wood are considered, softwoods have a higher percentage of mannose units and more galactose units than hardwoods. Hardwoods on the other hand have a higher proportion of xylose units and more acetyl groups than softwoods. The amount of hemicellulose of the wood dry weight is usually between 20-30%.<sup>61</sup> The composition and structure of the hemicelluloses in

softwoods differ from those in hardwoods. Considerable differences also exist in the hemicellulose content and composition between the stem, branches, roots and bark.<sup>48</sup> The main types of hemicelluloses found in softwood are galactoglucomannans, arabinoglucuronoxylan and arabinogalactan. Beside these types of hemicelluloses, softwoods also contain other polysaccharides present in very small amounts that include starch (composed of amylose and amylopectin) and pectic substances. The predominant types of hemicelluloses found in hardwoods are glucuronoxylan and glucomannan. A brief description of the types of hemicelluloses found in softwoods follows.

### ***Galactoglucomannans***

Galactoglucomannans are the principal hemicelluloses in softwoods at about 20%.<sup>48</sup> Their backbone is a linear or sometimes slightly branched chain built up of (1→4)-linked β-D-glucopyranose and β-D-mannopyranose units.

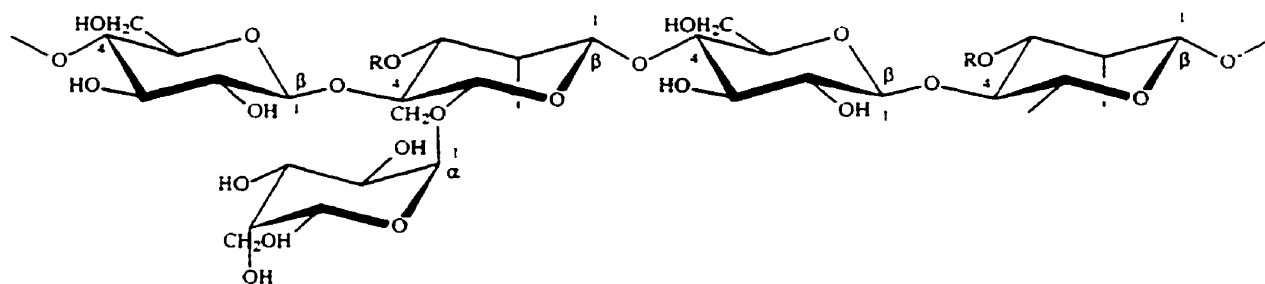


**Figure 1.13** Principal structure of galactoglucomannan.<sup>48</sup>

Galactoglucomannans can be divided into two fractions having different galactose contents. In the fraction which has a low galactose content the ratio of galactose to glucose to mannose is about 0.1 : 1 : 4.<sup>91</sup> In the galactose rich fraction the corresponding ratio is 1 : 1 : 3.<sup>91</sup> The low galactose content fraction is often referred to as glucomannan. The α-D-galactopyranose residue is linked as a single unit side chain to the framework by (1→6) bonds. An important structural feature is that the hydroxyl groups at C2 and C3 positions in the chain units are partially substituted by O-acetyl groups at every 3 – 4 units. Galactoglucomannans are easily depolymerised by acids especially between galactose and the main chain.

### *Arabinoglucuronoxylan*

Arabinoglucuronoxylan makes up for about 5-10% of the hemicellulose in softwoods.<sup>48</sup> It is composed of a framework containing (1→4)-linked β-D-xylopyranose units which are partially substituted at C2 by 4-O-methyl-α-D-glucuronic acid groups, about every two residue units per ten xylose units. In addition the framework also contains α-L-arabinofuranose units on average 1.3 residue units per ten xylose units.

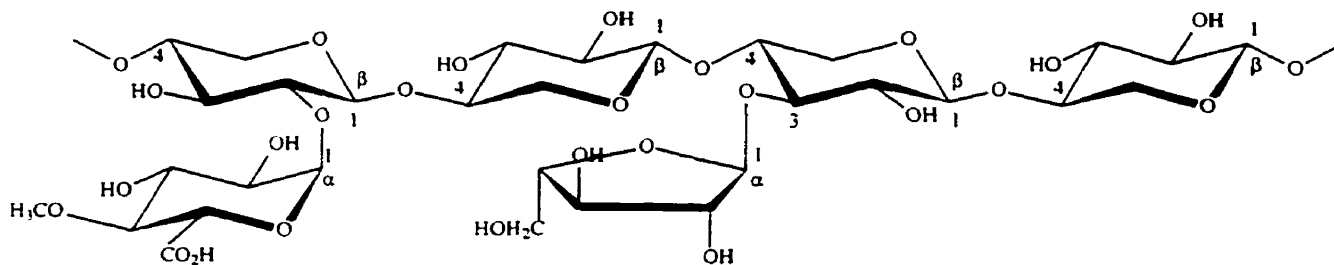


**Figure 1.14** Principal structure of arabinoglucuronoxylan.<sup>48</sup>

Because arabinoglucuronoxylan has a furanosidic structure, the arabinose side chains are easily hydrolysed by acids. Both the arabinose and uronic acid substituents stabilise the xylan chain against alkali catalysed degradation.

### *Arabinogalactan*

Arabinogalactan is only a minor constituent in softwood.<sup>48</sup> Its backbone is built up by (1→3)-linked β-D-galactopyranose units. Almost every unit carries a branch attached to position 6 that are (1→6)-linked β-D-galactopyranose residues. There are also a few glucuronic acid residues present in the molecule. The highly branched structure is responsible for the low viscosity and high solubility in water.

### **1.3 Methods of Crystallinity Determination**

There are a number of different techniques that have been proposed in the literature for the determination of the relative degree of crystallinity in pulps and cellulosic materials. Of these methods the most common are water retention value, near infrared, x-ray diffraction, FTIR and solid state NMR. The latter three are most widely used. A brief description of each method follows.

### **1.3.1 Water Retention Value (WRV)**

The method of water retention was first proposed and used by Ferrus and Pages.<sup>92</sup> Due to the hydrogen bonding that occurs in cellulosic material, water can be taken up into the fibres of the cellulose. The amount of water depends on the humidity of the sample's environment and on the nature of the packing of the fibres themselves.<sup>93</sup> A more highly packed and ordered sample absorbs less water than a less packed and ordered sample of cellulose.

In this method a calibration curve must first be constructed from cellulose samples that have a known water retention value. The calibration curve is determined in conjunction with another technique that is used for crystallinity determination to get relative values for comparison. The technique that Ferrus and Pages chose to compare their results with was infrared spectroscopy (IR). They chose this method because the water retention value shows a better correlation with the accessibility measurements from IR than from x-ray diffraction.

In their procedure 0.2 grams of the sample is soaked in distilled water for 15 hours. The sample was then removed and slightly squeezed with their fingers. The sample was then placed in a centrifuge and spun for 10 minutes at 5200 rpm after which time the sample weight was recorded. The sample was then dried in an oven at 105 °C and weighed again after allowing time for cooling in a dessicator. The water retention value is taken as a percentage of water on a dry weight basis and is compared to the calibration curve to determine the relative degree of crystallinity.

The inherent disadvantage of this method is that it relies on another method for its precise value in the construction of the calibration curve. Furthermore, it is very time consuming.

### **1.3.2 Near Infrared (NIR)**

The near infrared region is between 4 000  $\text{cm}^{-1}$  and 10 000  $\text{cm}^{-1}$ . This method is able to distinguish intermolecular hydrogen bonding and crystal lattice forces since both C-O and O-H stretching as well as their deformations are dominant in the near infrared region. The method was used by Basch *et al.* in 1974 as a new method for obtaining crystallinity ratios of cellulose.<sup>94</sup>

In this procedure the sample is wiley milled to an 80 mesh and then dried at 105 °C. The sample is then conditioned by allowing it to equilibrate for 48 hours in a desiccator with distilled water. A potassium bromide pellet is then made using 10 mg of sample and 260 mg of potassium bromide. In making this pellet, 15 tons of pressure are applied for 5 minutes. The sample is then placed in a spectrophotometer and flushed with nitrogen before running the test to eliminate the effects of oxygen and carbon dioxide present in the air.

Calculation of the relative degree of crystallinity is determined by the following method. A straight line is drawn from 5300  $\text{cm}^{-1}$  to 4500  $\text{cm}^{-1}$ . The peaks of interest are at 4760  $\text{cm}^{-1}$  and 5190  $\text{cm}^{-1}$ . The peak at 4760  $\text{cm}^{-1}$  varies directly with crystallinity while the peak at 5190  $\text{cm}^{-1}$  varies inversely with crystallinity. Thus the relative degree of crystallinity by near infrared is calculated by the NIR ratio.

$$\text{NIRRatio} = \frac{\text{Absorbance}(4760 \text{ cm}^{-1})}{\text{Absorbance}(4760 \text{ cm}^{-1} + 5190 \text{ cm}^{-1})} \quad (1.1)$$

The disadvantage of this method is that the instrumentation for obtaining the measurements cannot be as commonly found in laboratories today than the instrumentation needed for some of the other methods. This procedure can be quite time consuming in comparison to some of the other methods available.

### **1.3.3 X-ray Diffraction**

#### ***Fundamentals of the Technique***

X-rays like ordinary light follow the laws of reflection and refraction. The main difference is in their high penetration power. Reflection does not occur only at the outer surface of a crystal but can occur hundreds of molecular layers within a crystal.<sup>72</sup> Bragg, who was a pioneer in x-ray crystallography developed the following simple concept and laws governing the reflection of x-rays by crystals.<sup>91</sup>

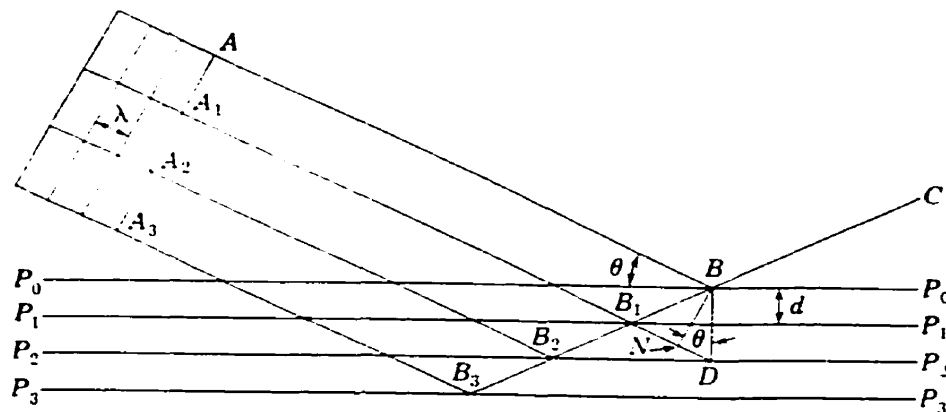


**Figure 1.15** Diagrammatic sketch of reflection of x-rays.<sup>91</sup>

The figure above represents four parallel atomic planes of a large perfect crystal that are spaced at equal distances,  $d$ .  $AB$ ,  $A_1B_1$ ,  $A_2B_2$  and  $A_3B_3$  represent rays of a beam of monochromatic x-rays having the wavelength  $\lambda$ , that strike the surface at an angle  $\theta$ . Only a small portion of the rays that strike the surface are reflected. Most of them penetrate the crystal and reflect at atomic planes further into the structure. When the rays are reflected, the angle of reflection is equal to the angle of incidence.

All beams reflected along  $B_3O$  from the different structural planes reinforce each other. Even though the amount of each reflection alone is hardly enough to detect, when it is reinforced a hundred or more times, it becomes readily measurable on a photographic plate or with an ionisation spectrometer. The angle of incidence ( $\theta$ ) of the x-ray beam on the crystal (at which reinforcement of the beam causes an increase in ionisation in the spectrometer) is related to the wavelength of the x-rays,  $\lambda$ , and the interplanar distance,  $d$ , by the following equation:

$$\lambda = 2d \sin \theta \quad (1.2)$$

Knowing the wavelength of the monochromatic beam of x-rays it is possible to calculate the interplanar distance, or when the interplanar distance is known, the wavelength of x-rays can be calculated. The wavelength most suitable for the study of the structure of crystals is from  $0.71 - 1.54 \text{ \AA}$ , which is the range of normal atomic



spacing in crystals.<sup>95</sup> X-rays with a wavelength of 1.54 Å can be generated with a copper target irradiated by electrons wire under high potential.<sup>96</sup> This wavelength is preferred for the study of organic crystals containing lighter atoms in which the atomic layer spacing may be as great as 10 Å.

X-rays are generated in cathode ray tubes when high energy electrons hit a metal target. When x-rays are focused on a sample, two types of scattering occur. If the sample is crystalline, the x-rays are scattered coherently.<sup>97</sup> This means that there is no change in wavelength or phase between the incident and scattering rays. This type of scattering is commonly referred to as x-ray diffraction. If the sample has a non-homogeneous morphology, such as that in the amorphous regions of cellulose, the scattering is incoherent. This means that there is a change in only the phase. Incoherent scattering is referred to as diffuse diffraction.<sup>97</sup> Coherent scattering is determined by wide angle measurements and incorporate scattering by small angle measurements. A wide angle diffraction pattern consists of a series of peaks arising from scattering by the crystal planes and is superimposed on a diffuse background of incoherent scattering. As the relative degree of crystallinity increases, the peaks become sharper and more well defined.

#### ***Lignin, Hemicellulose and Cellulose Considerations***

Lignin is not a regularly repeating molecule but is made up of units irregularly attached together.<sup>60</sup> For this reason it is impossible to obtain a x-ray diffraction pattern from lignin. Hemicellulose on the other hand can be considered to be made up of a somewhat regularly repeating pattern, however, due to the small amount that is present in pulp and the varying types of hemicelluloses that are present, obtaining a good x-ray pattern from pulp is highly improbable.<sup>48</sup>

In the solid state the hydrogen bonds between cellulose molecules are not arranged randomly, but a regular system of the hydrogen bonds results in the formation of an ordered system with crystal like properties. These properties were first detected by Nishikawa and Ono in 1913 using x-ray diffraction.<sup>61</sup> Further studies using this model were carried out by several scientists and led to the Meyer and Misch model in 1937 for the crystalline unit of cellulose.<sup>98</sup> Features of this model can still be applied today. There are various polymorphs of cellulose and native cellulose is termed cellulose I because of

its crystalline lattice.<sup>99,100</sup> This lattice as evaluated by x-ray diffraction is monoclinic,<sup>101</sup> in that it has three axes of different lengths and one non-90° angle. Furthermore, only the corners and centre of the crystalline unit cell are occupied and the latter is translated by  $\frac{1}{2}$  a glucose molecule.

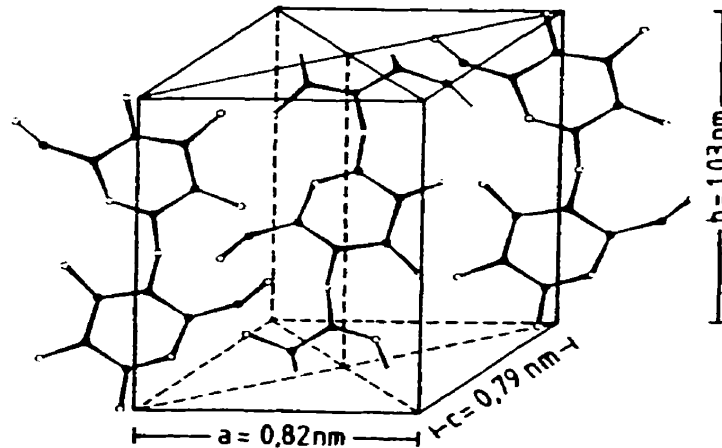


**Figure 1.16** Monoclinic unit cell of cellulose I.<sup>61</sup>

The figure above shows the central chain of the space unit runs counter to the chains arranged at the corners. As each chain forms a corner of the crystal unit every second cellulose chain is reversed. It can then be said that the cellulose lattice consists of counter running chain pairs. These chains are staggered by a distance of  $\frac{1}{4}$  along the b-axis (as can be seen from figure 1.16).

In recent years doubts have arisen as to whether cellulose chains are in fact counter running. Models have been proposed in which the cellulose chains of the adjacent 002 planes are arranged in the same direction. The main crystal planes for the cellulose space unit are shown below. These peaks are represented by peaks of different intensities in the x-ray diagrams.

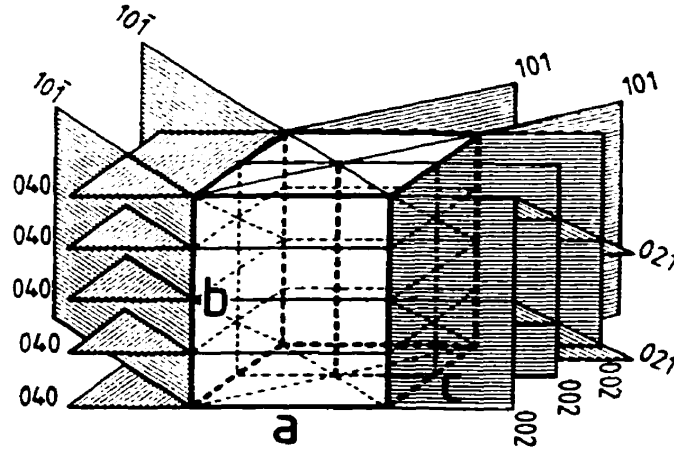


**Figure 1.17** Lattice planes of the space unit of cellulose I.<sup>61</sup>

According to Gardner and Blackwell there is closer agreement with the diffraction intensity data if parallel cellulose chains are assumed.<sup>102</sup> From the standpoint of sterical extension and the space requirement of the cellulose molecules an anti-parallel arrangement in the unit cell is possible. This arrangement allows hydrogen bonding within the 002 planes as well as between adjacent 002 planes.

***Obtaining Measurements with X-ray Diffraction***

X-ray diffraction measures the fraction of molecules that are arranged in a regularly repeating pattern.<sup>61</sup> As the crystallites get smaller the crystalline peaks get broader and the amorphous background increases. X-ray diffraction can also give information on the size of the crystallite by measuring the half height width of the crystalline peak.<sup>103</sup> The term crystallite is used to mean a crystalline domain within a microfibril. Only material within crystallites appears crystalline and so the size of the crystallite is important. The larger the crystallite the higher the relative degree of crystallinity. Conversely, the smaller the crystallite the lower the relative degree of crystallinity. Crystallites tend to be relatively larger in algae cellulose than in wood celluloses and so the relative degree of crystallinity tends to be higher.<sup>97</sup> In general cellulose crystallinities tend to be lower for hardwoods than for softwoods.<sup>104</sup>

The disadvantage of x-ray diffraction is that it gives relatively higher results compared to other methods. Material on the surface of the crystallite have a greater mobility and a lower degree of order. Material on the interior of the crystallite have a lower mobility and a higher degree of order. X-ray diffraction measures both of the above as being crystalline. Thus small defects within the crystalline region is included within the crystalline fraction. This happens because the crystalline regions are too small to distinguish them from regions of disorder.

By looking at an x-ray diffraction pattern or diffractogram, the peaks deriving from the various lattice planes are based not on the zero line but on a certain background which has to be attributed to a non-crystalline or amorphous portion in cellulose. The term amorphous is sometimes used loosely. The more correct term to use is non-crystalline since it refers to all matter excluding the crystalline portion. This includes amorphous cellulose and hemicellulose. The term amorphous is used in this thesis to mean non-crystalline material. The amorphous background varies in its intensity depending on the origin of the cellulose. The relative degree of crystallinity which represents the crystalline portion in a cellulose sample is calculated by subtraction of the background of the curve from either the height of the most resolved and intense peak (ie. the 002 peak in cellulose) or the integral area.

### **1.3.4 Fourier Transform Infrared (FTIR) Spectroscopy**

#### ***Fundamentals of the Technique***

Emission or absorption spectra arise when molecules undergo transitions between quantum states corresponding to two different internal energies.<sup>105</sup> The energy difference between the states is related to the frequency of the radiation emitted or absorbed by the quantum relation  $\Delta E = h\nu$  where  $\Delta E$  represents the change in the energy,  $h$  represents Planks constant and  $\nu$  represents the frequency. Infrared frequencies in the wavelength range of  $10,000 - 200 \text{ cm}^{-1}$  are associated with molecular vibration and vibration-rotation spectra. FTIR spectroscopy looks at these variations and rotations in the infrared region, between  $4,000 \text{ cm}^{-1}$  to  $400 \text{ cm}^{-1}$ . Infrared spectroscopy has been used to study the conformation of cellulose.<sup>106</sup> The early work on infrared showed spectral differences between the celluloses from algae and bacteria and from cotton and ramie. Polarised

infrared studies identified the orientation of hydrogen bonds within the crystalline regions. Early work also established the differences between native cellulose and other polymorphs. Infrared determination of crystallinity has been used by many scientists.<sup>107</sup>

There are two instrumental variations in infrared spectroscopy. The older dispersive method uses prisms or gratings to disperse the infrared radiation.<sup>72</sup> The newer method of Fourier transform infrared (FTIR) spectroscopy uses the principle of interferometry.<sup>72</sup> The disadvantage of dispersive infrared spectroscopy is its low sensitivity. Since a substantial amount of the incident energy reaches the detector, the technique is limited to only sampling. This has now been overcome by the combined application of interferometry and Fourier transform techniques with digital computers. Good quality infrared spectra can now be obtained from almost any type of sample by a variety of techniques. Other advantages of Fourier transform infrared spectroscopy is the ability for spectra to be developed rapidly. The instrument can have a dedicated computer and store and manipulate spectra.

FTIR spectroscopy is one of the most widely used methods for identifying chemical compounds and studying their changes in various chemical reactions. The observed bands from the test are derived from functional groups in the molecules and information about both the type and quantity of the groups is provided. FTIR spectroscopy offers greater versatility to structural studies because spectra can be scanned, recorded and transformed in a matter of seconds. Thus the technique can facilitate studies of reactions such as degradation.

Intensities of certain infrared bands have been found to be sensitive to variations in crystallinity.<sup>108</sup> An absorbed band that is affected by crystallinity is compared to a band that is relatively insensitive to changes in crystallinity. The technique is advantageous because it requires only a small amount of sample. The challenge of this technique is standardising the operating conditions to obtain reproducibility.

#### ***Obtaining Measurements with FTIR Spectroscopy***

FTIR spectroscopy is a relatively simple and fast method for determining cellulose crystallinity. The intensities of certain bands in infrared spectra have been found to be sensitive to variations in crystallinity.<sup>108</sup> The infrared absorption spectra of the same

sample of cellulose in the crystalline and amorphous states can differ for at least two reasons. First, specific intermolecular interactions may exist in the crystalline cellulose which lead to sharpening or splitting of certain bands.<sup>109</sup> Second, some specific conformations may exist in one but not the other phase, leading to bands which are characteristically exclusive of either crystalline or amorphous material.<sup>109</sup>

Usually an absorbance band affected by cellulose crystallinity is compared to a band that is relatively insensitive to changes in crystallinity. This work was first reported by O'Connor *et al.* in 1958.<sup>106</sup> They defined a crystalline band as one that decreases in intensity progressively with an increase in temperature and then disappears when the polymer becomes molten. They defined an amorphous band as one that does not appear in the spectra of a crystalline polymer but becomes more intense with increasing amorphous character. To determine the crystallinity (also known as the crystallinity index) the ratio of absorbance at 1429  $\text{cm}^{-1}$  to absorbance at 893  $\text{cm}^{-1}$ . The peak at 1429  $\text{cm}^{-1}$  is a  $\text{CH}_2$  symmetric bending (or a  $\text{CH}_2$  scissoring).<sup>110</sup> The peak at 893  $\text{cm}^{-1}$  is an antisymmetric out of phase stretching (or a C1 group vibration).<sup>110</sup> The relative degree of crystallinity is calculated by dividing the peak absorbance value at 1429  $\text{cm}^{-1}$  into the sum of the peak values at 1429  $\text{cm}^{-1}$  and 893  $\text{cm}^{-1}$ . A ratio of 1372  $\text{cm}^{-1}$  to 2900  $\text{cm}^{-1}$  can also be used to estimate the crystallinity of cellulose I and cellulose II.<sup>111</sup> A more complicated method is also used in which the combined areas of the 1370  $\text{cm}^{-1}$ , 1335  $\text{cm}^{-1}$  and 1315  $\text{cm}^{-1}$  peaks are compared to the 670  $\text{cm}^{-1}$  peak.<sup>112</sup>

Although the infrared technique is convenient and requires only a small amount of sample, it requires careful standardisation of the operating conditions for reproducibility purposes. In any case, such determinations give only relative crystallinities because there is neither a 100% crystalline standard nor a 100% amorphous cellulose for crystallinity determinations.

### **1.3.5 CP/MAS Solid State Nuclear Magnetic Resonance Spectroscopy**

#### ***Fundamentals of the Technique***

<sup>13</sup>C nuclear magnetic resonance (NMR) spectra can be obtained on solid materials with a resolution comparable to or approaching that of solution NMR for some materials.<sup>113</sup> Obtaining significant results in these tests depend upon the physical nature

of the system and the application of several techniques known as magic angle spinning,<sup>114</sup> cross polarisation<sup>115</sup> and high power decoupling.

In a  $^{13}\text{C}$  solution spectrum of a molecule, absorptions at a particular field frequency value are characteristic of the environment or magnetic shielding of the carbons in the molecule.<sup>116</sup> The chemical shifts recorded are the isotropic values from the averaging of all possible orientations of the nucleus to the magnetic field by the random motion of the molecules. In a solid crystalline powder material, all orientations are possible and the signals from each orientation overlaps the other. This is known as a shift anisotropy pattern and may be averaged with its isotropic value by spinning the sample about an axis at a magic angle of  $\theta=54.74^\circ$ . This happens because the anisotropy is modified by the term  $(3\cos^2 \theta - 1)$ , where  $\theta$  is the angle between the spinning axis and the magnetic field vector. When  $\theta = 54.74^\circ$  the term  $(3\cos^2 \theta - 1)$  is reduced to zero. This gives rise to the single isotropic shift value which is the same net result for the random motion of the molecule.

Another advantageous refinement applied in solid-state NMR studies is the technique of cross polarisation. This technique increases the signal to noise ratio of the dilute  $^{13}\text{C}$  nucleus being observed.<sup>117</sup> In the case of a dilute system like the  $^{13}\text{C}$  nuclei, the maximum increase in signal to noise ratio is approximately fourfold. The repeat time of the experiment depends only on the proton spin-lattice relaxation time which are much shorter than the carbon values. A much more efficient experimental technique results.

In an abundant spin system, for example the case of protons, the  $^1\text{H}$ - $^1\text{H}$  dipolar interactions completely dominate the spectrum and other interactions such as spin-spin coupling and chemical shifts are negligible.<sup>118</sup> It is possible to reduce the dipolar interactions by pulse techniques, however, in practice they are so large and the chemical shift range of protons so small that it is not possible to obtain analytically useful information from the spectra of this nucleus.<sup>119</sup> In a dilute system like  $^{13}\text{C}$  this is not the case. Although there are more interactions and the  $^1\text{H}$ - $^{13}\text{C}$  dipolar interactions are still substantial, it is possible to obtain high resolution spectra. The  $^1\text{H}$ - $^{13}\text{C}$  interactions are between different nuclei and may be decoupled using very high power decoupling fields at the proton resonance frequency. Also because of the low natural abundance of the  $^{13}\text{C}$  nuclei (around 1.1 %), the  $^{13}\text{C}$ - $^{13}\text{C}$  dipole-dipole interactions are negligible.<sup>118</sup>

### ***Proton Spin Relaxation Time ( $T_{1H}$ )***

There has been quite an interest in the past two decades to study NMR relaxation parameters.<sup>120</sup> This interest has sparked mainly due to the fact that it is easy to measure NMR relaxation parameters using a Fourier transform NMR spectrometer. It is important that in using this type of spectrometer of these parameters are well understood. Spectroscopists have been able to use these parameters to provide critical information that includes molecular rotational and angular momentum correlation times, translational diffusion constants, and inter- and intramolecular exchange rates.<sup>121</sup> There is also a dependence of some relaxation parameters on bond lengths, allowing these parameters to probe molecular mobility. Two of the most common relaxation times measured are the spin-lattice relaxation time  $T_1$ , and the spin-spin relaxation time  $T_2$ . The spin-lattice relaxation time is a longitudinal measurement and represents the amount of time required for energy to pass from the spin system to other degrees of freedom.<sup>122</sup> The spin-spin relaxation time is a transverse measurement and takes into account thermal equilibrium.<sup>122</sup> The advantage of these relaxation times is in obtaining information at a molecular level to analyse molecular motion.

Spin relaxation times calculated for pulps can be influenced by many parameters such as water content within the sample,<sup>123</sup> paramagnetic metals,<sup>121</sup> pH,<sup>124</sup> magnetic field<sup>125</sup> and temperature.<sup>125</sup> Each of these factors either increases or decreases the relaxation times. Careful effort must be taken to control these factors so that accurate measurements are attained.

The presence of water is known to plasticise wood. This plasticisation increases the mobility of the wood and so reduces the cross polarisation efficiency at room temperature.<sup>126</sup>  $T_{1H}$  values tend to be longer for dry woods,<sup>127</sup> however, some water is needed to enhance the signal to noise ratio to improve the spectra's resolution.<sup>123</sup> The presence of paramagnetic impurities such as iron (Fe), copper (Cu) and manganese (Mn) also affects the magnitude of the  $T_{1H}$  values.<sup>128</sup> Interaction of unpaired spins in paramagnetic impurities can cause fluctuations in magnetic intensity of the protons in the pulp components. A fluctuation of magnetic intensity at a nucleus can cause spin transition if its components are of suitable frequency. Since the magnetic moment of an



electron is about 650 times that of the nucleus. even small traces of paramagnetic impurities in a sample can drastically reduce the measured relaxation times. Care must be taken to treat the sample to reduce or eliminate the contribution of paramagnetic impurities.<sup>124</sup> In a comparative study, it is best to obtain the relaxation times in the same spectrometer to reduce the influence of the magnetic field. Measurements should be taken at room temperature because elevated temperature is not favourable.

### ***Obtaining Measurements with Solid State NMR Spectroscopy***

NMR measurements offer a relatively new approach to the study of chain conformation within crystalline regions. From splitting of the peak at C1, it is apparent that as many as four environments exist for that atom within an apparently homogeneous crystalline cellulose. Similar discrepancies exist for C6. The NMR method is sensitive to short range order. Carbon atoms in different environments have different chemical shifts and so the method is able to determine the number of carbon atoms in a particular environment.<sup>117</sup> Cellulose crystallinity is measured using the signal from the C4 appearing at 89 ppm (for highly ordered cellulose in the interior of the crystallite) and at 84 ppm (for the less ordered cellulose).<sup>129</sup> The earliest published <sup>13</sup>C NMR of solid cellulose show two peaks at 82 ppm and 91 ppm assigned to the C4 carbon of cellulose and was reported by Atalla *et al.*<sup>101</sup> Moistening the cellulose sharpens broad NMR peaks.<sup>123</sup> Peaks at 102 ppm and 82.6 ppm are assigned to hemicelluloses and do not appear in the spectra of purified celluloses.<sup>130</sup>

The fraction of crystalline cellulose determined by NMR is defined as the area of the peak at 89 ppm divided by the total area assigned to the C4 (89 ppm + 84 ppm).<sup>131</sup> This ratio is a measurement of the crystalline interior cellulose to the total cellulose in the sample. Since the first results on solid state <sup>13</sup>C NMR of cellulose by Atalla *et al.*<sup>101</sup> and Earl *et al.*<sup>132</sup> numerous investigations have confirmed the separation of the signals from ordered (crystalline) and disordered (amorphous) regions.<sup>61</sup> It has been shown that the intensity of the 89 ppm peak decreases while the 84 ppm peak considerably increases as a result of an increase in amorphous character of the sample. Proton spin relaxation times indicate much greater molecular movement for 84 ppm carbon atoms than in the case of 89 ppm.

### **1.3.6 Comparison of Techniques (X-ray, FTIR and Solid State NMR)**

Anhydroglucose units within cellulose can exist in regions with a wide range of degrees of order. From areas that are completely ordered (as in the interior of crystallites) to those that lack long range order (as in the amorphous regions). The sensitivity of a method to order and disorder within the cellulose indicates how the method distinguishes between crystalline and less ordered materials.

To be classified as crystalline by x-ray diffraction, the crystallites must be of a particular minimum size. The diffraction patterns of cellulose show a number of peaks superimposed on a broad background. These features are attributed to the crystalline and amorphous regions of the sample. The width of the peaks in the diffractogram are inversely proportional to the lateral width of the crystallites. As the crystallites get smaller the crystalline peaks get broader and the amorphous background increases. Material on the surface of the crystallite that has greater mobility and a lower degree of order than the material in the interior of the crystallite are measured as crystalline material. Small defects within the crystalline fraction are included in the crystalline fraction.

Infrared band ratios are used to measure changes in crystallinity because intensities of certain infrared bands are sensitive to variations in crystallinity. An absorbed band that is affected by crystallinity is compared to a band that is relatively insensitive to changes in crystallinity. This comparison shows variations in crystallinity between different samples with accuracy.

The NMR method is sensitive to short range order. In the NMR spectrum carbon atoms in different environments have a different chemical shift. This method measures the number of carbon atoms in a particular environment. Cellulose crystallinity is measured using signals from the C4 which appear at 89 ppm (for highly ordered cellulose in the interior of the crystallite) and at 84 ppm (for the less ordered cellulose). Material on the surface of the crystallites which exist in regions of lower order than those in the centre of the crystallites gives a signal at 84 ppm. Since only material within the crystallites appears as crystalline in the NMR spectrum, the relative degree of crystallinity depends on the size of the crystallites. For a constant fraction of crystalline cellulose, larger crystallites exhibit a higher relative degree of crystallinity. This implies that even

if a material is composed totally of small crystallites, the relative degree of crystallinity calculated by NMR can never reach unity.

Three comparisons have been reported on the relative degree of crystallinity by NMR and x-ray for a range of pure cellulose samples.<sup>133,134,135</sup> These results showed that as the proportion of material in ordered domains increased, the sizes of the crystallites increased resulting in an increase in the relative degree of crystallinity. In the current literature there are no comparisons between x-ray, FTIR and NMR or any combination thereof other than the one stated previously. The three methods used to determine the relative degree of crystallinity are all sensitive to different aspects of order and disorder. It is not surprising then that different methods provide different measurements of ordered and less ordered cellulose within the same sample.

## **1.4 Method to Monitor Cellulose Degradation**

### **1.4.1 Viscosity**

Viscosity is a measure of the degradation of high molecular weight carbohydrates, mainly cellulose, in pulp fibres caused by pulping and bleaching.<sup>136,137</sup> The fibres are dissolved in a 0.5% solution of cupriethylenediamine and the viscosity of the solution is determined under standard conditions in a capillary viscometer.<sup>138,139,140</sup> There is a relationship between viscosity and length of the cellulose molecules. The solution viscosity of the pulp gives an indication of the average degree of polymerisation of the cellulose. Thus this test provides a direct correlation between the viscosity and the molecular weight of the cellulose.<sup>141,142</sup>

Several factors affect the precision of this method. First, the reaction time between the cupriethylenediamine and the cellulose affects the viscosity. The longer the reaction time, the lower the viscosity. It is therefore important that the reaction time between adding the cupriethylenediamine to the sample and reading the efflux time remains consistent to minimise the variability. Second, the cupriethylenediamine solution deteriorates very quickly and it is important that the solution is stored under nitrogen to prevent oxidation. Finally, the temperature of the reaction is also important. An increase in temperature increases the speed of the reaction resulting in lower viscosity readings. Thus a constant temperature of  $25.00 \pm 0.05$  °C has to be maintained for all

measurements. The temperature of 25 °C is used to minimise cellulose degradation in the cupriethylenediamine solution and the  $\pm 0.05$  °C because viscosity of a solution is strongly dependent on the temperature.

#### **1.4.2 Conductometric Titration**

The conductance of a solution is the sum of all ions present in it. Correlating the unequal distribution of ions within a cellulose fibre (between the interior of the fibre wall and the external solution) is described in the early work of Donnan.<sup>143</sup> He was the first to observe the unequal distribution of low molecular weight ions on the two sides of a membrane that was able to confine a large molecular weight ion to one side due to the relatively small pore size of the membrane.

Two highly conducting ions are hydrogen and hydroxide.<sup>144</sup> Knowing the concentration of each ion at a given internal pH, both the conductance of the system and the amount of sodium hydroxide required to reach a given pH can be determined. The contribution of any ion to the conductance of a solution is the product of its concentration and its equivalent ionic conductance. The total conductance is the sum of these contributions. By taking relevant concentrations into account, the conductances of both internal and external solutions can be calculated. The amount of sodium hydroxide required to obtain a given internal pH is calculated from the fact that sodium hydroxide is the only source of sodium ion other than that originally present.<sup>145</sup> Thus the amount of sodium hydroxide is found by summing the amounts of sodium in the internal and external solutions and subtracting the sodium originally present. Conductometric titration curves can be constructed by repeating the procedure for a series of pH values.

A typical conductometric titration procedure starts with the ion exchange of the acidic groups in the pulp to hydrogen form by treatment with hydrochloric acid. Excess hydrochloric acid and the liberated cations are then washed from the pulp. The pulp is subsequently diluted to a specified consistency using deionised water and a dilute solution of sodium chloride. Finally the suspension is titrated with sodium hydroxide allowing sufficient time for equilibrium between additions.

At the start of the titration, the acid (in the case of cellulose, carboxylic acid) ionises to a small extent and a fraction of hydrogen ions leaves the fibres for the external

solution to exchange with sodium. As the titration proceeds, ionisation of the unneutralised acid is soon reduced to low levels and the hydrogen ion makes negligible contribution to the conductance of either solution. The main result is that until the end point is approached, most of the sodium added in the form of sodium hydroxide enters the fibre wall and is associated with neutralisation of the acid. The end point is marked by the accumulation of sodium hydroxide in the external solution.

Conductometric titration provides valuable information on the change that takes place on the cellulose fibres as degradation occurs.<sup>146</sup> Attack by oxygen on cellulose causes a series of oxidations to occur. These oxidations, if they do not result in chain cleavage of the cellulose chain, can be followed by the method of conductometric titration. Conductometric titration is able to quantify the amount of carboxylic acids present on the cellulose fibres.

## Chapter 2

### Scope and Aim of Thesis

---

The prime focus of this thesis is to gain an understanding of the physicochemical properties of cellulose as it undergoes the oxygen delignification process. During oxygen delignification, the removal of lignin involves an oxygen reaction that is not selective because the carbohydrate and lignin components are attacked simultaneously. The attack on the carbohydrate component may result in degradation leading to fibre strength loss. This loss is significant to the oxygen delignification process. Since the cellulose component of pulp contributes to its strength, it is therefore important to concentrate on the cellulose component of pulp during oxygen delignification.

The relative degree of crystallinity is a measure of the amount of crystalline material in cellulose. As the crystalline content changes during oxidation, the physicochemical changes in cellulose can be examined. Three instrumental analytical techniques, x-ray diffraction, Fourier transform infrared (FTIR) spectroscopy and  $^{13}\text{C}$  solid state nuclear magnetic resonance (NMR) spectroscopy were used to investigate the changes in the relative degree of crystallinity during oxidation. To date no attempts have been made in comparing these three instrumental techniques to determine the relative degree of crystallinity.

Furthermore, the extent of degradation during oxidation can be detected by examining the changes in the chain length (degree of polymerisation) and the amount of oxidation that takes place on the polymer (carboxylic acid content). The degree of polymerisation was calculated from the viscosity of the cellulose and conductometric titration measured the changes in carboxylic acid content.

Different types of cellulose were oxidised under carefully controlled conditions in a kettle reactor. The four types chosen were: fully bleached softwood pulp (Q-90), hemicellulose reduced pulp derived from Q-90, cotton cellulose and microcrystalline cellulose (Avicel). The composition of each cellulose chosen was different in that Q-90

is derived from wood whereas cotton is from a plant, and Avicel is manufactured from a wood cellulose. The supermolecular structure of each cellulose type is different and presents an interesting basis for comparison.

This thesis initially presents the methodology of the experiments conducted to measure changes in relative degree of crystallinity, degree of polymerisation and carboxylic acid content during oxidation. Chapter 3 outlines the procedure used to oxidise the cellulose, the preparation of the samples, the instrument types and conditions and the method of calculating properties of cellulose structure. The four cellulose samples were all analysed by the techniques listed above.

In Chapter 4, one cellulose type (Q-90) was selected and characterised using all three instrumental techniques. This provided an evaluation of the capability of each technique in measuring the relative degree of crystallinity. The accuracy and reproducibility of the data were also examined.

In Chapter 5, the relative degree of crystallinity for the four celluloses were examined by the same techniques validated in the previous chapter. A comparison of the techniques for each sample and a comparison of the samples using each technique are presented. A theory is proposed to rationalise the observed trends in the changes of the relative degree of crystallinity as a function of time.

In Chapter 6, cellulose degradation is examined using viscosity measurements and conductometric titration for each cellulose. The relationship between carboxylic acid content and degree of polymerisation is critically discussed. In addition, the number of scissions in a cellulose chain (chain scission number) is compared to the carboxylic acid content. A relationship is thus developed between viscosity measurements and conductometric titrations.

Chapters 7 and 8 summarise the conclusions of this study and recommendations for further studies are made.

## Chapter 3

### Experimental

---

#### 3.1 Oxidation of Pulp

##### 3.1.1 Q-90, Cotton and Hemicellulose reduced Pulp

All pulp samples were prepared as follows: 50 g (based on oven dry weight) of pulp were added to water to form a slurry. Sodium hydroxide (NaOH) was then added at a concentration of 2.5%. Additional water was added to bring the slurry to a 10% consistency. The mixture was then fluffed in a Hobart mixer for 3 minutes. The pulp was subsequently preheated by transferring the mixture in a plastic bag and heating it at a high temperature setting for 2 minutes per side in a microwave oven. The mixture was then placed into the preheated 2.5 L kettle reactor. (A schematic of the kettle reactor appears in Appendix I). The reactor was pressurised with oxygen or nitrogen at  $6.895 \times 10^5$  Pa (100 psi) and heated at 95°C while being stirred at 10 rpm. The reaction times varied for the pulp samples. At the end of the reaction, the pulp was removed and placed in water to a 1% consistency. It was disintegrated for 45 seconds using a counter rotating blade and then washed. The fines were collected separately and stored. The pulp was made into hand sheets for further analyses. For all pulps, a control sample prepared with the same workup, was also tested. The control sample was not exposed to reactor mixing.

##### *Q-90*

Q-90 is commercially prepared from fully bleached black spruce kraft pulp. The designation “Q” is an abbreviation for the Quevillon mill in northern Québec, and the number “90” is the ISO brightness of the sample. When the gas used to pressurise the reactor was oxygen, reaction times of 0, 5, 10, 15, 30, 60, and 90 minutes were used. When the gas used was nitrogen, times of 5, 15, 60 and 90 minutes were used. Nitrogen gas was also applied to an autoclaved sample of cellulose for 50 and 90 minutes.



### ***Cotton***

A cotton pulp was chosen with approximately the same degree of polymerisation as the Q-90 sample. Pressurised oxygen with reaction times of 0, 5, 15, 30, 60 and 90 minutes was applied. Nitrogen with reaction times of 5, 50 and 90 minutes on autoclaved cotton cellulose was used.

### ***Hemicellulose Reduced Pulp***

The hemicellulose reduced pulp was generated by treating the Q-90 pulp to remove a significant amount of hemicellulose according to a modified procedure outlined by Beelik.<sup>147</sup> Such a pulp was obtained via a treatment causing a reduction in the amount of its hemicellulose content. However, not all the hemicellulose was removed from the original pulp. The amount of hemicellulose removed was determined by performing a carbohydrate analysis on the pulp before and after removal. The results of these analyses can be found in Table 5.1. This removal was carried out in three stages.

During the first stage, 375 g (based on oven dry weight) of pulp were slurried for 20 minutes at room temperature in 4181 mL of aqueous sodium hydroxide containing 37.5 g of sodium hydroxide. The final volume of the solution was 9375 mL, containing pulp at 4% consistency. The sodium hydroxide concentration of the extraction liquor was 1%. The mixture was stirred intermittently. The pulp was washed through a filtered funnel three times with deionised water. In the second stage, the procedure was repeated using 3577.5 mL of aqueous sodium hydroxide containing 468.75 g of sodium hydroxide, giving a sodium hydroxide concentration in the extraction liquor of 4%. In the third stage, the procedure was repeated once again using 4 L of aqueous sodium hydroxide containing 937.5 g of sodium hydroxide, giving a sodium hydroxide concentration in the extraction liquor of 10%.

This pulp was subjected to pressurised oxygen treatment at reaction times of 5, 15, 30 and 90 minutes. Autoclaved hemicellulose reduced pulp at 90 minutes reaction time was also examined with pressurised nitrogen.

### **3.1.2 Avicel**

Avicel is a commercial microcrystalline cellulose (FMC Corporation) obtained from the acid hydrolysis treatment of a high “alpha” cellulose softwood pulp. Avicel was prepared in a different manner for the reactor than the Q-90, cotton and hemicellulose

reduced pulps because it was a powder sample. 100 g of powdered Avicel (based on oven dry weight) was added to form a slurry. Sodium hydroxide (NaOH) was then added at a concentration of 2.5%. Additional water was added to bring the slurry to a 25% consistency. The mixture was then mixed for 3 minutes and transferred to a plastic bag to preheat on high setting for 4 minutes in a microwave oven. The mixture was then transferred to a preheated 2.5 L kettle reactor. The reactor was pressurised with oxygen for 0 and 60 minutes to  $6.895 \times 10^5$  Pa (100 psi) and heated at 95°C while being stirred at 50 rpm. At the end of the reaction, the pulp was removed and washed with water on a Buchner funnel. The pulp was then collected using a centrifuge, freeze dried and stored.

### **3.2 Crystallinity Determination**

The relative degree of crystallinity for each sample was determined using x-ray diffraction, Fourier transform infrared (FTIR) spectroscopy, and solid state nuclear magnetic resonance (NMR) spectroscopy whose details follow.

#### **3.2.1 X-ray Diffraction**

##### ***Preparation of the Sample Mount***

##### ***Q-90, Cotton and Hemicellulose reduced Pulp***

Approximately 0.150 g (based on oven dry weight) of pulp were dispersed in 40 mL of deionised water and stirred moderately for 10 minutes. The sample was filtered using a 30 mm diameter coarse glass sintered Buchner funnel. The resulting cellulose “cake” was then placed between blotter paper and hand pressure was applied for five minutes. The pressed cellulose cake was allowed to air dry overnight. The sample was then cut to fit a 24 mm diameter mount and affixed to the mount using carpenters double sided tape.

##### ***Avicel***

Approximately 0.50 g (based on oven dry weight) of powder were pulverised in a mortar with a pestle until a fine free flowing powder was achieved. About 0.150 grams of the fine powder was then spread evenly over the 24 mm diameter mount. The sample was then mechanically pressed for a few minutes to obtain a flat pellet.

### ***Instrument and Conditions***

Sample characterisation was performed using a RIGAKU D/Max 2400 automated powder diffractometer with a 12 KW rotating anode. Copper K $\alpha$  radiation was used. The sample mounts were analysed at a voltage of 40 V and a current of 160 Amp. The width of the scan was 14 mm on a 24 mm mount with a receiving slit set to 0.10. The scan axis used was theta over 2 theta ( $\theta / 2\theta$ ). The mounts were spun at 60 rpm. The angles scanned were 10° to 30° and took a total of 12 minutes to scan.

### ***Calculation of Crystallinity***

The data was processed using the JADE software supplied with the x-ray diffraction equipment. The resulting spectra were printed and the relative degree of crystallinity was calculated by taking the ratio of the intensity at ~22.4° (which represents the 002 plane in the crystal regions of cellulose) to the sum of the intensity at ~22.4° plus ~18.5°.

## **3.2.2 FTIR**

### ***Preparation of the Sample Mount***

#### ***Q-90 and Cotton***

Approximately 15 mg (based on oven dry weight) of pulp were dispersed in 25 mL of deionised water and stirred moderately for 10 minutes. Using a coarse glass sintered Buchner funnel of 30 mm diameter the sample was filtered. The resulting cellulose wafer was then placed between blotter paper and hand pressure was applied for five minutes. The pressed cellulose wafer was allowed to air dry overnight. The sample was then cut with the aid of tweezers and scissors to avoid contamination from oil or dirt from finger contact. The sample was cut to fit the diameter of the pellet size. The resulting wafer weighed about 2 mg.

Infrared grade potassium bromide (KBr) was dried overnight in an oven set at 110 °C. 350 mg of KBr was then ground to a fine powder in a mortar. Approximately half of the powder was placed in the well of the pellet maker. The wafer sample was then placed on top and the remaining KBr powder covered it. The pellet maker was then evacuated using a vacuum pump for 2 minutes after which 10 tons of pressure were applied while still under vacuum for an additional 4 minutes. The resulting pellet was then removed.

### *Hemicellulose Reduced Pulp*

Infrared grade potassium bromide (KBr) was dried overnight in an oven set at 110 °C. 350 mg of KBr was then ground to a fine powder with a mortar. Approximately half of the powder was placed in the well of the pellet maker. Approximately 2 mg of the hemicellulose reduced pulp fibres were then manually disintegrated with tweezers and spread uniformly across the cross sectional area of the pellet well. The remaining KBr powder was used to cover the pulp fibres. The pellet maker was then connected to a vacuum for 2 minutes after which 10 tons of pressure were applied while still under vacuum for an additional 4 minutes. The resulting pellet was then removed.

### *Avicel*

Infrared grade potassium bromide (KBr) was dried overnight in an oven set at 110 °C overnight. 2 mg of Avicel powder and 350 mg of KBr were then weighed out and ground together to a fine powder with a mortar and pestle. The resulting mixture of powder was placed in the well of the pellet maker. The pellet maker was then hooked up to a vacuum for 2 minutes after which 10 tons of pressure were applied while still under vacuum for an additional 4 minutes. The resulting pellet was then removed.

### *Instrument and Conditions*

Infrared spectra were recorded on a Bruker IFS-48 spectrometer. A blank pellet was first made which contained only 350 mg of KBr in the same manner as stated above for the samples. It was then placed in the sample holder of the FTIR machine and was purged with nitrogen gas for 20 minutes before any measurements were taken. 60 scans at a resolution of 4.0 cm<sup>-1</sup> for the background were recorded to determine the contribution of KBr. The sample was then run in a similar fashion but with 120 scans and the background scan subtracted. This ensured that there was no KBr contribution to the spectra.

### *Calculation of Crystallinity*

Spectral manipulations were made using the Bruker OPUS software supplied with the computer connected to the spectrometer. A baseline correction was performed using the rubberband method, excluding carbon dioxide, with 200 base points. The plot was then smoothed using 23 points by the standard Savitsky-Golay method provided on the

software. The spectra were then plotted for analysis. The relative degree of crystallinity was calculated by taking the ratio of the absorbance at  $1429\text{ cm}^{-1}$  to the total absorbance at  $1429\text{ cm}^{-1}$  plus absorbance at  $893\text{ cm}^{-1}$  after the standard baseline correction was applied to these two peaks.

### **3.2.3 Solid State NMR**

#### ***Sample Preparation to Remove Metal Ions***

Approximately 2 grams (based on oven dry weight) of cellulose were dispersed in 300 mL of a 0.2% (w/v) diethylenetriaminepentaacetic acid (DTPA) solution prepared in deionised water. The dispersion was then stirred for 1 hour at  $60\text{ }^{\circ}\text{C}$ . The cellulose was then filtered through a glass sintered Buchner funnel and washed with 500 mL of deionised water. The washed cellulose was then redispersed in a 600 mL solution of sulphuric acid (1.1 mL/L) and stirred gently at room temperature for 2 hours. The sample was then filtered and washed with 500 mL of deionised water. The cellulosic material was then broken up into small sized fragments and allowed to air dry for 2 days at room temperature.

Cellulose samples prior to and after metal ion removal were sent to an independent laboratory to determine the metal ion content of iron, copper and manganese. This verified the effectiveness of the metal ion removal. Data for these tests measurements are provided in Appendix II.

#### ***Sample Conditioning in the Dessicator***

Prior to NMR measurements all samples were kept in a dessicator under reduced pressure for a period of one week over Drierite (anhydrous calcium sulphate). All samples were then placed in another dessicator that contained a 100 mL of 45.41% sulphuric acid solution to create a 45% humidity environment. The solution concentration is expressed as a percentage of anhydrous solute by weight. The dry samples were kept in the second dessicator for a period of one week prior to any measurements.

#### ***Instrument and Conditions for $^{13}\text{C}$ CP MAS NMR and Proton $T_1$ Measurements***

All samples were conditioned at  $45\pm 5\%$  relative humidity prior to any measurements, so as the effect of moisture content on the measured parameters was

eliminated.<sup>124</sup> Proton spin-lattice relaxation time measurements were carried out via carbon. All solid state NMR experiments were carried out on a Chemagnetics CMX-300 spectrometer operating at a frequency of 75.4 MHz. All spectra CP/MAS experiments were performed with a spin rate of 3.5 kHz, a contact time of 0.5 ms and proton  $\pi/2$  pulses of 4.0  $\mu$ s duration. Endcaps with O-ring type construction were used to prevent loss of moisture. (No change in sample weight occurred after several hours of spinning.)

The proton spin-lattice relaxation times were measured with a Torchia style CP experiment (where the proton magnetisation is followed by monitoring the carbon-13 signal) employing a Freeman-Hill type sequence.<sup>148</sup> The proton signal decays exponentially to zero as a function of tau. Usually 80-100 transients were acquired on each of 7 tau values. The proton T1 values were calculated from the slope of a  $\ln(I)$  versus tau plot where I is the intensity of the cellulose peak at 72 ppm.

#### ***Deconvolution for the Calculation of Crystallinity***

The spectra were transferred to a Chemagnetics CMX-270 spectrometer that has Spinsight NMR software installed. The spectra were fit using lineshapes that were assumed to be 50% Lorentzian and 50% Gaussian. The area for the peaks at 89, 84, 65 and 63 ppm were noted for each spectrum and the appropriate calculations were carried out.

### **3.3 Viscosity**

#### **3.3.1 Q-90 / Cotton / Hemicellulose reduced Pulp / Avicel**

Approximately 0.12 g (based on oven dry weight) of sample, weighed to four decimal places, was placed in a 40 mL vial. Deionised water was added using a burette to obtain a 1% consistency. Two glass beads were added to the vial and placed on a shaker for 20 minutes to disperse the sample. Cupriethylenediamine was added to the vial using a burette in the same amount as the water to yield a 0.5% consistency. A timer was started once the cupriethylenediamine was added. The vial was then placed in a water bath set at exactly  $25.00 \pm 0.05$  °C. After exactly 20 minutes, the solution was poured into a glass viscometer until its large sphere was half full. The efflux time was then measured after exactly 25 minutes from when the cupriethylenediamine was added.

The efflux time was measured by drawing up with a pipette bulb the liquid in the viscometer above the second etch mark and recording the time it took for the meniscus to pass between the two marks. This was done at least twice for each reading and the average was recorded in seconds. The viscosity was obtained by multiplying the average efflux time by the K-factor of the viscometer.

### **3.4 Conductometric Titration**

#### **3.4.1 Sample Preparation**

Approximately 2 grams (based on oven dry weight) of cellulose were dispersed in 400 mL of standardised 0.1N hydrochloric acid solution (8.31 mL of concentrated HCl per litre of deionised water) and mixed for 45 minutes at room temperature. The sample was then filtered through a glass sintered Buchner funnel and then redispersed in 400 mL of fresh 0.1 N hydrochloric acid solution and mixed for another 45 minutes. The sample was filtered and washed with at least 500 mL of deionised water until a low and constant filtrate conductance of 0.1  $\mu\text{s}/\text{cm}$  was obtained.

The sample was then dispersed in 500 mL of 0.001N sodium chloride (NaCl) solution (0.0580 g / L of deionised water passed through an ion exchange resin). 5 mL of 0.1N standardised hydrochloric acid (HCl) solution was then added to the sample. The electrodes for the titration were placed in the sample container. The sample was then sealed with plastic wrap, mixed moderately, and nitrogen gas was bubbled through the solution. After the titration the sample was filtered, washed and dried at 105 °C for 4 hours. The dry sample was allowed to cool in a dessicator over Drierite for 30 minutes and then accurately weighed.

#### **3.4.2 Instrument Criteria and Conditions**

A Dosimat 655 titrator connected (through a computer interphase that was built by the Pulp and Paper Research Institute of Canada) to an IBM based computer was used to deliver exactly 0.10 mL of sodium hydroxide solution. The interval time between reading the conductance of the solution and the delivery of the next portion of titrant was set at 180 seconds. The wait time needed to obtain a equilibrated conductance reading after delivery of titrant was set at 120 seconds. Conductance measurements were obtained

using a CDM 83 Copenhagen conductivity meter. All measurement readings were recorded and stored on the IBM computer before being plotted and analysed.

### 3.4.3 Calculations

A plot of the conductance versus the titrant volume was constructed. The endpoints for the titration curve and the volume of titrant used for each endpoint were determined. The amount of carboxylic acid contained in the sample was calculated using the following equation:

$$\text{Amount of -COOH (mmole/Kg)} = \frac{[(\text{Endpoint 2 (mL)}) - (\text{Endpoint 1 (mL)})](N_{\text{NaOH}})(1000)}{\text{Oven dry weight of sample (g)}} \quad (3.1)$$



## Chapter 4

### Results & Discussion – Part I

#### Evaluation of Techniques

---

To understand the changes in cellulose during oxygen delignification, several cellulose types were oxidised at various times with pressurised oxygen, along with a control sample not subjected to oxidation, to observe the changes in the relative degree of crystallinity. This chapter presents the results for three methods of analysis: x-ray diffraction, Fourier transform infrared (FTIR) spectroscopy and  $^{13}\text{C}$  solid state nuclear magnetic resonance (NMR) spectroscopy with cross polarisation and magic angle spinning. In determining the relative degree of crystallinity, each method focuses on a specific aspect of the supermolecular structure of cellulose. To date, no data comparison for these three methods is available. Consequently the first part of the results and discussion section for this thesis critically evaluates the ability of these techniques to examine the behaviour of cellulose under oxygen delignification conditions. The cellulose of a fully bleached softwood pulp was used in this evaluation.

#### 4.1 Relative Degree of Crystallinity

When a polymer has a highly stereo-regular structure with little or no chain branching or when it contains highly polar groups with very strong dipole-dipole interactions, it may exist in a crystalline form.<sup>72</sup> Such crystallinity is unlike that of low molecular weight compounds but instead it exists in regions of the polymer matrix where polymer molecules order themselves in a thermodynamically favourable alignment. The fringed micelle model defines crystallinity in terms of such ordered regions, called crystallites, in which any particular polymer chain may exist within a number of crystallites.<sup>150</sup>

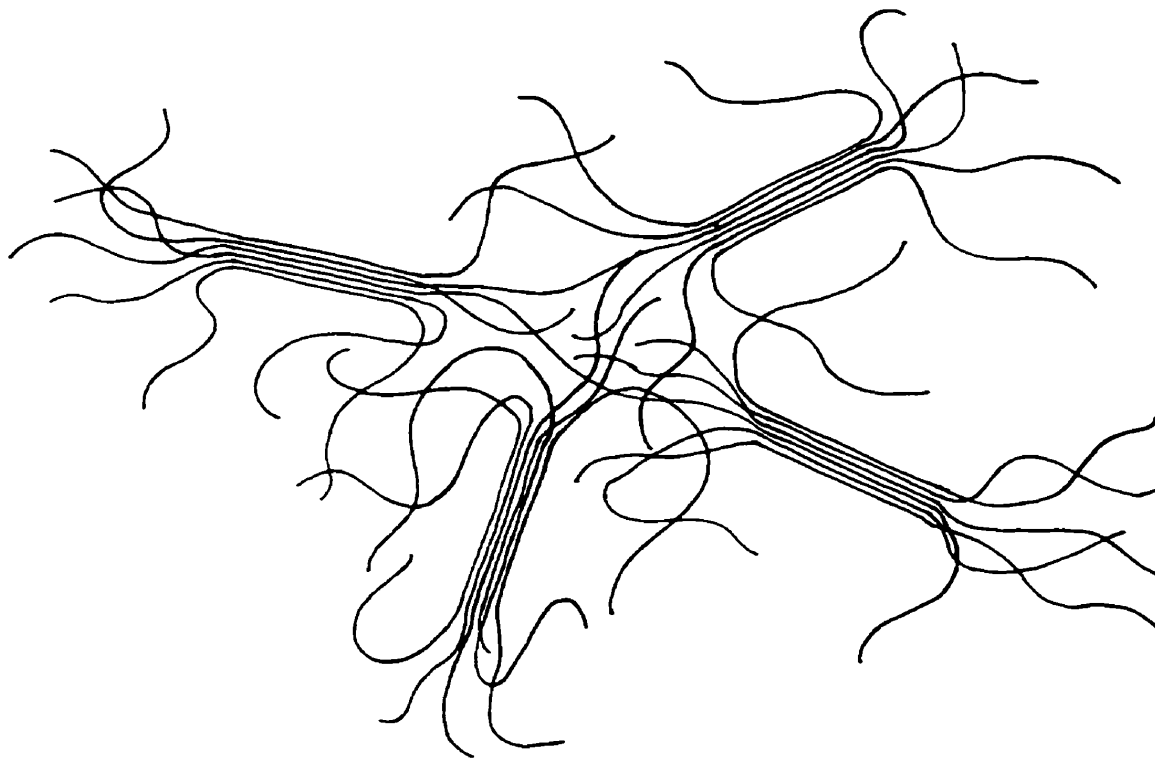


**Figure 4.1** Schematic representation of the fringed micelle model.<sup>72</sup>

Cellulose can be considered a polymer chain with crystallites because it displays a paracrystalline morphology.<sup>97</sup> The cellulose molecules are linked laterally by hydrogen bonds to form linear bundles.<sup>48</sup> The extremely large number of hydrogen bonds results in a strong lateral association of the linear cellulose molecules. The strong association and almost perfect alignment of the cellulose molecules give rise to crystallinity. X-ray diffraction measurements in previous studies have shown that the crystalline regions are interrupted every 600 Å with non-crystalline amorphous regions.<sup>61</sup> The reason for this is not completely understood. In general, cellulose crystallinity regards the molecules as having a highly oriented (crystalline) length for a distance of about 600 Å with an adjacent length of poor orientation (amorphous) and then again a crystalline length. This pattern repeats throughout the length of a cellulose molecule. Two neighbouring cellulose molecules may originate from the same crystalline bundle but on entering and re-entering different amorphous regions, may not end up in the same crystallite bundle.<sup>71</sup>

Each individual crystalline region is interconnected by amorphous regions. Crystalline regions may contain occasional kinks or folds in the polymer chain, called defects. Depending on the type of cellulose, the number of defects varies.<sup>102</sup>

As stated in the Introduction, cellulose is highly susceptible to oxidising chemicals such as molecular oxygen.<sup>75</sup> The two most susceptible portions of the cellulose molecule are the terminal reducing end group and the hydroxyl sites.<sup>76</sup> There are three main oxidation sites of attack on cellulose. The first is oxidation occurring at the reducing end groups to cause a “peeling” reaction.<sup>77</sup> The second is oxidation at the glycosidic linkage within a cellulose molecule to cause chain scission.<sup>77</sup> These oxidation sites (particularly the second one) can significantly reduce the degree of polymerisation of an individual cellulose molecule. The third type of oxidation attack occurs at the C3 carbon position. This causes the C2 and C3 carbons to be transformed into carboxylic acid groups and some oxidation may occur at the C6 carbon.<sup>78</sup> This type of oxidation does not cause chain cleavage and therefore the degree of polymerisation remains the same. Since attack on the terminal groups do not cause significant changes in the average degree of polymerisation, more attention should be focused on the oxidation that causes random chain cleavage by attack at the glycosidic linkage.

If the amorphous domains of cellulose are attacked, chain scission and “peeling” reactions occur which reduce the total amount of amorphous cellulose.<sup>151</sup> The reduction in the total amorphous cellulose effectively increases the relative degree of crystallinity. There is also the possibility that random cleavage of the cellulose occurs at the accessible chains within the crystalline domains.<sup>151</sup> The chains at the outer portions of the crystallites can randomly cleave and dangle like “hair” from the crystalline domain. The “hairs” can now be considered amorphous since they are not part of the crystallite. If this occurs, there is a significant increase in the total amorphous character of the cellulose, and the relative degree of crystallinity decreases.

The cellulose is oxidised at an elevated temperature (100 °C). Roffael and Schaller have found that the thermal treatment of isolated cellulose resulted in a decrease in the degree of polymerisation at temperatures in excess of 100 °C.<sup>152</sup> They also observed an increase in the crystallinity in thermally treated cellulose up to temperatures

of 120 – 160 °C. The thermal degradation of cellulose is not restricted to the cleavage of molecular chains, but there are additional dehydration and oxidation restrictions. Hernadi has shown that chain cleavage and dehydration follow a zero-order reaction whereas oxidation is a first-order reaction.<sup>153</sup> Heating in air causes oxidation of the hydroxyl groups resulting in an increase of carbonyl and subsequently carboxyl groups.<sup>154</sup> All samples of cellulose were oxidised in the kettle reactor at a temperature of 100 °C, and so there is no contribution of thermal degradation.

## **4.2 Q-90**

Q-90 is a softwood pulp that has been fully bleached which means that practically all the lignin has been removed from the pulp. The result is a high cellulose content pulp with some hemicellulose present.

### **4.2.1 X-ray Diffraction**

Samples for x-ray diffraction were prepared with Q-90 pulp that had been oxidised using oxygen in the kettle reactor. In addition, samples of regular and autoclaved pulp that were treated with pressurised nitrogen gas were examined by x-ray diffraction. Oxidation times in the kettle reactor for these oxygen and nitrogen treated samples ranged from 0 to 90 minutes. For each oxidation time, three separate mounts were prepared. Triplicate sets of data were required to establish the relative error associated with the x-ray diffraction method. The relative degree of crystallinity was calculated for each sample and plotted against the oxidation time. This plot is shown in Figure 4.2.

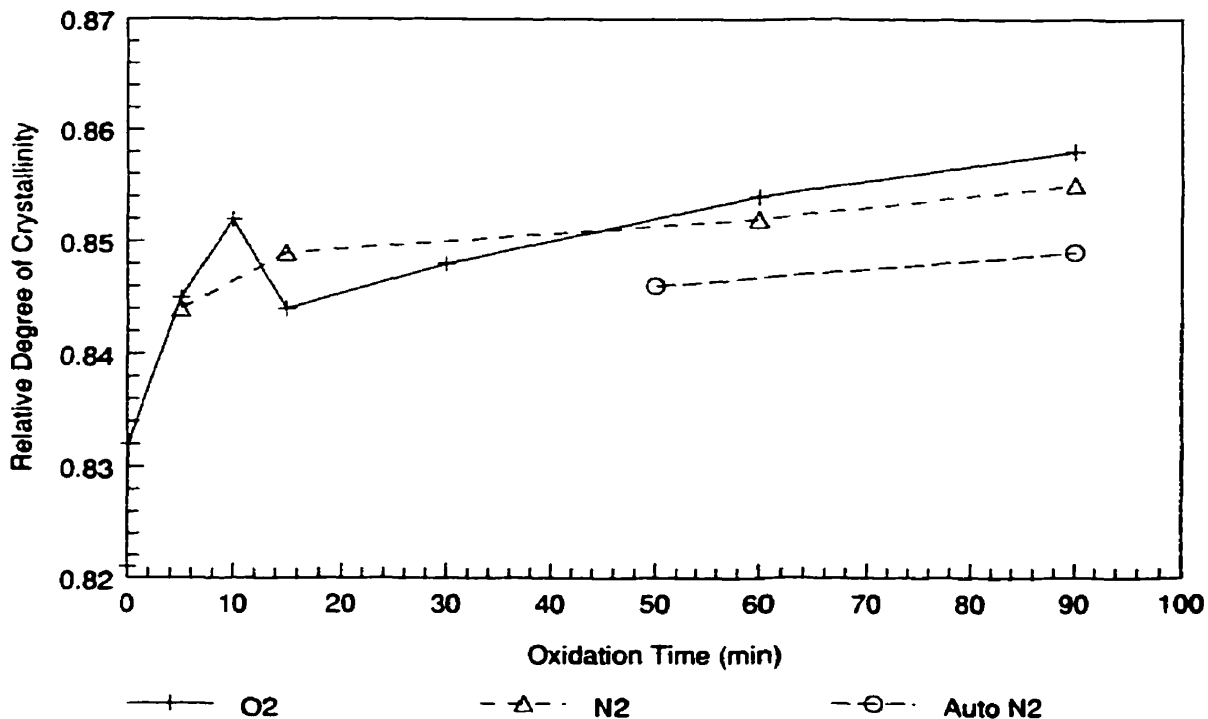


**Figure 4.2** X-ray diffraction data for Q-90 showing the relative degree of crystallinity as a function of oxidation time.

It is interesting to note that the relative degree of crystallinity initially increases rapidly for the oxygen and nitrogen treated samples. This is due to the fact that oxygen present within the fibres is reacting with cellulose immediately.<sup>155</sup> This is occurring so rapidly that even within the preheating stage of the pulp, prior to it being placed in the reactor, oxidation takes place. The oxidation of the cellulose, prior to treatment in the reactor, may also occur due to the thermal oxidation and dehydration reactions that can occur (outlined in section 4.1). This is best illustrated by closely examining the oxygen data curve. Between the control sample and the unoxidised (0 minute) sample there is a significant increase in the relative degree of crystallinity. Within the next five minutes, the slope is less steep indicating that the reaction is somewhat slower. In the next five minutes, between 5 and 10 minutes of oxidation time, the slope decreases slightly. The change in slope is more pronounced for the samples exposed to nitrogen.

It is worth noting that in later reaction times, where autoclaved nitrogen samples were examined, the slopes of the curves for both nitrogen treated samples are almost

parallel. This suggests that the oxygen present in the pulp fibres has been depleted or that a reaction is taking place with the caustic present. It is of no surprise that the autoclaved sample data shows a lower relative degree of crystallinity than the non-autoclaved sample curve. This is because there is almost no oxygen present in the autoclaved sample<sup>156</sup> and so the reaction of the caustic with the cellulose predominates.

The reason for the dramatic drop in the relative degree of crystallinity at 15 minutes for the oxygen curve cannot be explained with the data presented thus far. It may be due to a number of factors. One such factor is that the oxidation procedure was flawed in some way and was not accurately reproduced between samples. Another factor may be caused by some hemicellulose present which may contribute in some way to the decrease. Furthermore, variations in the initial pulp could also be considered. These possible factors are further discussed as more data is presented in this work. This drop is not due however to the reproducibility of the x-ray diffraction data because the error associated with the triplicate measurements is much smaller than the actual decrease. This suggests that the decrease in the relative degree of crystallinity is significant and deserves further investigation.

It is noteworthy to mention at this point that x-ray diffraction measures the fraction of cellulose molecules that are arranged in a regularly repeating pattern.<sup>61</sup> Small defects present within the crystallite, or amorphous material on the surface of the crystallite are however not likely to be distinguished.<sup>157</sup> This results as an apparent overestimation of the crystalline material in the pulp. As such it is prudent to also examine other techniques of measuring the relative degree of crystallinity.

#### **4.2.2 FTIR Spectroscopy**

FTIR spectroscopy is convenient since it requires only a small amount of sample for the analysis.<sup>107</sup> The disadvantage of this technique is that a very rigorous procedure is needed and must be carried out painstakingly to ensure that for each analysis the data is comparable.<sup>72</sup> The procedure outlined in the experimental section was therefore carried out with precision. The quantities were precisely measured on an analytical balance to four decimal places. The time required to make the pellet and the purging of the sample chamber was carefully monitored with a stop watch. In addition triplicate measurements

were carried out to ascertain reproducibility and determine the accuracy of the data as a function of oxidation time.

Q-90 samples were used in the FTIR spectroscopic analysis as in the x-ray diffraction method. The samples were similarly treated with oxygen and nitrogen in the kettle reactor at the previously specified reaction times. Figure 4.3 shows the data for these measurements where the relative degree of crystallinity is plotted as a function of oxidation time.

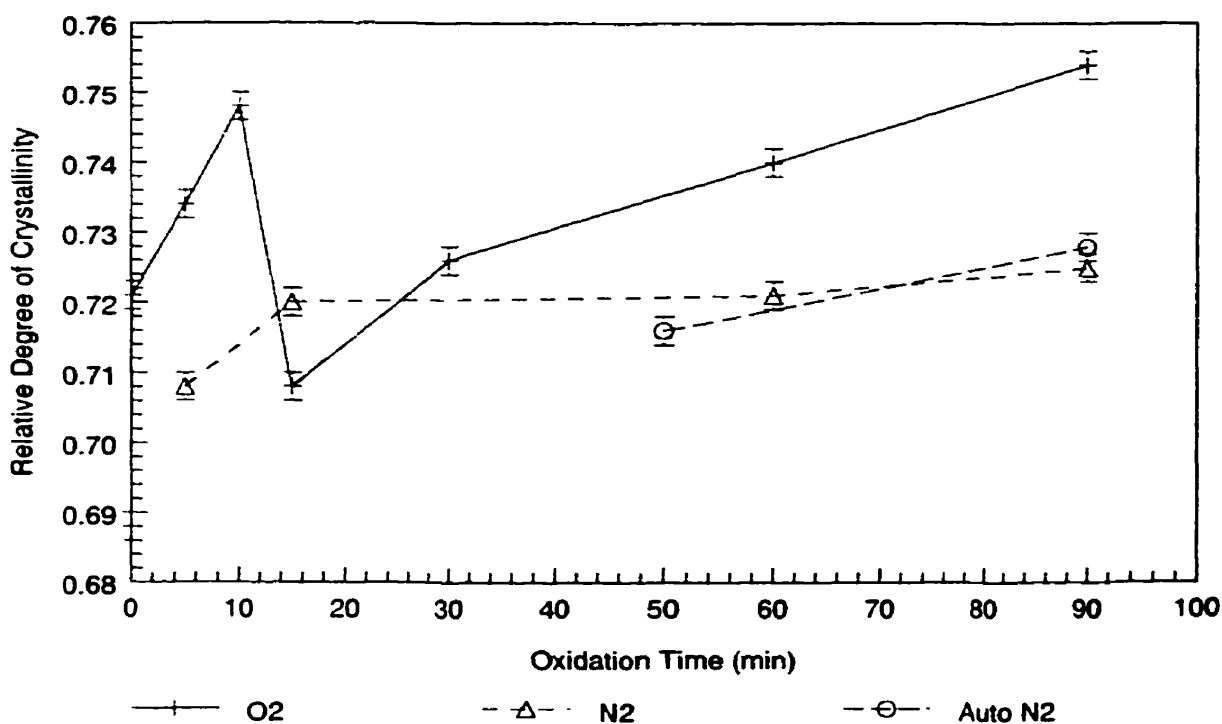


**Figure 4.3** FTIR spectroscopy data for Q-90 showing the relative degree of crystallinity as a function of oxidation time.

The Q-90 samples treated with oxygen show an identical profile as that of Figure 4.2 that deals with the x-ray diffraction analysis. There is a steady increase in the profile at the beginning of oxidation then a sharp decline followed by another less dramatic increase. Once again the decrease in crystallinity occurs at 15 minutes. In comparing the two sets of data determined by independent techniques, it is evident that the decrease in the relative degree of crystallinity at 15 minutes may be somewhat more significant than at first thought.

The two nitrogen curves show virtually identical data within the last 40 minutes in the reactor. Nitrogen and autoclaved nitrogen samples were also tested to examine how the oxygen initially present within the cellulose samples, contribute to cellulose degradation. The autoclaved nitrogen sample curve does not appear to be significantly lower than the non-autoclaved curve. This can be attributed to the fact that FTIR spectroscopy measures the intensity of certain bands in the infrared spectra that are sensitive to variation in the relative degree of crystallinity.<sup>108</sup> This method is able therefore to distinguish between the amorphous character of cellulose that surrounds the crystallites, unlike x-ray diffraction. It cannot, however, distinguish the amorphous domains that may lie within a crystallite as a defect from the crystallite itself.<sup>109</sup> Thus, oxygen that may have been present in the two series of nitrogen samples appeared to act on the cellulose in a similar way.

A third method is needed to confirm the results that have been presented thus far. This leads to the following discussion on  $^{13}\text{C}$  solid state NMR spectroscopy with cross polarisation and magic angle spinning.

#### **4.2.3 $^{13}\text{C}$ Solid State NMR Spectroscopy**

The method of  $^{13}\text{C}$  nuclear magnetic resonance (NMR) spectroscopy with magic angle spinning and cross polarisation is sensitive to short range order.<sup>114,115</sup> Carbon atoms in different environments have different chemical shifts and the sensitivity of this method is able to determine the number of carbon atoms in a particular environment.<sup>117</sup> The relative degree of crystallinity is determined by probing the cellulose structure down to the molecular level. This method disregards the defects that are normally present within the cellulose crystallites from the relative degree of crystallinity calculations. Not only is the material surrounding the crystallite considered part of the amorphous domain but also the defects within the crystallite.

The relative degree of crystallinity can be interpreted using solid state NMR in two ways: deconvolution and proton spin-lattice relaxation times. Triplicate measurements were not carried out on any of these Q-90 samples because of the long time required to obtain each spectra. There may be doubt regarding the reliability of similar results but since there is a consistent trend in the results from this NMR method



and the x-ray diffraction and FTIR spectroscopy methods, the analysis appears to be valid. The data is presented in the following sections.

### ***Deconvolution of NMR Signals***

In the same manner as for x-ray diffraction and FTIR, Q-90 pulp samples were subjected to oxygen, nitrogen and autoclaved nitrogen in a kettle reactor from 0 to 90 minutes and then characterised using solid state NMR. Nitrogen and autoclaved nitrogen samples were examined to locate any possible contribution of the oxygen, initially present within the cellulose samples, to cellulose degradation. To determine the area under each peak of the resulting spectra, the method of deconvolution was first examined.

The first relevant application of  $^{13}\text{C}$  solid state NMR to cellulose was by Maciel<sup>158,159</sup> and VanderHart.<sup>132,160</sup> In these studies it was shown that the C4 and C6 carbons exhibit two distinct resonances, each with the relative intensities within each pair, varying with the origin of the cellulose. As in the case of both C4 and C6, one of the peaks was considerable broader, it was concluded that the two peaks arose from crystalline and amorphous regions in the solid state. Furthermore, it was determined that these regions were in fact cellulose units in the interior and at the surface, respectively, of the cellulose fibrils. The surface units apparently experience a more variable local environment leading to a larger shift dispersion. Knowing that there are two environments, crystalline and amorphous, for each of the C4 and C6 carbons, a ratio of the areas is calculated to give the relative degree of crystallinity. Once the spectra were obtained a deconvolution of both the environments for the C4 and C6 carbons was carried out. The plots of the relative degree of crystallinity versus oxidation times are seen in Figures 4.4 and 4.5 for the C4 and C6 carbons respectively.

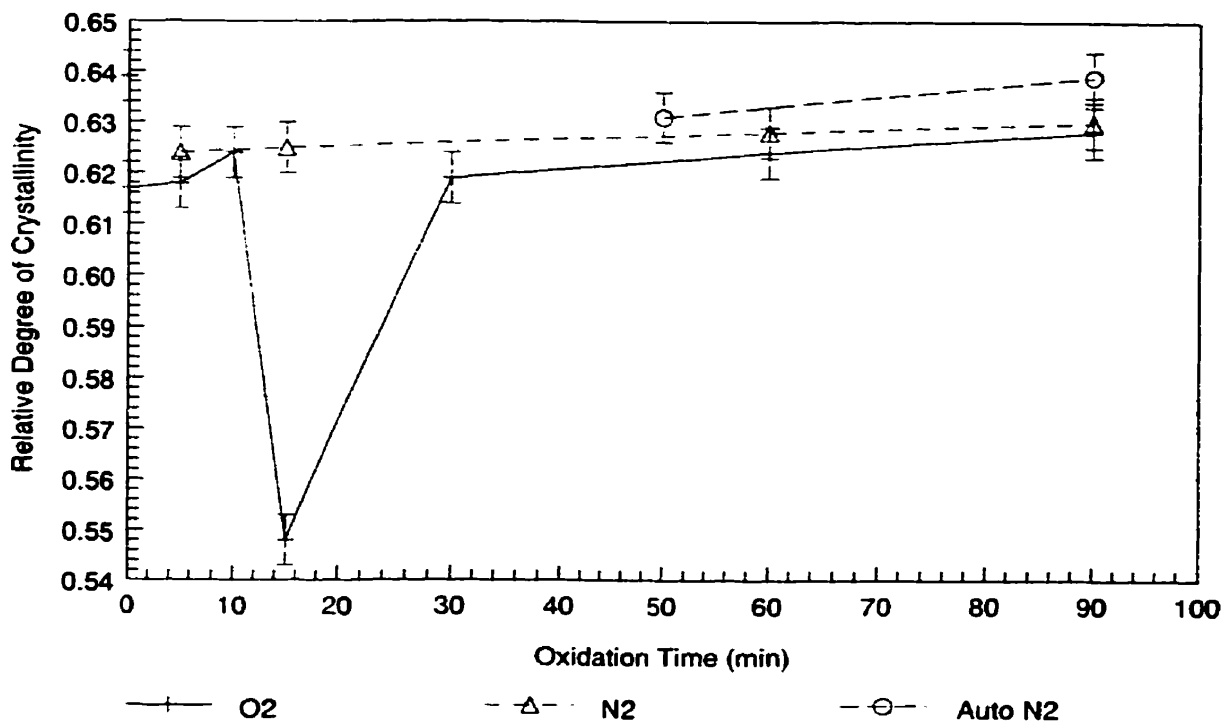


**Figure 4.4** Solid state NMR data for Q-90 showing the relative degree of crystallinity calculated from the C4 carbon contribution as a function of oxidation time.

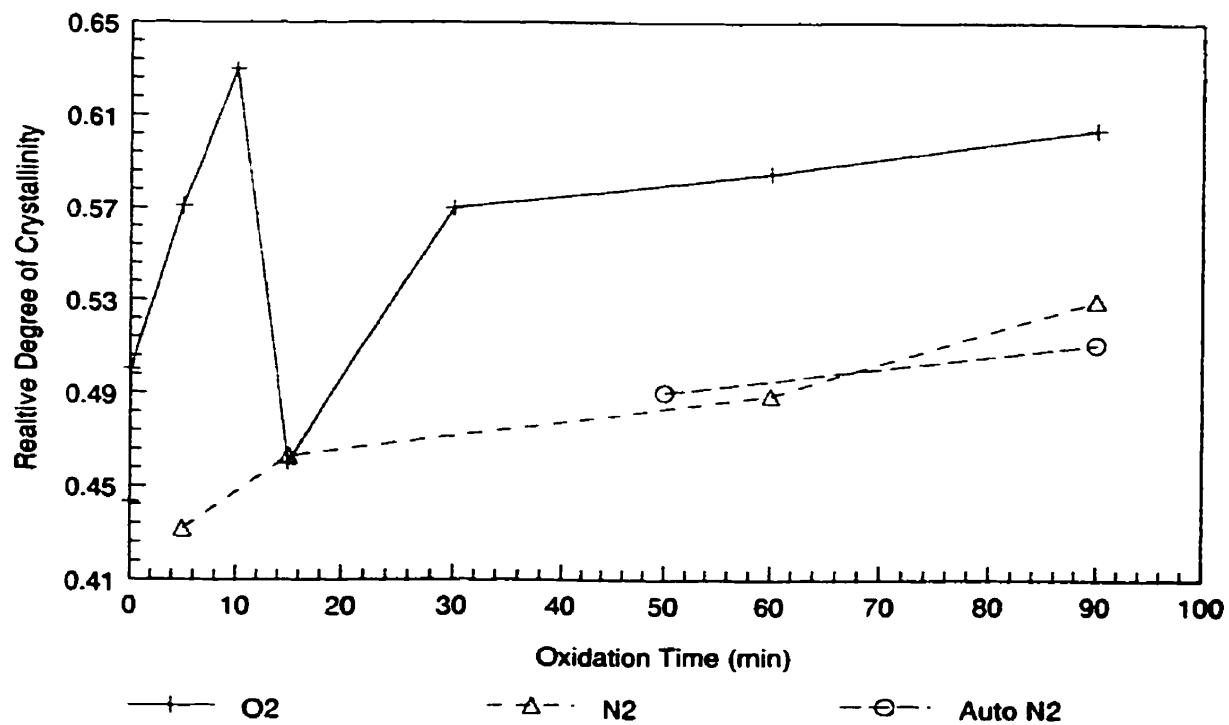


**Figure 4.5** Solid state NMR data for Q-90 showing the relative degree of crystallinity calculated from the C6 carbon contribution as a function of oxidation time.

In calculating the relative degree of crystallinity for the C4 carbon, a ratio of the areas for the peak indicating the crystalline environment was compared to the area of the peak for the amorphous and crystalline environments. The crystalline peak occurs at 89 ppm while the amorphous peak at 84 ppm on the NMR spectra.<sup>131</sup> In a similar fashion the degree of crystallinity for the C6 carbon was calculated. In this case the crystalline peak occurs at 65 ppm and the amorphous one at 63 ppm.<sup>132,159</sup>

Both Figures 4.4 and 4.5 show similar profiles with an initial increase in the degree of crystallinity followed by a decrease and then another increase for oxygen treated samples. The precise magnitude of the relative degrees of crystallinity are however somewhat different. When comparing these two plots to the ones obtained from the x-ray diffraction and FTIR spectroscopy there does not appear to be an obvious correlation. However, when the effects of the two crystalline environments are compared with the summed values for both the crystalline and amorphous environments a clear understanding emerges. This analysis is presented in Figure 4.6.

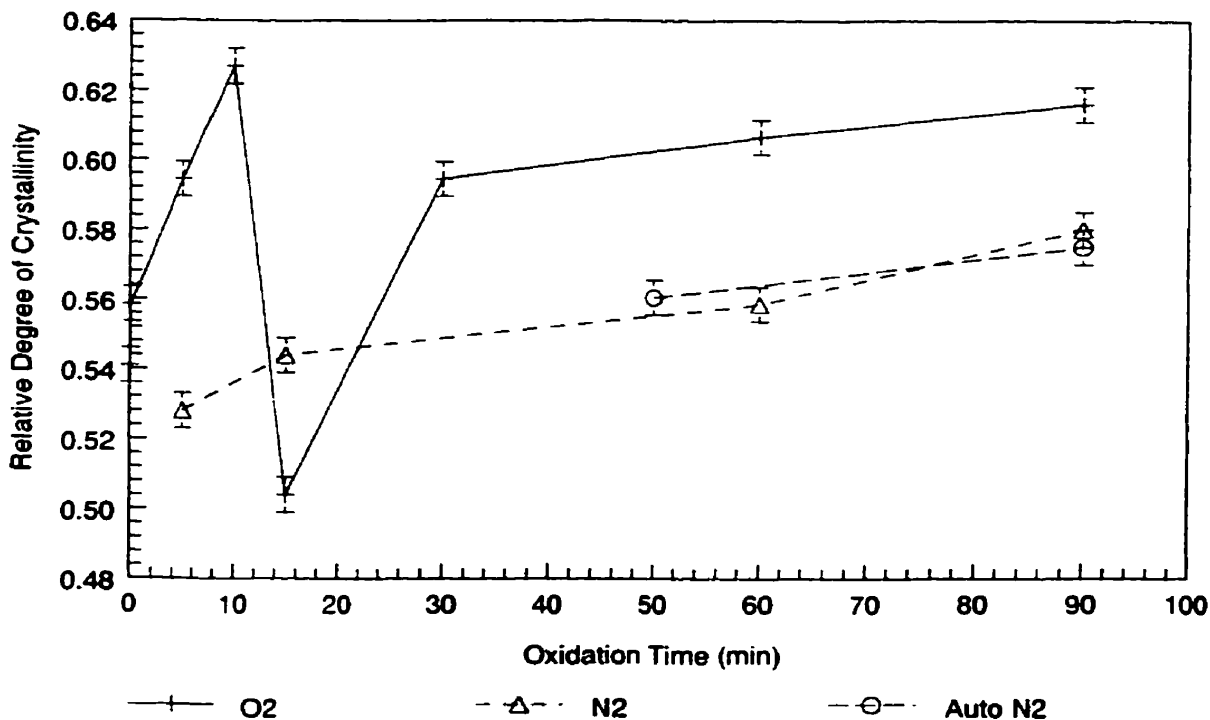


**Figure 4.6** Solid state NMR data for Q-90 showing the relative degree of crystallinity calculated from the total C4 and C6 contributions as a function of oxidation time.

The relative degree of crystallinity is calculated from the ratio of the sum of the areas under the two peaks at 89 ppm and 65 ppm to the total sum of the areas for the four peaks. The combined data of the C4 and C6 analyses are analogous to the plots presented from the x-ray diffraction and FTIR spectroscopic analyses. In Figure 4.6, initially there is a steady rise in the relative degree of crystallinity in the oxygen curve followed by a dramatic decrease at 15 minutes after which there is a steady rise again. The nitrogen and autoclaved nitrogen sample curves appear to be the same for the same reason noted previously for the FTIR spectroscopic analysis.

### ***Proton Spin-Lattice Relaxation Time***

Relaxation times can be related to molecular motion. The variation in proton spin-lattice relaxation times for cellulose can be attributed to the modification of its macromolecular structure. Large variations may affect the functional groups of the cellulose by inducing hydrogen bonding interactions. The formation of hydrogen bonds by free OH groups can alter the physical and dynamic mechanical properties of cellulose and their proton spin-lattice relaxation times.<sup>161</sup> Documented literature showing the variation of spin-lattice relaxation times for a number of chemically modified wood samples provided information regarding small changes in the composition of carbohydrates caused by various chemical agents.<sup>162</sup>

The time a proton takes to relax in an amorphous domain is different than the time it takes to relax in a crystalline domain. The relaxation time is longer for the protons in the crystalline domains than within the amorphous regions because of the restrictions imposed on their mobility by hydrogen bonding.<sup>122</sup> Hydrogen bonding in the crystalline cellulose chains are more numerous than in the amorphous domain. The relaxation time is an average measurement of both these times.<sup>122</sup> An increase in the overall relaxation time indicates that the relative degree of crystallinity is increasing.

The proton spin-lattice relaxation time is an alternative method of calculating the relative degree of crystallinity in cellulose samples. The relative degree of crystallinity cannot be calculated from the relaxation time although relaxation time is directly related to relative degree of crystallinity. The relaxation times for the samples that were

pressurised in the kettle reactor with oxygen were determined. Figure 4.7 shows a plot of these relaxation times versus the oxidation times.

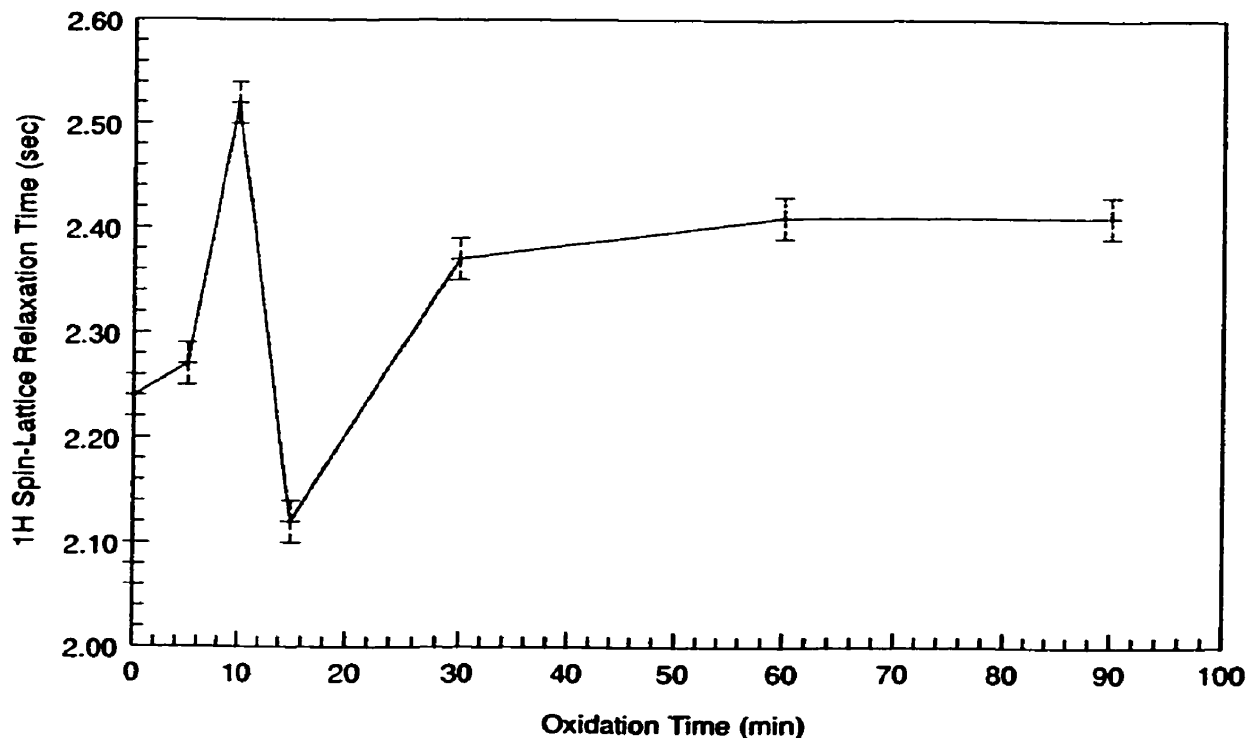


**Figure 4.7** Proton spin-lattice relaxation times for Q-90 as a function of oxidation time.

The curve is strikingly similar to all other curves presented so far for oxidised samples. Initially there is an increase in the proton spin-lattice relaxation time followed by a decrease at 15 minutes of oxidation and then a steady increase. These trends in relaxation times can be correlated to variations in the crystalline and amorphous domains. In the amorphous domain there is less intramolecular hydrogen bonding between cellulose molecules compared to the number of hydrogen bonds that are present in the crystalline domains. Molecules in the amorphous domain have a greater mobility and as such take a shorter time to relax. The longer relaxation times shown in the figure above most likely indicate an increase in the relative degree of crystallinity. Relaxation times for control samples are similar to literature values.<sup>124,125</sup>

### 4.3 Reproducibility of the Methodology

Three methods of determining the relative degree of crystallinity on Q-90 pulp have been presented for which the data shows a sudden decrease in the relative degree of

crystallinity towards an oxidation time of approximately 15 minutes. This pattern was typical for all oxygen treated samples. To ascertain the significance of this decrease in the relative degree of crystallinity, the oxidation of additional samples were repeated a second time with specific emphasis around the 15 minute time range. The oxidation times chosen were 5, 10, 15 and 30 minutes to determine if the minimum could be repeated with any degree of accuracy. For each time, two oxidations were carried out and the data was analysed in duplicate using x-ray diffraction and FTIR spectroscopic techniques. For the case of solid-state NMR analysis, triplicate measurements were recorded for each of the two oxidations.

#### 4.3.1 X-ray Diffraction

The data of both oxidation tests analysed by x-ray diffraction are shown in the following figure.

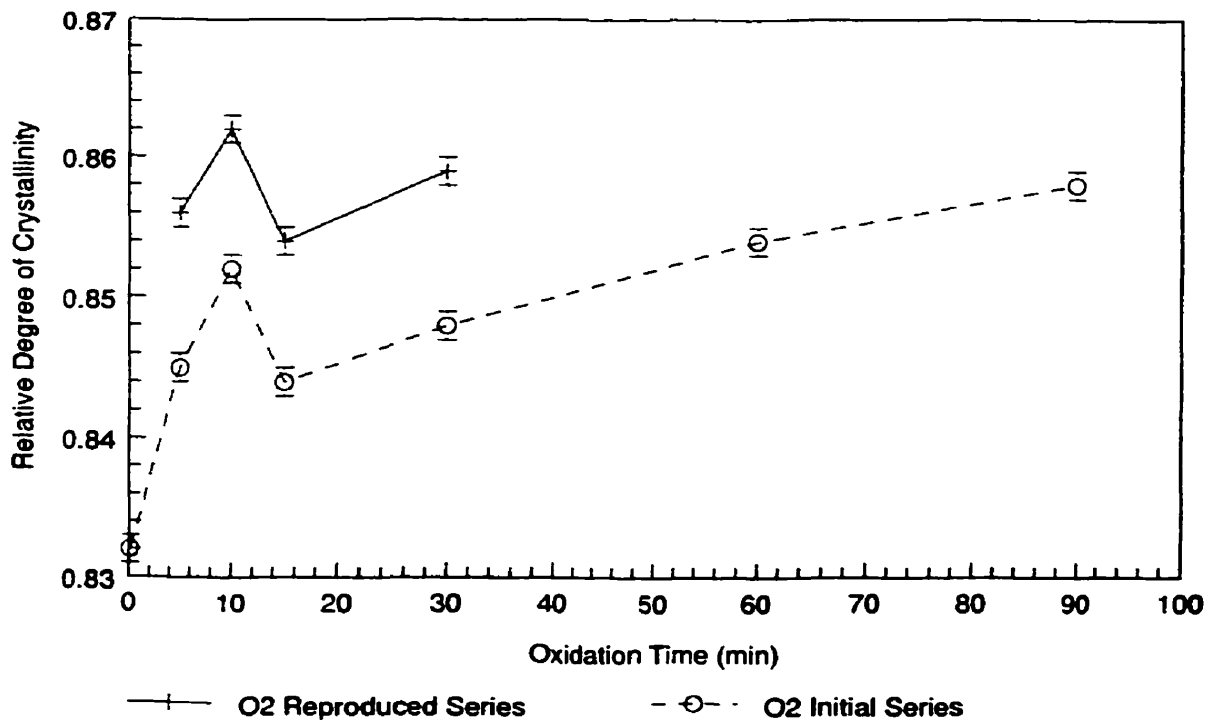


**Figure 4.8** X-ray diffraction data for the Q-90 reproducibility measurements of the relative degree of crystallinity as a function of oxidation time.

The changes in the relative degree of crystallinity for both series of tests are virtually identical except for a shift upward of the repeated data. The error associated with each

value in both curves is by far smaller than the change in the relative degree of crystallinity from one point to the next. A possible reason for the variation in the data for each series of curves may be due to the elapsed time of several months between the original measurements and reproducibility runs. Since several months had elapsed before the duplicate measurements were carried out a real but explainable discrepancy is apparent. The Q-90 pulp was placed in a large plastic bag from which only a relatively small amount of sample was required for each measurement. In the time that passed between the original and the repeat measurements, the pulp was used for other unrelated experiments. It was assumed that the pulp within the bag was well homogenised, however, the technique of x-ray diffraction is able to detect slight variations in homogeneity.<sup>91</sup> These variations translated to the shift upward in the new curve. Despite this it is still interesting to note that the minimum in the curve is obvious for both oxidation runs.

#### **4.3.2 FTIR Spectroscopy**

In carrying out the second series of FTIR spectroscopic measurements, the same care was used to prepare the pellets, the pulp and the potassium bromide concentrations within it. The purge time in the instrument chamber was regulated to the same degree as the initial measurement and the spectra obtained and analysed in an identical manner. The data showing the original and duplicate curves are shown in Figure 4.9.

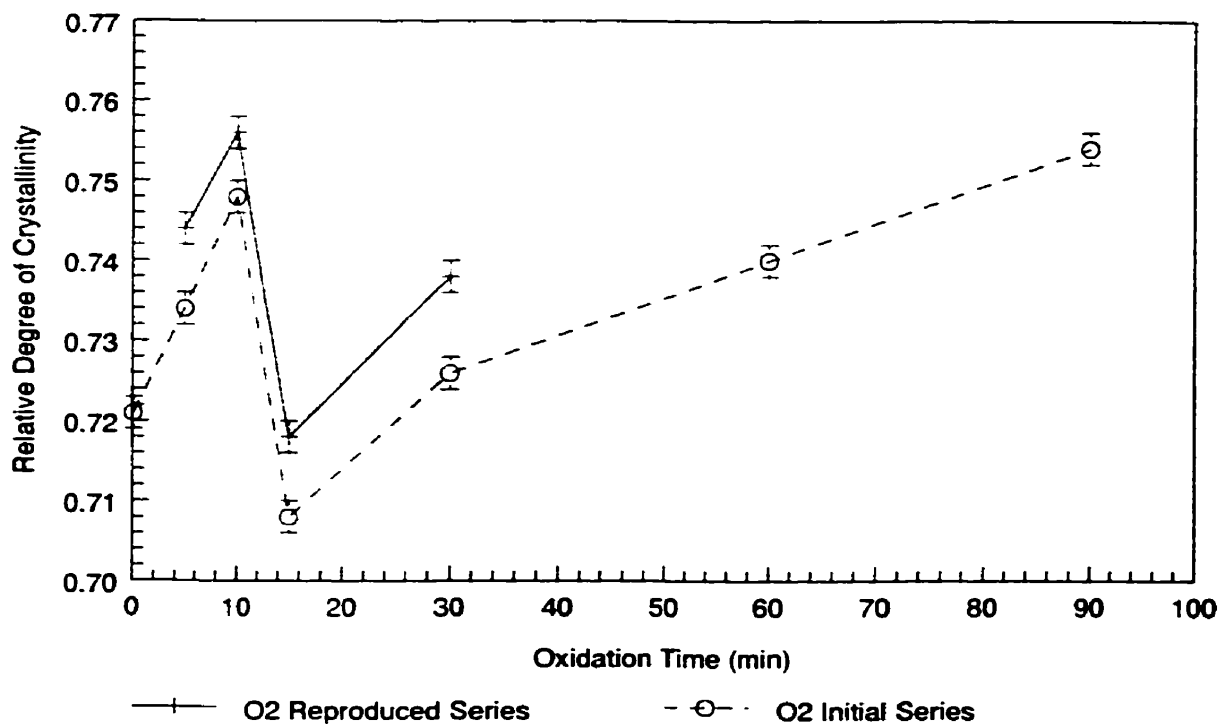


**Figure 4.9** FTIR data for the Q-90 reproducibility measurements showing the relative degree of crystallinity as a function of oxidation time.

Once again the data for the duplicate measurements concur well with the original curve. The profile of the curve is reproducible with a consistent upward shift, possibly due to the homogeneity difference between the Q-90 samples discussed in section 4.3.1.

#### 4.3.3 <sup>13</sup>C Solid State NMR Spectroscopy

The same analyses were used to examine duplicate measurements of the relative degree of crystallinity by the solid state NMR technique.

##### *Deconvolution of NMR Signals*

The second set of measurements was carried out in triplicate for each oxidation time to obtain the spectra. The acquisition of the data was performed in the same manner as previously discussed in section 4.2.3. Deconvolutions and graphs for both the C4 and C6 carbons were plotted and identical data were produced. Figure 4.10 shows the relative degree of crystallinity obtained by taking the total of the areas under the peaks at 89 ppm and 65 ppm for C4 and C6 and dividing by the sum of the area of the four peak.



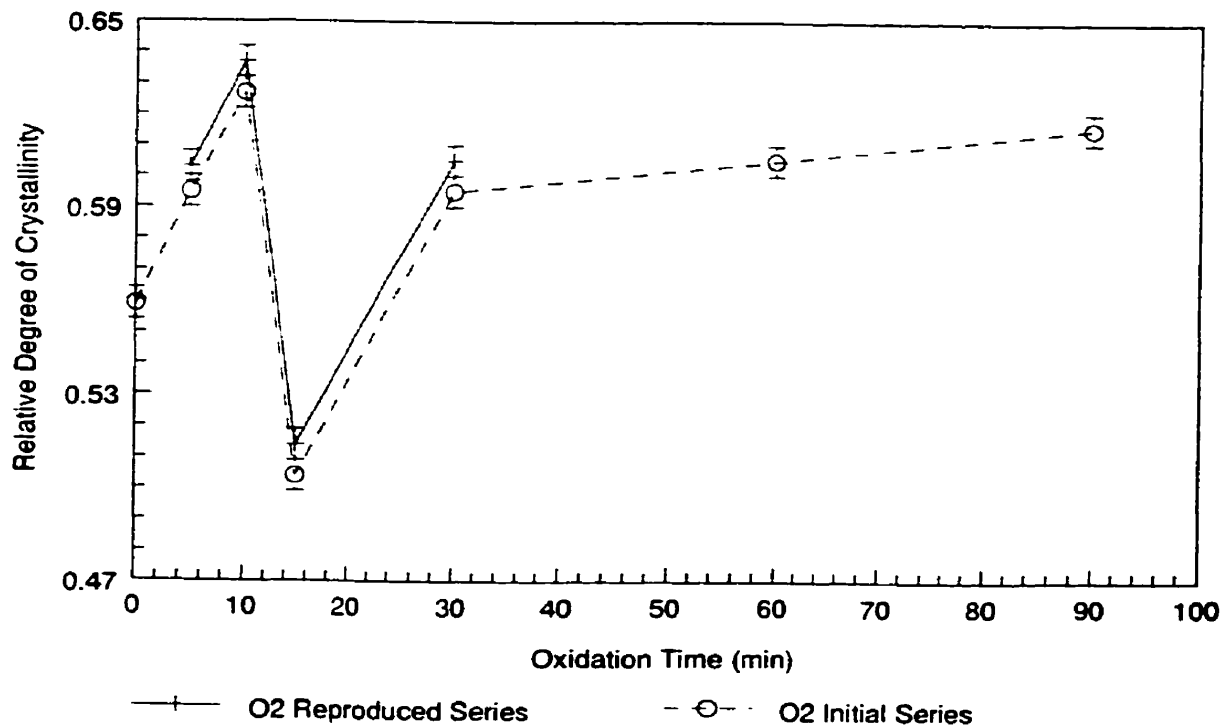


**Figure 4.10** Solid state NMR data for the Q-90 reproducibility measurements showing the relative degree of crystallinity (calculated from the total C4 and C6 contributions) as a function of oxidation time.

Once again the data are virtually identical. The two curves almost overlap with each other but the duplicate measurement seems to be somewhat higher. The difference in the two curves is much smaller than the difference in the curves for the x-ray diffraction and FTIR. This is because solid state NMR takes into account fewer defects within the crystallite and excludes the amorphous character around the crystallite when determining the crystalline component.<sup>101</sup>

#### ***Proton Spin-Lattice Relaxation Time***

The samples were conditioned in the same way prior to measurement and subjected to the same conditions as the initial series of measurements to obtain the proton spin-lattice relaxation times. The plot of the duplicate measurement along with the original curve is seen in Figure 4.11.

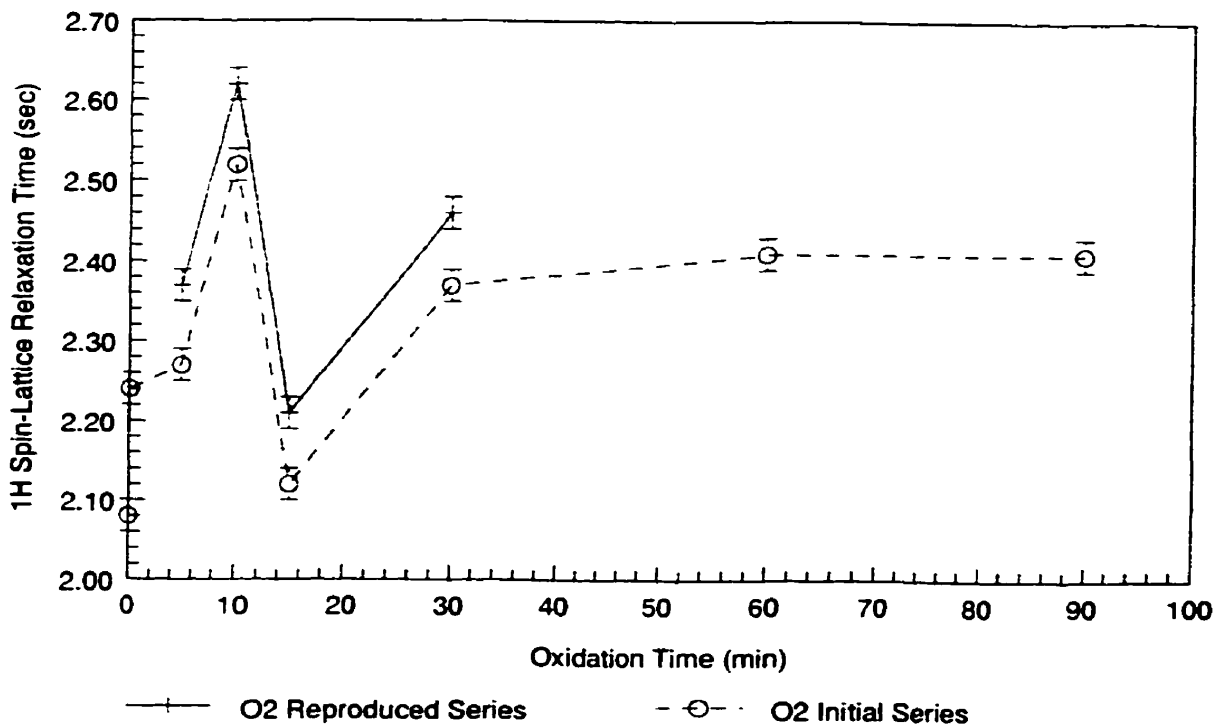


**Figure 4.11** Proton spin-lattice relaxation times for the Q-90 reproducibility samples as a function of oxidation time.

Once again the two curves are identical in shape. Due to the slightly higher crystalline character in the duplicate sample, the relaxation times are longer.

#### 4.3.4 Summary of Q-90 Reproducibility Measurements

By carrying out duplicate oxidations on the Q-90 pulp and by repeating the crystallinity determinations using three different and independent techniques, it was shown that a minimum in the relative degree of crystallinity occurs at 15 minutes. Evaluation of the x-ray diffraction, FTIR spectroscopy and solid state NMR spectroscopy data concludes that these techniques are valid to examine changes in pulp crystallinity. All three techniques provided reproducible and consistent data. The error associated with each point on any curve is much less than the change in the relative degree of crystallinity. The error associated with reproducibility runs was insignificant.

In all cases this reproducible profile shows three different areas where the kinetics of the reaction are different. The first area occurs from 0 to 10 minutes. In this range of oxidation a steep rise in the relative degree of crystallinity takes place. In the second

segment of the curve, there is a dramatic decrease in the relative degree of crystallinity. This occurs between 10 and 15 minutes. The remaining area is from 15 minutes onward. Here it is evident that there is, once again, an increase in the relative degree of crystallinity.

It can be concluded that the minimum in the relative degree in crystallinity that occurs at 15 minutes is significant and is due to some other factor than experimental technique. This critical point suggests that the overall kinetics of the reaction may be influenced by the hemicellulose content within the Q-90 pulp. Q-90 pulp contains approximately 80% cellulose and 20% hemicellulose. Like cellulose, hemicellulose can be oxidised by oxygen. The changes in the hemicellulose due to its oxidation may impact the relative degree of crystallinity. The contribution of the hemicellulose in the oxidation reaction therefore merits further investigation to understand the change in crystallinity of pulp.

## Chapter 5

### Results & Discussion – Part II

#### Relative Degree of Crystallinity for Various Celluloses

---

The evaluation of three instrumental techniques to examine changes in the relative degree of crystallinity for one pulp (Q-90) was previously discussed. An effort was initially made to ascertain that the oxidation and crystallinity evaluation methodology used in this work was valid and reproducible. Having established that the effect of oxygen on cellulose displays a peculiar behaviour on the relative degree of crystallinity, attention on further understanding this effect is examined. In order to delineate the effect of hemicellulose on the observed outcomes, the logical choice at this stage was to oxidise a cellulose sample whose hemicellulose content was dramatically reduced.

Cellulose varies in terms of the size of the crystallite, the packing, the number of defects present within the crystallite, the amount of amorphous character initially present, and the purity of the cellulose.<sup>70</sup> Cellulose crystallites from varying sources of cellulose can differ in crystallite width and crystallite packing.<sup>104</sup> Moreover, the interior of the crystallite may vary in other ways. Some celluloses may have more crystallite kinks causing a less orderly molecular arrangement which increases the percentage of defects within the crystallite.<sup>97</sup> The purity of cellulose is an indication of whether other contaminants such as lignin and hemicellulose are present.

This chapter examines hemicellulose reduced pulp, cotton and Avicel using the proven instrumental techniques (x-ray diffraction, FTIR spectroscopy and solid state NMR spectroscopy) to observe oxygen attack and the regions in which it occurs. The relative degree of crystallinity is used as an indicator of how the carbohydrate component in the pulp is altered during oxygen delignification.

##### 5.1 Hemicellulose Reduced Pulp

A hemicellulose reduced pulp was produced by treatment of the Q-90 fully bleached softwood pulp. The treatment was modified from a procedure outlined by

Beelik.<sup>147</sup> In Beelik's procedure, three stages were followed to selectively extract hemicellulose from a similar softwood pulp. In the first stage, barium hydroxide was used to remove xylan. In the second and third stages, potassium hydroxide and sodium hydroxide were used respectively to remove galactoglucomannan and glucomannan. The drawback of this procedure is that it does not remove any arabinose sugars which make up part of the hemicellulose content. In addition the high caustic content used could somewhat change the conformation of the cellulose.<sup>163</sup> The change that occurs is due to mercerisation of some of the cellulose in which cellulose I is converted to cellulose II in an irreversible manner.<sup>163</sup> However, the total conversion is low since the concentration of sodium hydroxide used does not exceed 10%.

Many chemical and thermal treatments cause changes in the crystal lattice of cellulose.<sup>61</sup> If a cellulose sample is treated with alkali solution the cellulose swells to various extents depending on the temperature and the concentration of alkali. The sodium ion has a favourable diameter (0.276nm) which is able to widen the smallest pores down to the space between the lattice planes and advance into them.<sup>164</sup> With increasing alkali concentration the hydroxyl groups become more and more accessible for water. Alkali treatment with sodium hydroxide causes not only a widening up of the lattice but also a change in the conformation and a shift of the lattice planes.<sup>165,166</sup>

The swelling of cellulose with an aqueous solution of sodium hydroxide is an important commercial treatment. It is called mercerisation after its discoverer, John Mercer, who took a patent on the process in 1850.<sup>167</sup> Changes in fine structure that occur when cellulose is mercerised include a conversion of the crystal lattice from cellulose I to II, a reduction in the crystallite length and a reduction in the degree of crystallinity.<sup>73</sup> These changes have been tracked using x-ray diffraction.<sup>167</sup>

The most important alternative crystalline form is cellulose II. This form results from treatment of cellulose in concentrated alkali, such as 18% sodium hydroxide, followed by thorough rinsing in water.<sup>167</sup> The treatment of cellulose in milder alkali concentrations, amounts mainly to a disruption and decrystallisation rather than a total transformation to a good cellulose II crystalline structure, however, some cellulose I is converted to cellulose II.<sup>168,169</sup> At low concentrations of sodium hydroxide, the diameter

of the hydrated ions is too large for easy penetration into the fibres.<sup>170</sup> As the concentration increases, the number of water molecules available for formation of hydrates decreases and therefore their size decreases. Small hydrates can diffuse into the crystalline regions as well as the pores of the low order regions. The hydrates can form hydrogen bonds with the cellulose molecules.

Beelik's technique was modified in this study because it requires large quantities of base. Instead three successive extractions were applied to the pulp using sodium hydroxide each time. A carbohydrate analysis was conducted on the original pulp and on the hemicellulose reduced pulp using both treatment methods. The result of this analysis is noted below.

Sample Pulp	Treatment	Arabinose	Xylose	Mannose	Galactose	Glucose	Total (%)
Q-90	Original	0.7	10.1	6.6	0.8	80.6	98.8
Hemicellulose Reduced	Beelik's Extraction	0.0	1.5	2.4	0.0	88.5	92.4
Hemicellulose Reduced	Modified Extraction	0.0	0.9	3.9	3.5	78.2	86.5

**Table 5.1** Carbohydrate analysis for Q-90 and hemicellulose reduced pulp obtained by two methods.

As can be seen from the glucose content for the original Q-90 sample the percentage of cellulose was roughly around 80%. After both extraction procedures the glucose content rose to above 90%. This implies that the hemicellulose content was reduced by more than half the original amount present in the Q-90 pulp. Although the hemicellulose is not totally eliminated a significant portion of it has been removed.

“Hemicellulose reduced pulp” in this study refers to the Q-90 pulp treated with sodium hydroxide to reduce the hemicellulose content of the pulp. The hemicellulose reduced pulp was oxidised in the kettle reactor for times of 5, 15, 30, and 90 minutes using pressurised oxygen. In addition using pressurised nitrogen an autoclaved sample

was also placed in the reactor. Each sample was analysed using the techniques of x-ray diffraction, FTIR spectroscopy and  $^{13}\text{C}$  solid state NMR spectroscopy.

### 5.1.1 X-ray Diffraction

The hemicellulose reduced pulp was prepared for analysis in the same manner as that of the Q-90 samples. The conditions for the analysis were also conducted as before. Figure 5.1 indicates the data of the hemicellulose reduced pulp using x-ray diffraction analysis.

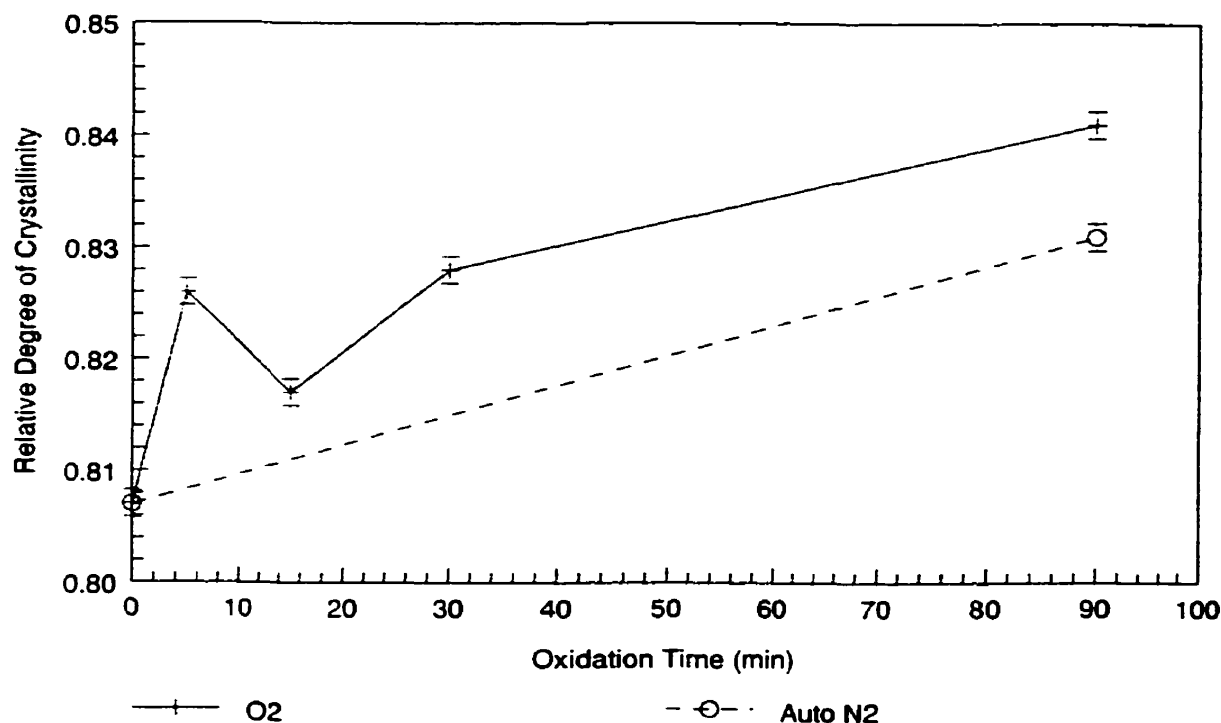


**Figure 5.1** X-ray diffraction data for hemicellulose reduced pulp showing the relative degree of crystallinity as a function of oxidation time.

In a manner similar to the Q-90 data shown in Figure 4.2, the features of the relative degree of crystallinity curve versus oxidation time are the same. The autoclaved nitrogen sample curve appears to be lower than the oxygen sample curve. The curve between the 0 and 90 minute oxidation times for the autoclaved nitrogen sample is provided as an illustration. Further investigation is required to examine if the curve is actually a straight line. To facilitate a comparison, Figure 5.2 shows the oxygen pressurised samples for the hemicellulose reduced and Q-90.

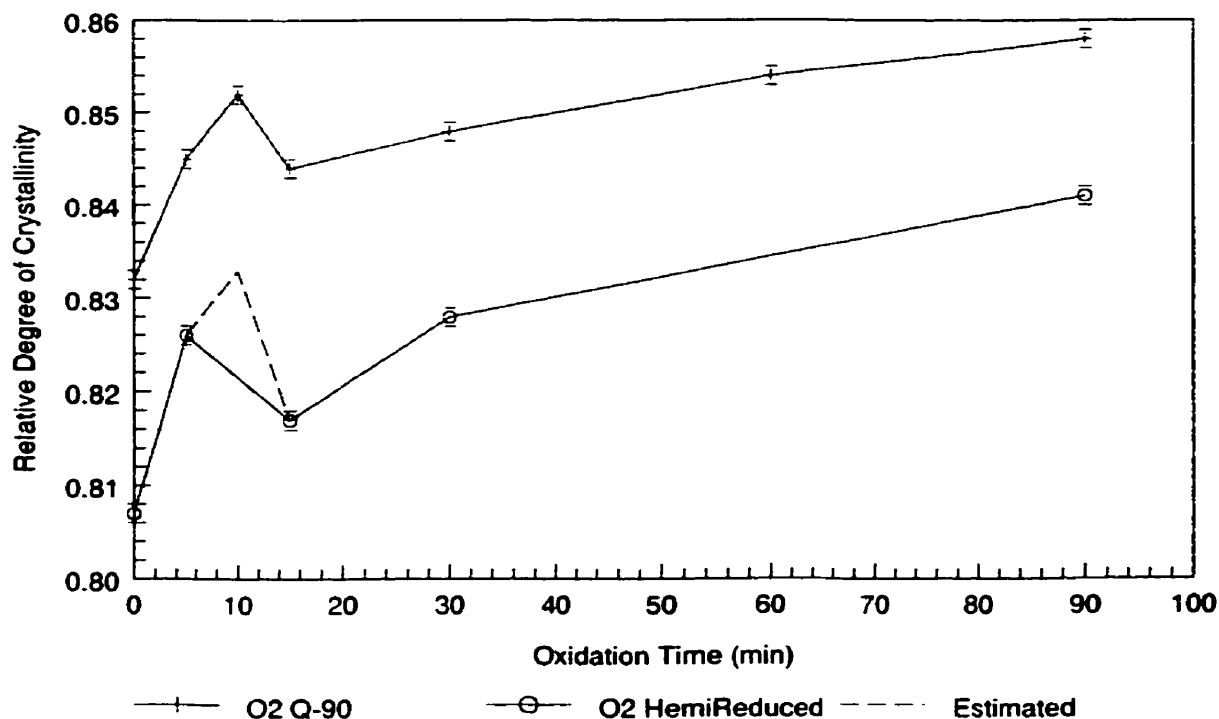


**Figure 5.2** A comparison of the x-ray diffraction data for Q-90 and hemicellulose reduced pulp showing the relative degree of crystallinity as a function of oxidation time.

Since a 10 minute time trial was not performed for the hemicellulose reduced samples an estimated value has been shown. This is illustrated by the dotted line on the hemicellulose reduced curve. Here it can be seen that the two curves are very similar in profile. The hemicellulose reduced curve is translated downward because some of the cellulose I originally present was converted to cellulose II as outlined in section 5.1. This conversion is most likely caused by the mercerisation that took place in removing the hemicellulose from the original pulp.<sup>163</sup>

### 5.1.2 FTIR Spectroscopy

The plot of the hemicellulose reduced samples showing the relative degree of crystallinity versus oxidation time is presented in Figure 5.3.



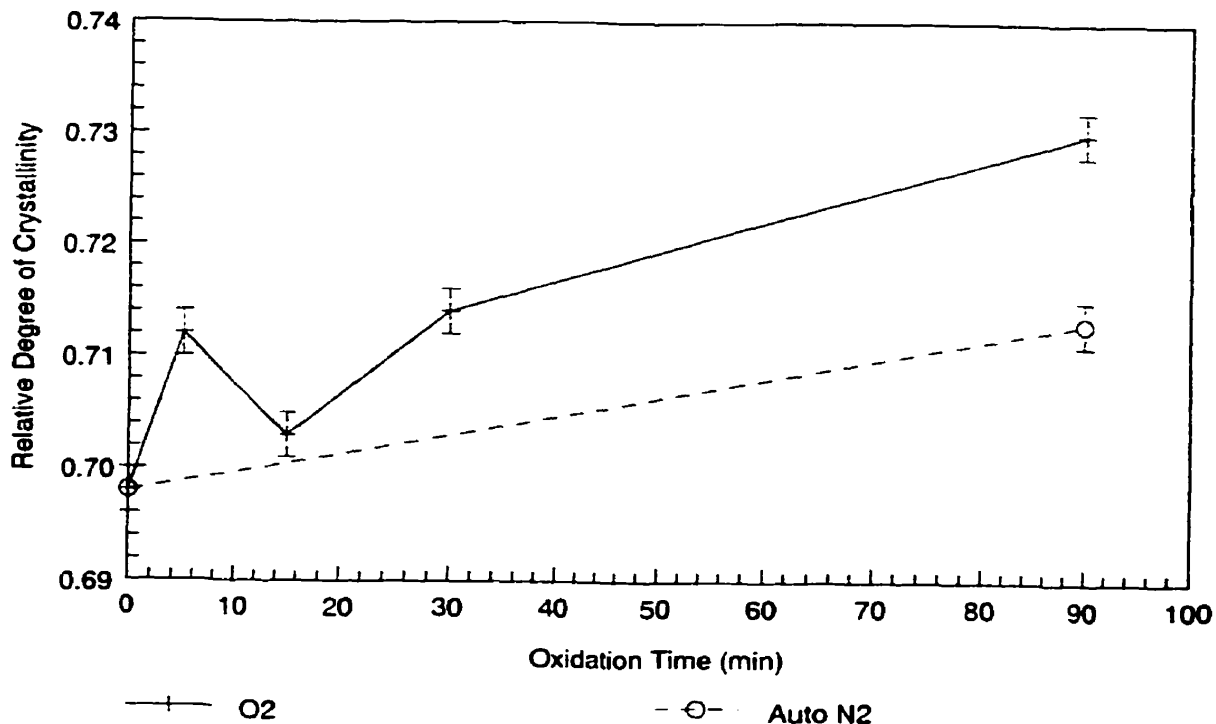


**Figure 5.3** FTIR data for hemicellulose reduced pulp showing the relative degree of crystallinity as a function of oxidation time.

FTIR data for hemicellulose reduced pulp are similar to Q-90 data.

### 5.1.3 $^{13}\text{C}$ Solid State NMR Spectroscopy

Solid state NMR spectroscopy was also used to analyse the hemicellulose reduced pulp samples. Both the methods of deconvolution and proton spin-lattice relaxation times were examined. These results appear in the following sections.

#### *Deconvolution of NMR Signals*

Figure 5.4 shows the relative degree of crystallinity obtained by taking the total of the areas under the peaks at 89 ppm and 65 ppm for C4 and C6 and dividing by the sum of the area of the four peaks.<sup>160</sup>

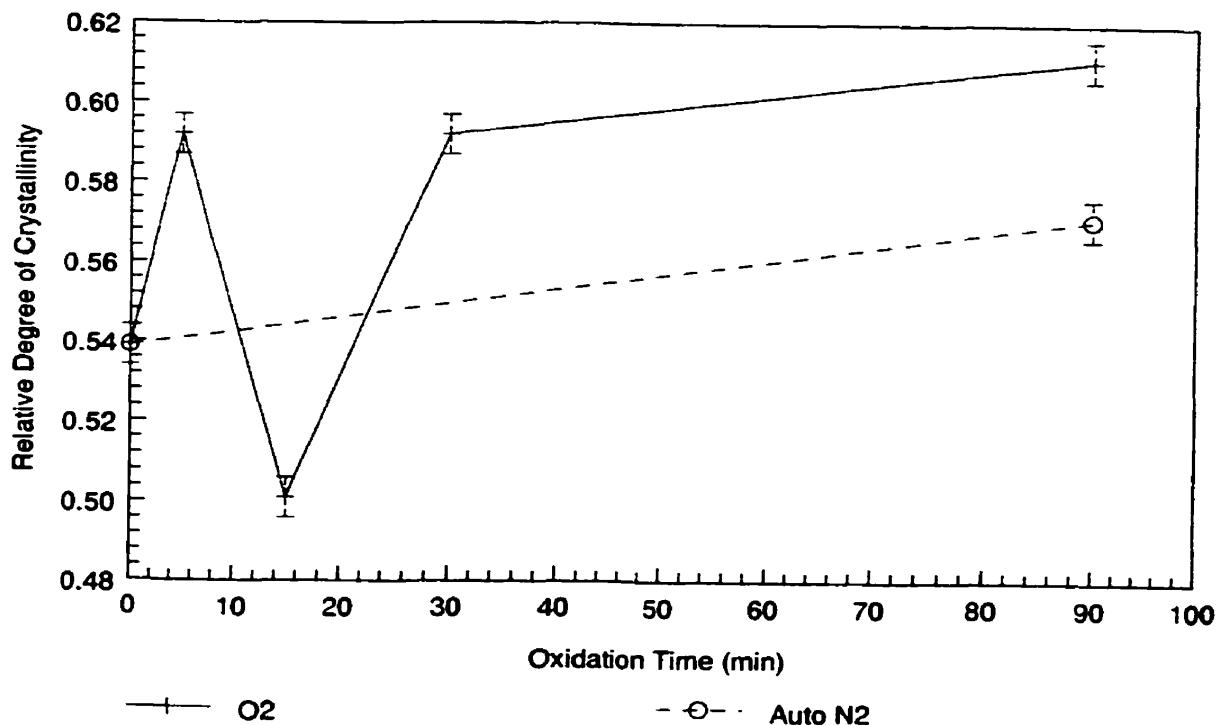


**Figure 5.4** Solid state NMR data for hemicellulose reduced pulp showing the relative degree of crystallinity calculated from the total contribution of the C4 and C6 carbons as a function of oxidation time.

The data observed from the curve above show the same consistent trends with that from the x-ray diffraction and FTIR spectroscopy. The prevalent increase, decrease and then increase is evident at the same times that had been outlined prior.

#### ***Proton Spin-Lattice Relaxation Time***

The proton spin-lattice relaxation times were measured for the hemicellulose reduced pulp samples that had undergone oxidation in the kettle reactor using pressurised oxygen. The data of these measurements are plotted against oxidation time in Figure 5.5 presented below.

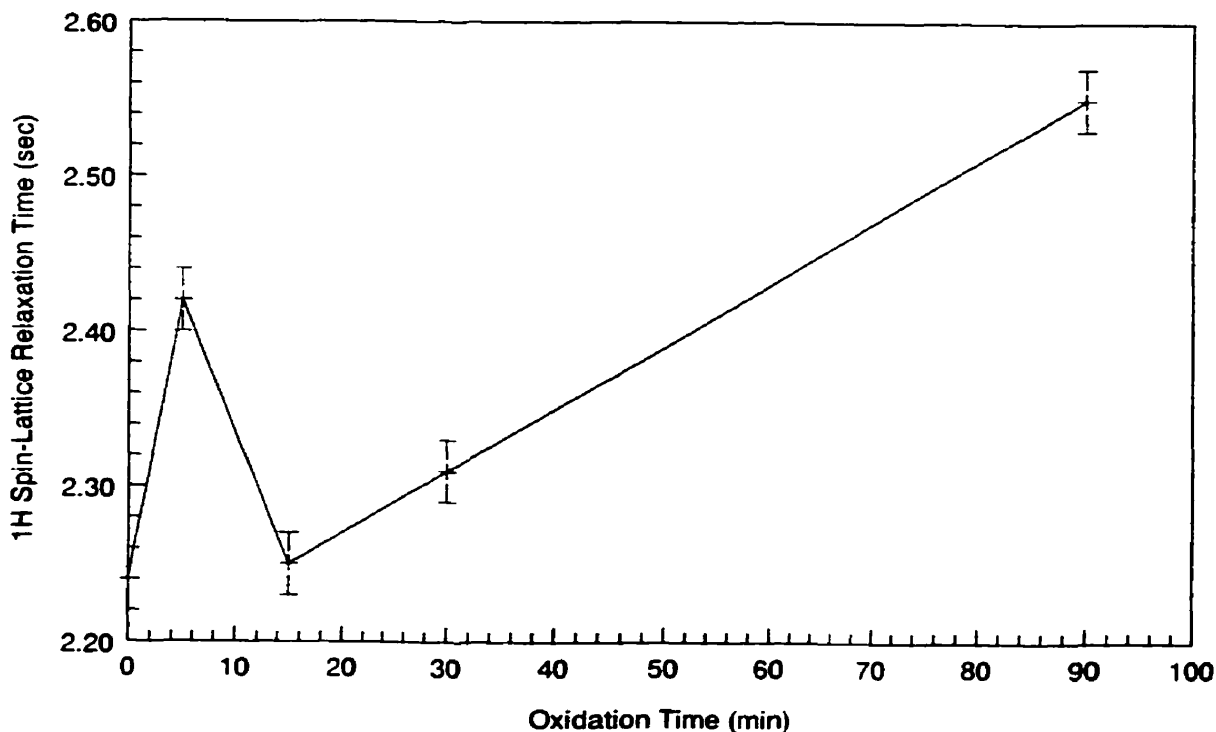


**Figure 5.5** Proton spin-lattice relaxation times for hemicellulose reduced pulp as a function of oxidation time.

The proton spin-lattice relaxation times portrayed above for the hemicellulose reduced pulp are longer than the Q-90 pulp relaxation times outlined in Figure 4.7. The profile of the curves in both the figures are the same. A possible speculation for the reason why the relaxation times are longer for the hemicellulose reduced pulp is due to the amount of cellulose I and II present in the samples. In removing the hemicellulose from the pulp some of the amorphous cellulose could have easily be transformed to cellulose II crystallites by mercerisation.<sup>163</sup> The total crystalline content (from cellulose I and II) would then be marginally higher for the hemicellulose reduced pulp. As such it would have longer relaxation times because solid state NMR spectroscopy is not able to distinguish between the two forms of cellulose present.<sup>99</sup> The results are consistent with the observations in the literature outlined in section 5.1.

#### **5.1.4 Summary of Hemicellulose Reduced Results**

For each of the three techniques, x-ray diffraction, FTIR spectroscopy and solid state NMR spectroscopy, the results of the hemicellulose reduced samples paralleled

those of the original Q-90 sample results. It appears that the cellulose was changed from cellulose I to II (Figure 5.2) due to mercerisation when removing hemicellulose from the pulp. This conversion was confirmed by examining at the x-ray diffraction spectra of the Q-90 pulp and comparing them to the hemicellulose reduced pulp.

Based on the data presented in this section it is clear that the minimum in the relative degree of crystallinity, occurring at 15 minutes, is still prevalent in these hemicellulose reduced samples. Hence, hemicellulose does not appear to contribute to this phenomenon. The minimum in the relative degree of crystallinity was still visible at the 15 minutes of oxidation. Initial and later increases in the relative degree of crystallinity were present with a dramatic decrease in between.

The critical change in crystallinity in the oxygen treated samples indicates that oxygen plays an important role in degrading the pulp. Oxygen acts on the cellulose in several ways as discussed earlier to change the overall relative degree of crystallinity with time. Experimental and procedural technique variations as well as the contribution of hemicellulose in oxygen delignification can be ruled out as playing a significant role.

## **5.2 Cotton Cellulose**

To better understand what may be taking place as oxygen attacks cellulose another cellulose model was chosen. Cotton cellulose with the same degree of polymerisation as the Q-90 sample was used. Both the Q-90 pulp and cotton cellulose samples initially had a degree of polymerisation of about 1000 (actual data for the degree of polymerisation determined by viscosity measurements can be found in Table 6.1). The difference between these two types of cellulose is predominantly in the crystallite composition. The crystallites of cotton cellulose are packed in a more orderly fashion than softwood cellulose such as Q-90.<sup>171</sup> The packing of cotton cellulose is also more dense.<sup>97</sup> In addition, the width of the crystallites are larger in cotton cellulose than in softwood cellulose.<sup>171</sup>

Q-90 pulp is a cellulose that has undergone delignification and bleaching to achieve a high cellulose content. Delignification and bleaching impart stress on the crystalline domains. This stress causes more defects to occur within the crystallite.<sup>157</sup> Cotton cellulose is derived from a cotton plant instead of a tree. This implies less

variation in the cellulose as a whole because within different parts of a tree, the cellulose structure varies. The process to extract cellulose from a cotton plant is less intrusive than delignification and bleaching. Therefore more uniform crystallites and fewer defects exist. In addition the hemicellulose content is less than 2%.<sup>61</sup>

Variations in cotton cellulose exist when comparison is made with Q-90 cellulose. This makes it an ideal subject for a comparative study. The cotton cellulose samples were prepared in a manner similar to that of the Q-90 samples in the kettle reactor. The procedure was not modified in any way so that direct comparisons could be made. Oxidation times using pressurised oxygen were set at 0, 5, 15, 30, 60 and 90 minutes. A control sample was prepared but not placed in the reactor. Autoclaved samples were prepared using pressurised nitrogen in the kettle reactor for times of 5, 50 and 90 minutes. The samples were then analysed by x-ray diffraction, FTIR spectroscopy and solid state NMR spectroscopy.

### **5.2.1 X-ray Diffraction**

The preparation of the x-ray diffraction mounts and the procedure to obtain the diffractogram were executed under the same conditions as in previous tests. Triplicate measurements were made for each sample. The data is presented in Figure 5.6.

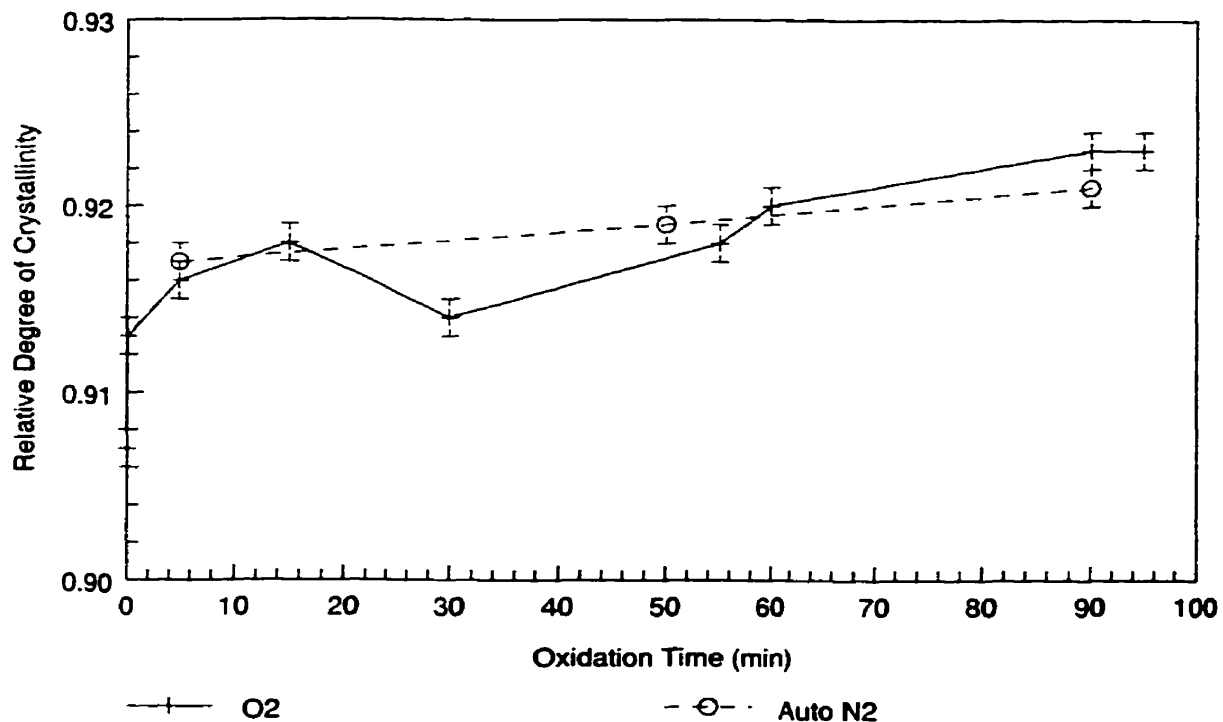


**Figure 5.6** X-ray diffraction data for cotton cellulose showing the relative degree of crystallinity as a function of oxidation time.

The curve for the oxygen pressurised samples appear to have a similar profile to the curves encountered for the Q-90 pulp. There is an initial increase in relative degree of crystallinity followed by a decrease and then another increase. The curves however differ in two ways. First, the initial increase in relative degree of crystallinity is not as sudden as the increase seen in the Q-90 data. Second, the minimum in the degree of crystallinity occurs at 30 minutes rather than at 15 minutes. Third, cotton is more crystalline possessing a relative degree of crystallinity of 0.91 as compared to Q-90 having a relative degree of crystallinity of 0.85 (as seen in Figure 4.2).

The autoclaved nitrogen curve overlaps the oxygen curve for the cotton cellulose. This was not evident before in other samples. Since there is better packing within the crystallites in cotton cellulose than in Q-90, and there are fewer defects within the crystallites, less oxygen is likely to be trapped within the cotton fibres.<sup>97,171</sup> The reduction in the amount of oxygen that is present means that there is less likelihood for chemical reactions to occur between the cellulose and oxygen.

### 5.2.2 FTIR Spectroscopy

Pellet preparation and sample analysis were conducted in the same way as previous FTIR spectroscopic measurements. The measurements for cotton cellulose were performed in triplicate. The data from FTIR spectroscopy analysis is provided in Figure 5.7.

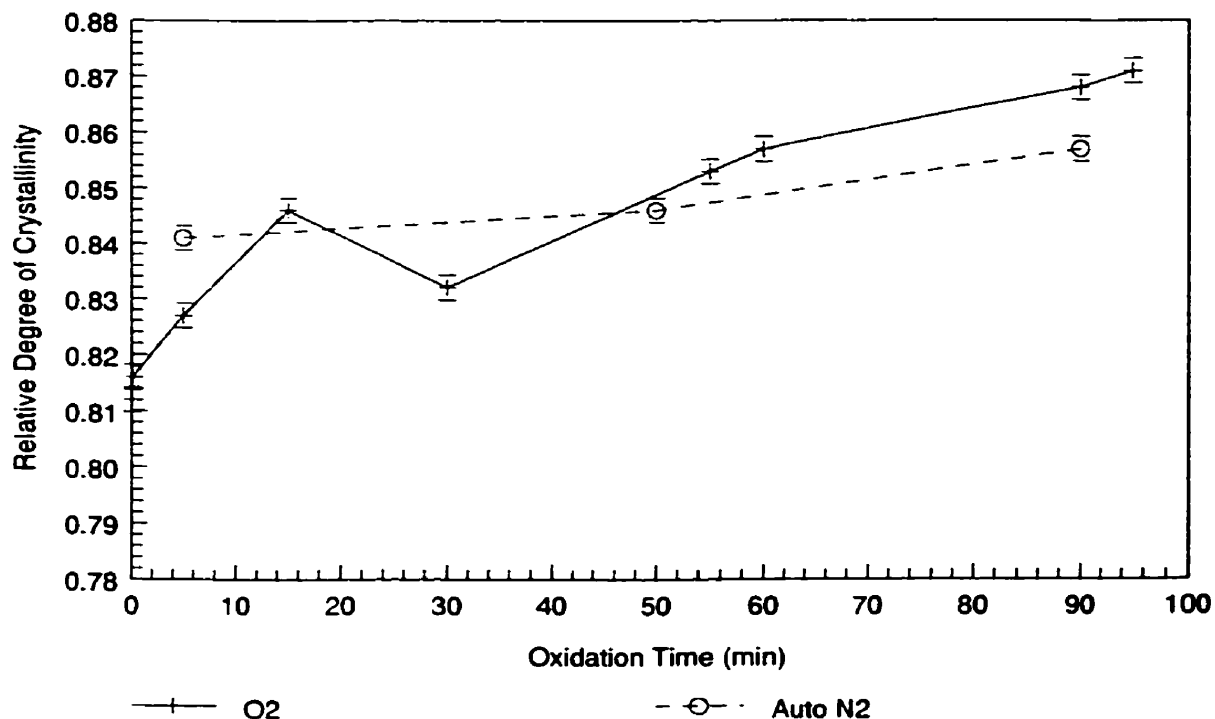


**Figure 5.7** FTIR data for cotton cellulose showing the relative degree of crystallinity as a function of time.

The curves of both the oxygen and the autoclaved nitrogen samples appear to have the same profile as those determined by x-ray diffraction analysis. There is an obvious decline in the relative degree of crystallinity at 30 minutes. In addition, the autoclaved nitrogen curve intersects with the oxygen curve in a similar fashion as before.

### 5.2.3 <sup>13</sup>C Solid State NMR Spectroscopy

To further confirm the results achieved so far for the cotton cellulose a third analysis was performed using solid state NMR spectroscopy. Once again the relative degree of crystallinity was determined by a deconvolution of the NMR spectra. In

addition to this, the proton spin-lattice relaxation times were also calculated. Although very time consuming all measurements were performed in triplicate.

### ***Deconvolution of NMR Signals***

The relative degrees of crystallinity calculated by deconvolution of both C4 and C6 carbons are shown in Figure 5.8.

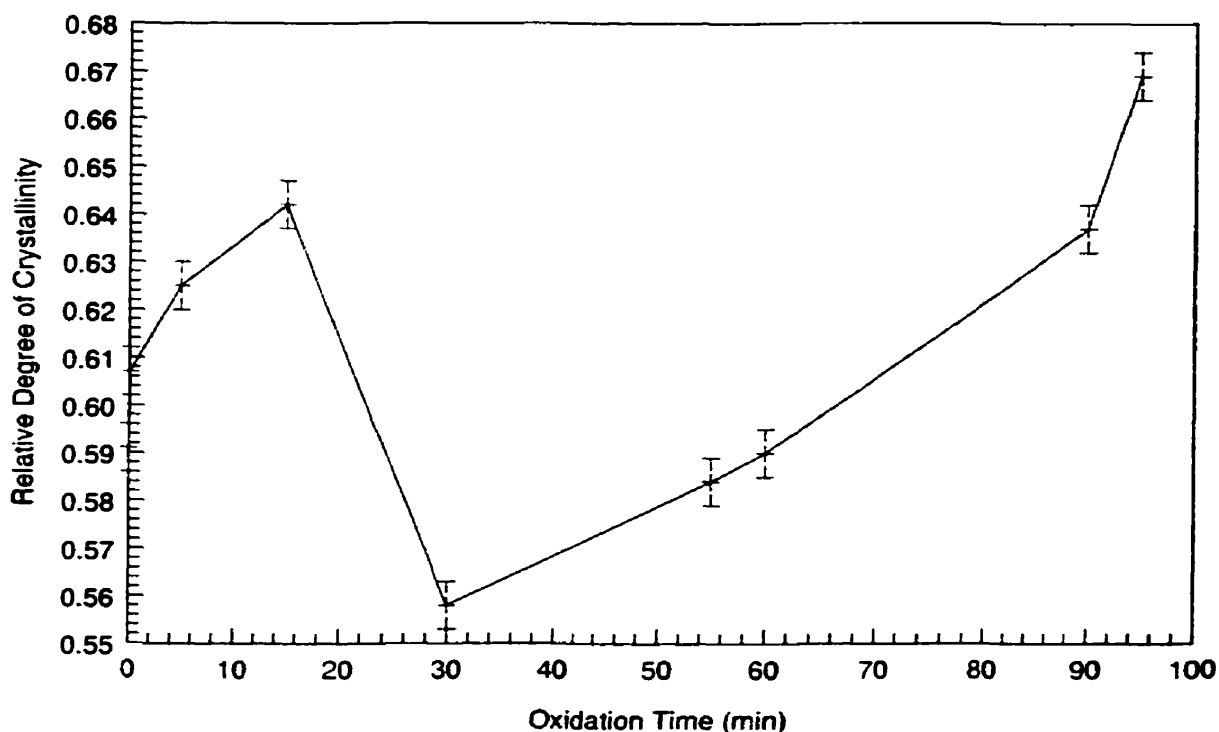


**Figure 5.8** Solid state NMR data for cotton cellulose showing the relative degree of crystallinity (calculated from the total contribution of the C4 and C6 carbons) as a function of oxidation time.

The figure indicates that the profile resembles the data obtained by measurements with x-ray diffraction and FTIR spectroscopy. The similarity of these curves is remarkable.

### ***Proton Spin-Lattice Relaxation Time***

The proton spin-lattice relaxation time measurements for the oxygen treated samples were also performed and the results obtained confirmed the trends that have shown up so far. There was a steady increase in the relaxation time initially followed by a drastic drop approaching 30 minutes. The relaxation times then increased again after 30 minutes of oxidation.



#### **5.2.4 Summary of Cotton Cellulose Results**

The data obtained by x-ray diffraction, FTIR spectroscopy and solid state NMR spectroscopy shows a consistent trend for oxygen pressurised samples. An increase in the relative degree of crystallinity followed by a decrease at 30 minutes and another increase. The change from decreasing relative degree of crystallinity to increasing relative degree of crystallinity occurred consistently at the 30 minute sample point and the profiles for the relative degree of crystallinity versus oxidation times using each technique were remarkably similar. When these curves are compared with the curves obtained with the Q-90 and hemicellulose reduced samples it is evident that the minimum in the relative degree of crystallinity moves from 15 minutes (for Q-90 and hemicellulose reduced pulp) to 30 minutes. Also the increasing slope of the relative degree of crystallinity in the first few minutes of oxidation is much steeper for the Q-90 and hemicellulose reduced samples than it is for the cotton samples. The curve for the nitrogen autoclaved sample appears throughout as a steady increase in the relative degree of crystallinity with time and appears at relatively the same values as the oxygen curve.

The error associated with any one point for the cotton cellulose samples is in the same range as those for the Q-90 and hemicellulose reduced samples. The minimum in the graphs is significant since the change in relative degree of crystallinity is greater than the error associated with the data points in the vicinity of the minimum.

#### **5.3 Avicel**

Since the data for the Q-90 and cotton cellulose samples are reproducible but vary in the time where a marked change in relative degree of crystallinity occurs in the profile, another type of cellulose called Avicel was chosen. Avicel is a manufactured microcrystalline cellulose rather than naturally occurring.<sup>149</sup> It is made by taking a natural cellulose sample like Q-90 and extensively purifying it to remove contaminants such as hemicellulose.<sup>149</sup> Avicel then undergoes a severe acid hydrolysis to remove as much of the amorphous portions as possible.<sup>138</sup> Some amorphous character is still present which links the crystallites of Avicel together.<sup>120</sup> The hydrolysis isolates the crystallites and reduces them in size.<sup>138</sup> The average degree of polymerisation for this material is about

50 compared to Q-90 which is about 1000 (see Table 6.1 for DP analysis). Having such a small degree of polymerisation the Avicel examined was in the form of a powder.

The powdery nature of the Avicel necessitated modification to the experimental methodology used for the other celluloses (Q-90, hemicellulose reduced and cotton). For this reason a larger amount of sample was used in the kettle reactor to ensure adequate mixing. In addition the reactions were performed at a higher consistency. Reaction times using pressurised oxygen were performed at 0 and 60 minutes. Furthermore, a control sample that was prepared in the same way but not placed in the reactor was also examined.

The samples were all examined using x-ray diffraction, FTIR spectroscopy and solid state NMR spectroscopy.

### **5.3.1 X-ray Diffraction**

The preparation of the Avicel for x-ray diffraction was carried out in a slightly different manner than the preparations for the other types of cellulose. In preparing the x-ray diffraction mount a small portion of the Avicel was placed in the cavity of the mount and then force applied to press the powder to form a large flat pellet with a 24 mm diameter. This modification should have no bearing on the outcome of the data. It is critical that the sample mount has an infinite thickness so that when the x-rays penetrate the sample, it only detects Avicel and nothing else below which is not part of the Avicel sample. The mounts were prepared in triplicate for each oxidation time.

The data for the relative degree of crystallinity versus oxidation time is shown in Figure 5.9. The relative degree of crystallinity does not change throughout the 60 minutes of oxidation time. The data shows an indication that attack on the cellulose crystallites are primarily on the reducing end groups. The oxygen attacks the cellulose similar to a chain “peeling” reaction.

### **5.3.2 FTIR Spectroscopy**

In making the pellet for analysis by FTIR spectroscopy some modifications were implemented. Instead of a thin wafer of cellulose between the potassium bromide powder, the Avicel powder was ground up together with the potassium bromide and then

made into a pellet. The concentration of the Avicel to potassium bromide still remained the same as the other tests. The conditions for the analysis also remained the same.

Figure 5.9 shows the data for the relative degree of crystallinity versus the oxidation time for Avicel using FTIR spectroscopic analysis.

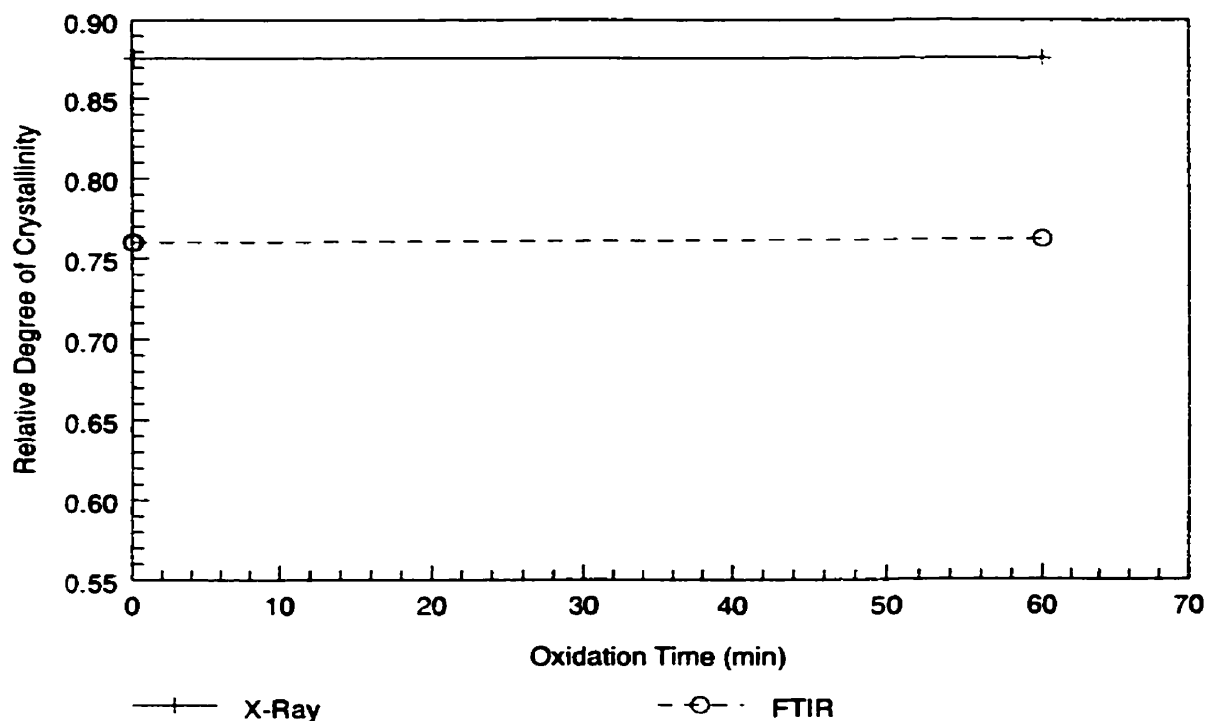


**Figure 5.9** X-ray diffraction and FTIR data for Avicel showing the relative degree of crystallinity as a function of oxidation time.

The data of the FTIR spectroscopic analysis are the same as that from the x-ray diffraction analysis. Both results show no change in the relative degree of crystallinity from 0 to 60 minutes.

### 5.3.3 $^{13}\text{C}$ Solid State NMR Spectroscopy

Although Avicel is a powder no modifications were required in the procedure to prepare the Avicel for solid state NMR spectroscopic analysis. The relative degree of crystallinity was tracked directly by the deconvolution method and indirectly by proton spin-lattice relaxation times.

### Deconvolution of NMR Signals

The NMR spectra was deconvoluted and analysed with respect to the C4, C6 and combined C4 and C6 carbons. The data showing the relative degree of crystallinity as a function of oxidation time are shown in Figure 5.10.

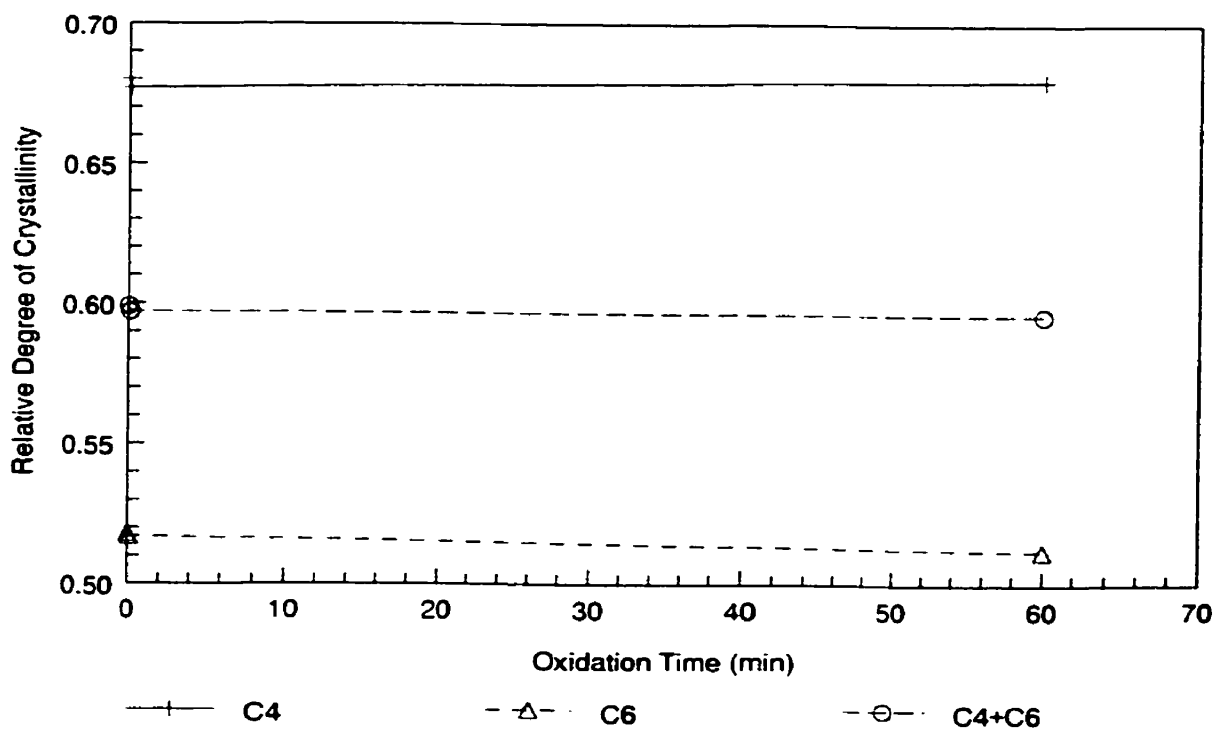


**Figure 5.10** Solid state NMR data for Avicel showing the relative degree of crystallinity (from the C4, C6 and total C4 and C6 carbons) as a function of oxidation time.

All three curves in Figure 5.10 show no changes in crystallinity. It is interesting to note that the relative degree of crystallinity associated with the C4 carbon is much higher than the C6 carbon. It is important to bear in mind that solid state NMR spectroscopy probes at the molecular environments surrounded by atoms. The C4 carbon has only one orientation possible within a crystallite while the C6 carbon can have more.<sup>117</sup> The C6 carbon can have free rotation around its bond between the ring of carbon atoms. The crystallite is held in place by intramolecular hydrogen bonding.<sup>48</sup> It is possible that this bonding does not necessarily take place for all C6 carbons within a crystallite since the energy required to break it is less than that needed to break a bond

between carbon atoms. Thus the higher crystallinity for the C4 carbon are displayed in the data of Figure 5.10. The C4 carbon has less freedom than the C6 carbon and a distinction is evident.

#### ***Proton Spin-Lattice Relaxation Time***

When the data for the proton spin-lattice relaxation times were plotted against the oxidation times for the Avicel samples they showed no visible difference from the deconvolution data. As discussed earlier, the relative degree of crystallinity can be paralleled to the relaxation times. There is no change in the relative degree of crystallinity as the oxidation times increase because relaxation times were relatively constant with time.

#### **5.3.4 Summary of Avicel Results**

By using the techniques of x-ray diffraction, FTIR spectroscopy and solid state NMR spectroscopy to analyse various oxidised Avicel samples, it was found that there was no change in the relative degree of crystallinity with time. The sample that was oxidised in the kettle reactor for 60 minutes had the same relative degree of crystallinity as the initial sample.

Since Avicel has an average degree of polymerisation of about 50, the makeup of Avicel is such that there is very little amorphous material for the oxygen to attack. It is likely that the oxygen reaction with cellulose takes place through chain “peeling”. This was evident in the data as the relative degree of crystallinity showed no change as time progressed.

#### **5.4 Comparison of Techniques by Sample**

Further key conclusions are apparent when the three instrumental techniques are compared concomitantly. The x-ray diffraction, FTIR spectroscopy and solid state NMR spectroscopy data are presented together for a particular cellulose sample. As discussed in previous sections of this work, there are consistent and common trends in the data of the relative degree of crystallinity as a function of oxidation time for all cellulose types. To avoid redundant repetition, two cellulose types, namely Q-90 and cotton, are now examined in detail.

### 5.4.1 Q-90

When the relative degree of crystallinity determined by all three techniques is plotted as a function of oxidation time for Q-90 pulp, Figure 5.11 emerges.

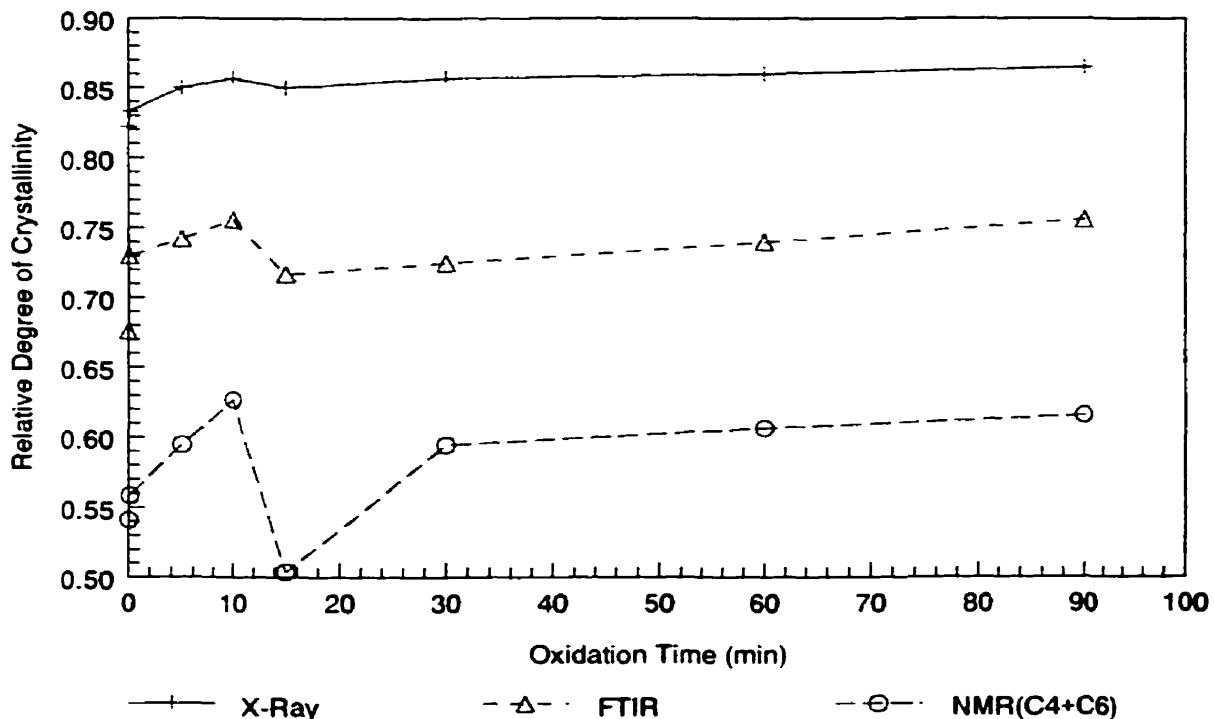


**Figure 5.11** Comparison of Q-90 samples using three analytical techniques.

The initial observation that emerges from Figure 5.11 is that the relative degree of crystallinity measured by x-ray diffraction is invariably higher than the data derived by FTIR spectroscopy and solid state NMR spectroscopy. The lowest relative degree of crystallinity results are generated from solid state NMR spectroscopy measurements. This can be attributed to the extent that each technique interprets the relative degree of crystallinity. X-ray diffraction measures the fraction of molecules that are arranged in a regularly repeating pattern.<sup>61</sup> The surface characteristics of a crystallite, including possible small defects and small amounts of amorphous material are rendered crystalline material by x-ray diffraction.<sup>103</sup> In the case of solid state NMR spectroscopy the environments around the carbon atoms are taken into consideration. The carbon atoms within a crystalline domain have a different chemical shift than the atoms within an amorphous domain.<sup>117</sup> In this way, small defects and amorphous material around the

crystallite is considered amorphous material rather than crystalline.<sup>101,132</sup> FTIR spectroscopy is able to distinguish some of the amorphous material associated with the crystallite but not all.<sup>109</sup> It probes the space between atoms and their vibration characteristics. It does not however, probe at the carbon atoms themselves.<sup>108</sup> FTIR spectroscopy's relative degree of crystallinity is thus not as detailed as NMR spectroscopy but provides more interpretation than x-ray diffraction. It stands to reason that FTIR spectroscopy provides intermediate data for the relative degree of crystallinity.

The second observation is that there are more significant variations in relative degree of crystallinity by the solid state NMR spectroscopic technique than by the other two methods. Similarly, the FTIR data shows greater variations than the x-ray diffraction data. This can also be attributed to the sensitivity of the various techniques to interpret the molecular structure of cellulose. X-ray diffraction is not able to distinctly separate the crystalline material from the amorphous material as well as FTIR spectroscopy. Likewise, FTIR spectroscopy does not distinguish the two structures as well as solid state NMR spectroscopy.

The slopes of the increases and decreases in the relative degree of crystallinity are also significant. For example, in the first 10 minutes of oxidation, the slope is greatest in the solid state NMR spectroscopy curve followed by the FTIR spectroscopy curve and then the x-ray diffraction curve. Since solid state NMR spectroscopy is best able to distinguish the amorphous from the crystalline regions, it gives the most accurate change in the relative degree of crystallinity.

#### **5.4.2 Cotton**

In a similar fashion for cotton cellulose, the three instrumental techniques used to determine relative degree of crystallinity can be compared. Figure 5.12 shows this comparison.

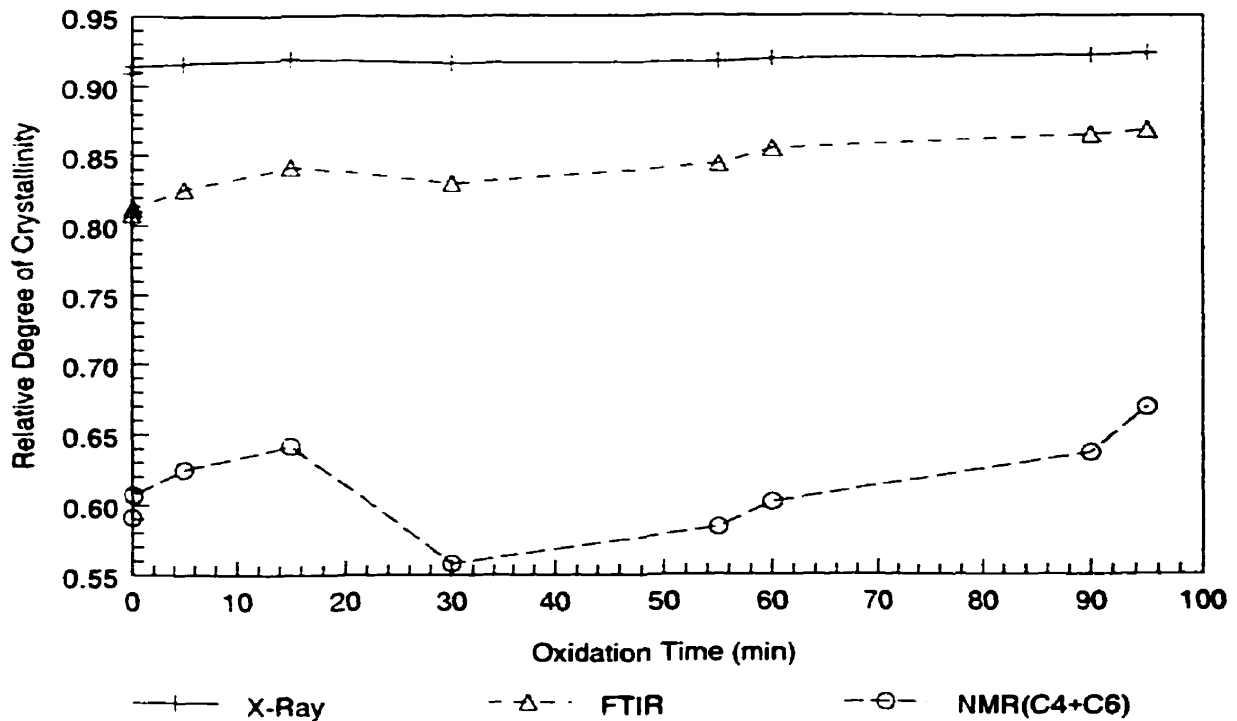


**Figure 5.12** Comparison of cotton cellulose samples using three analytical techniques.

Similar to Q-90 pulp, the x-ray diffraction curve for cotton cellulose shows the highest relative degree of crystallinity while the solid state NMR spectroscopy curve show the lowest. In addition, the variations in the relative degree of crystallinity are greatest for the solid-state NMR spectroscopy curve followed by the FTIR spectroscopy curve and then the x-ray diffraction curve.

### 5.5 Comparison of Samples by Analytical Technique

X-ray diffraction, FTIR spectroscopy and solid state NMR spectroscopy data for relative degree of crystallinity of the cellulose materials were compared. The following sections discuss each analytical technique and its capability.

#### 5.5.1 X-ray Diffraction

Figure 5.13 illustrates the data of four cellulose materials examined using x-ray diffraction.



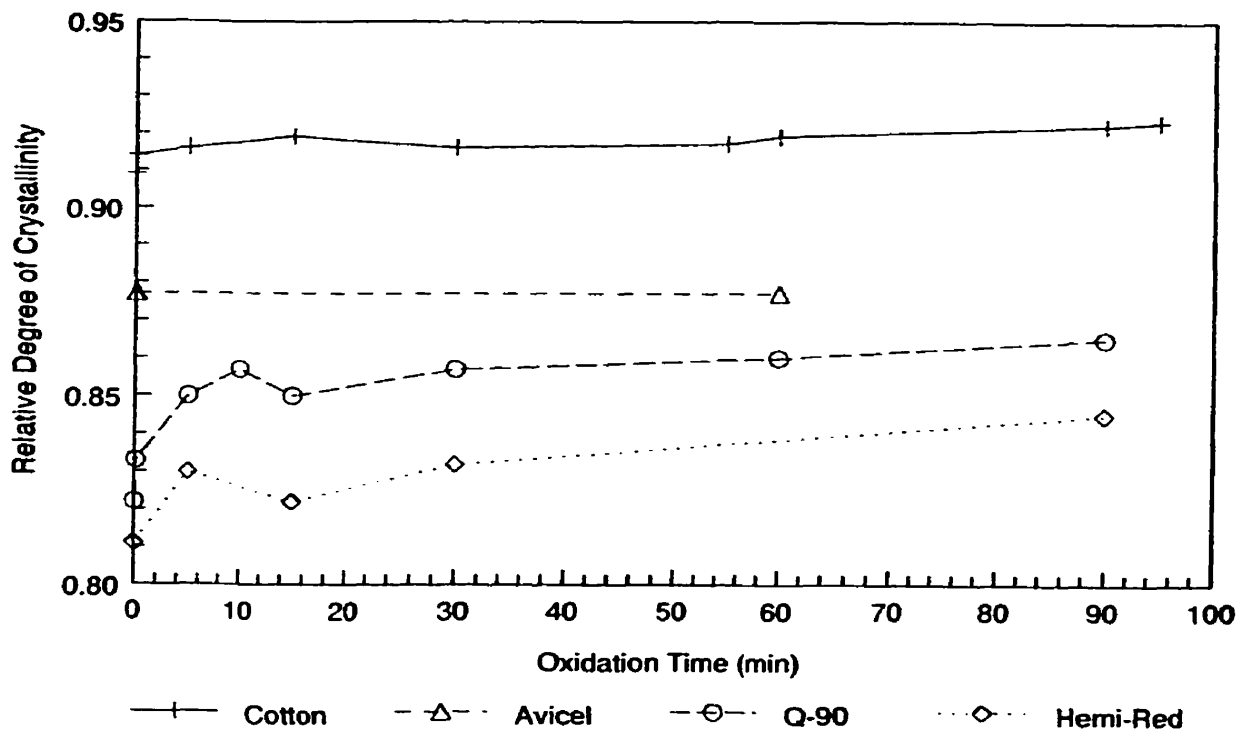


**Figure 5.13** Cellulose sample comparison by x-ray diffraction.

X-ray diffraction shows the highest relative degree of crystallinity for well packed and orderly crystallites. In Figure 5.13, cotton cellulose has the highest relative degree of crystallinity, however, Avicel has the best packed crystallites of all four celluloses and contains virtually no amorphous material.<sup>138</sup> One of the reasons that Avicel does not show the highest relative degree of crystallinity is because of its degree of polymerisation. Avicel has an average degree of polymerisation of 50, while cotton cellulose has an average degree of polymerisation of about 1000 or twenty times that amount. In addition, the width of the crystallite in cotton cellulose is larger than that of Avicel.<sup>171</sup> The technique of x-ray diffraction requires a minimum effective crystallite size on which the Avicel cellulose is bordering.<sup>91</sup> This results in an overall lower relative degree of crystallinity. The second reason why Avicel shows a lower relative degree of crystallinity than cotton is because it has been hypothesised that the individual cellulose chains in Avicel do not line up as orderly as in the cotton cellulose.<sup>97</sup> Individual Avicel cellulose chains appear to criss-cross each other forming a sort of “haystack”. Thus the Avicel sample shows less para-crystalline nature than the cotton cellulose.<sup>104</sup>

Furthermore, the Q-90 and hemicellulose reduced curves do not overlap although the two samples differ only in the hemicellulose content which is not detected by x-ray analysis.<sup>97</sup> The reason for the translation of the hemicellulose reduced curve downward is due to the amount of cellulose I present. Fengel *et al.* have demonstrated in a similar way that in preparing the hemicellulose reduced sample some of the cellulose I was converted to cellulose II by the conditions to which it was subjected.<sup>163</sup> The analysis of the diffractogram to calculate the relative degree of crystallinity is based on the cellulose I component in the sample. The results then confirm that the hemicellulose reduced samples have a lower cellulose I content which translated the curve downward.

Finally, the Q-90 cellulose curve shows a lower relative degree of crystallinity than the cotton cellulose. This is attributed to the composition of the crystallites in the two samples. As stated in section 5.2, the crystallites of the cotton cellulose are packed in a more densely and orderly manner than the Q-90 cellulose.<sup>97</sup> The cotton cellulose also has a larger crystallite width and fewer internal defects.<sup>154</sup> For these reasons the cotton cellulose possesses a higher relative degree of crystallinity than the Q-90 cellulose by x-ray diffraction analysis.

### **5.5.2 FTIR Spectroscopy**

The comparison of the relative degree of crystallinity analysed by FTIR spectroscopy for all cellulose samples studied is presented in Figure 5.14.

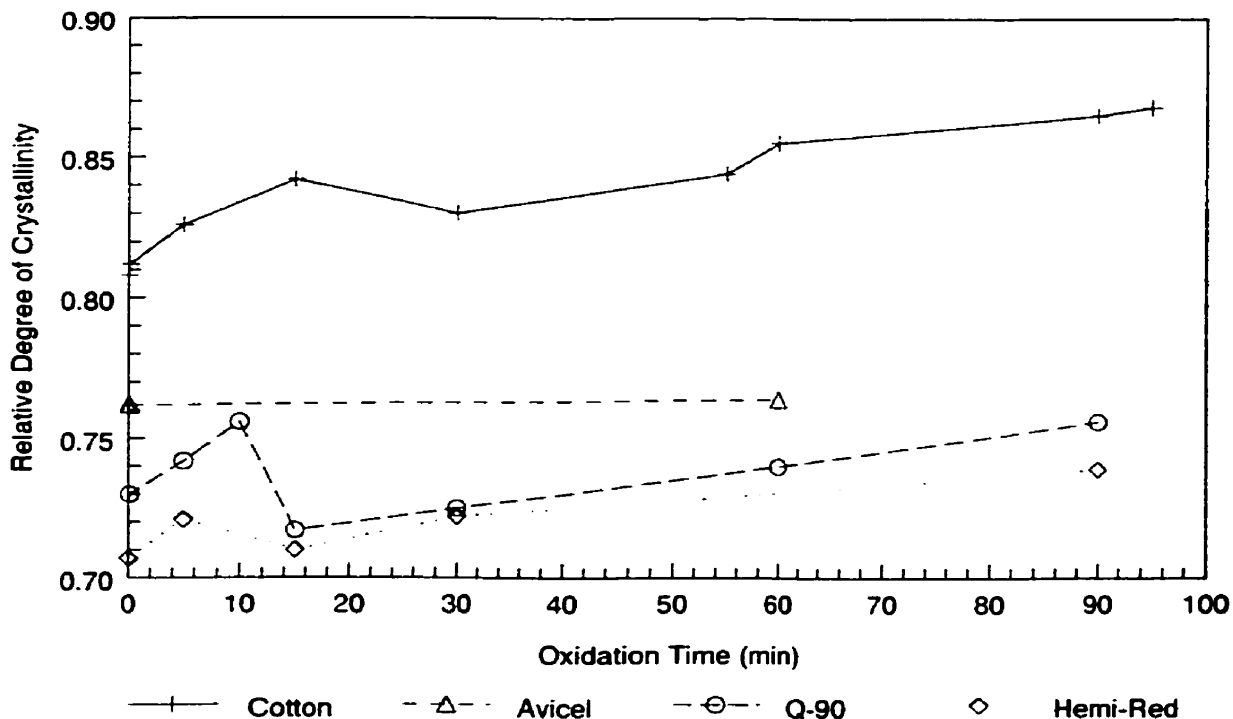


**Figure 5.14** Cellulose sample comparison by FTIR spectroscopy.

Two observations are apparent from this graph. The first is that the cotton cellulose has the highest relative degree of crystallinity and the second is that the Q-90 and hemicellulose reduced curves have very similar results. The cotton cellulose has a higher relative degree of crystallinity than the other cellulose curves shown for the same reasons outlined in the x-ray diffraction discussion earlier.

Q-90 and hemicellulose reduced curves both appear to be very similar because of the way the FTIR spectroscopic analysis calculates the relative degree of crystallinity. The relative degree of crystallinity is calculated using absorption bands in the spectra that are unique for the amorphous and crystalline domains of cellulose I. Thus the cellulose II generated when preparing the hemicellulose reduced sample is not taken into account.

### 5.5.3 $^{13}\text{C}$ Solid State NMR Spectroscopy

The curves for the four samples of cellulose analysed by NMR are compared in Figure 5.15. The relative degree of crystallinity shown in this figure is based on the

deconvolutions of the total amount of crystalline material from both the C4 and C6 carbon contributions.

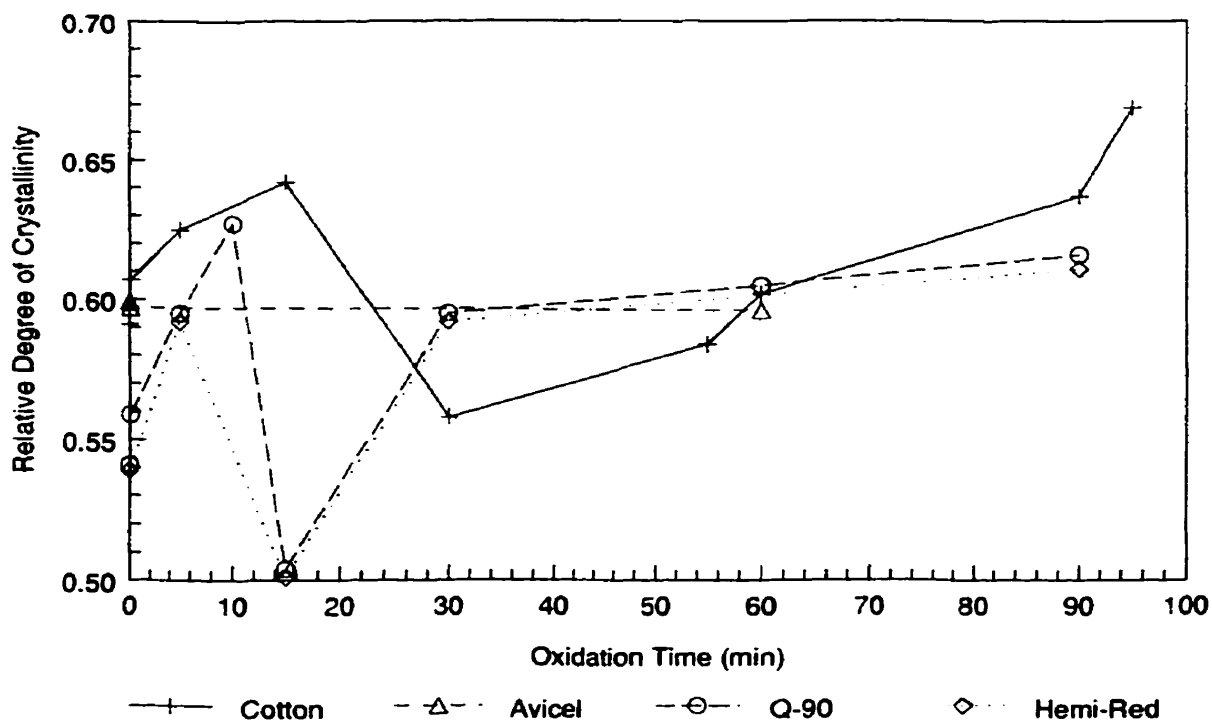


**Figure 5.15** Cellulose sample comparison by solid state NMR taking into account the total C4 and C6 carbon atom contribution.

The solid state NMR spectroscopic technique is the most sensitive of all three instrumental techniques studied here.<sup>132</sup> Hence a clear distinction between the amorphous and crystalline material is reflected in the relative degree of crystallinity. The Q-90 and hemicellulose reduced samples virtually overlap each other because in measuring the crystalline content of these two pulps no difference is made between the amount of cellulose I and cellulose II that is present.

All four cellulose materials have very similar relative degrees of crystallinity. In the x-ray diffraction comparison in Figure 5.13 it was shown that the difference in the relative degree of crystallinity between cotton and Q-90 was about 0.1. In this solid state NMR analysis the difference is about 0.05. The Avicel sample does not show the highest relative degree of crystallinity because this solid state NMR technique is sensitive to the size of the crystallites.<sup>117</sup>

## 5.6 Proposed Theory Based on Data

The three instrumental techniques applied to four types of cellulose offer several hypotheses about the physicochemical changes occurring within cellulose undergoing oxidation. In an effort to rationalise for the evaluated data a proposed theory is presented in this section.

The proposed theory is based on the fringed micelle model, not the chain folding model since cellulose is para-crystalline. Figure 5.16a shows a schematic illustration of the fringed micelle model. In order to understand why the relative degree of crystallinity changes during oxidation it is first important to understand how the crystallinity changes within cellulose. Assume that all the oxygen available attacks the cellulose only (excluding hemicellulose) causing a chain cleavage.

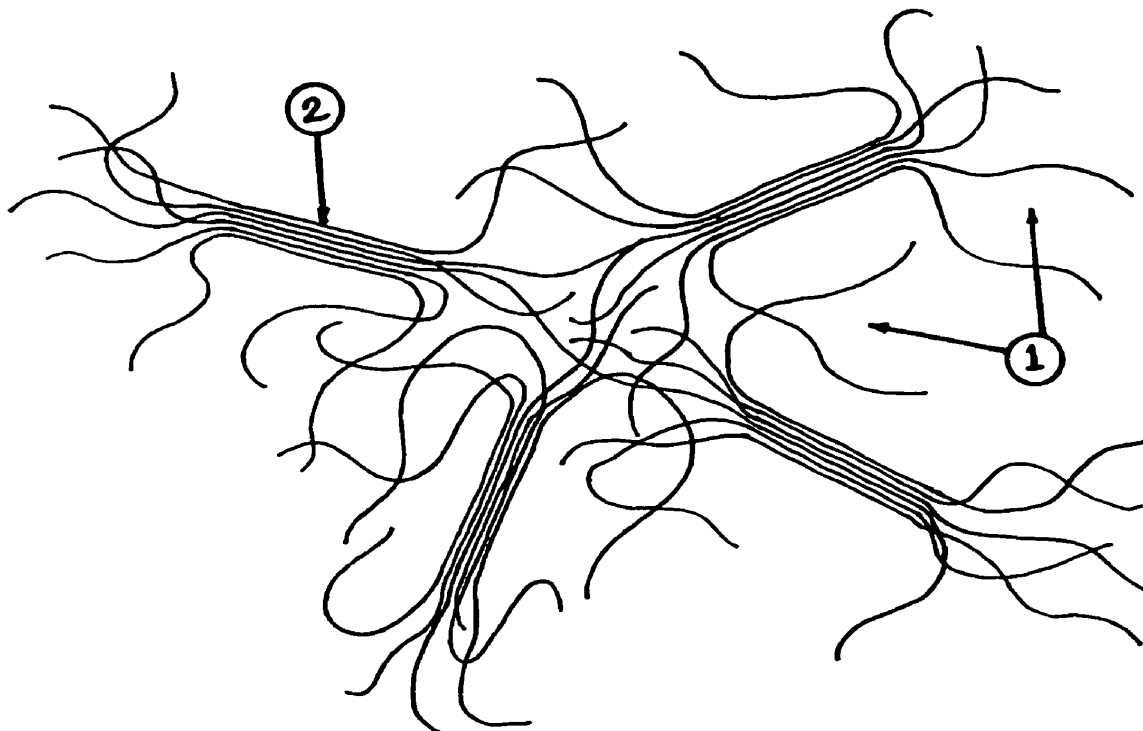


**Figure 5.16a** Schematic representation of cellulose by the fringed micelle model showing two possible points of attack by oxygen.

Consider first a simplistic assumption that oxygen can attack at either the amorphous or crystalline domains in cellulose as indicated in the positions identified in Figure 5.16a.

Attack on the amorphous domains of the cellulose is depicted by position 1. Attack on the crystalline domains of the cellulose is depicted by position 2.

Firstly, consider the attack of oxygen on the polymer at position 1. A chain cleavage in the amorphous domain results in the reduction of the polymer chain length. Further oxygen attack can then proceed to cut the amorphous chains of cellulose shorter or at different positions within the amorphous domain.

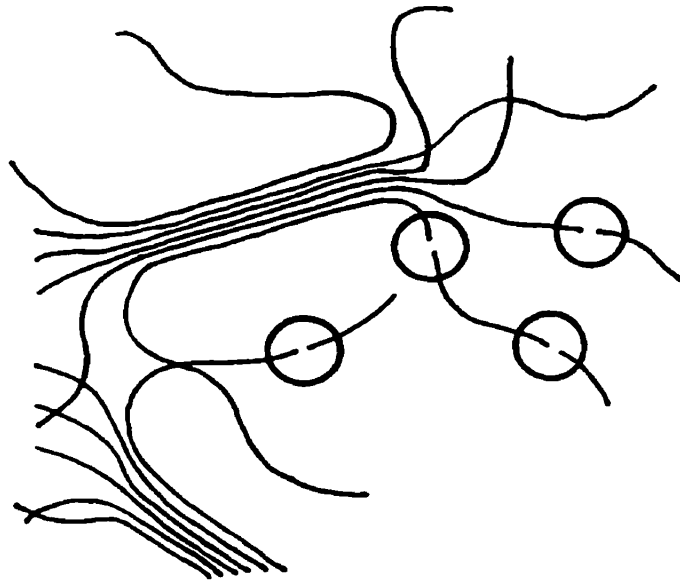


**Figure 5.16b** Attack on the amorphous domain.

At the same time that the oxygen attacks the glycosidic linkage in the cellulose molecule causing chain cleavage, attack at the reducing end groups of the cleaved chains could also take place. Such an event will start to reduce the total length of the cellulose chains within the amorphous domain by the “peeling” reaction (as described in section 1.2.3).

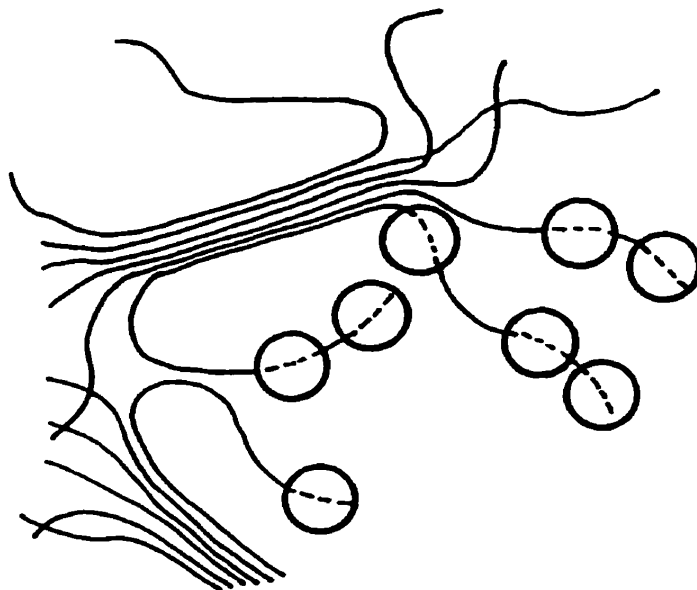


**Figure 5.16c** Chain “peeling” attack at the reducing end groups after scission in the amorphous domain.

Oxygen attack within the cellulose chains and at its ends leads to some of the amorphous chains becoming small independent fragments of cellulosic material. These fragments cannot be detected by x-ray diffraction, FTIR spectroscopy and solid state NMR spectroscopy and as such the overall relative degree of crystallinity increases.

Secondly, consider the attack of oxygen on the polymer at position 2 as depicted in Figure 5.16a. This represents attack of the crystalline domains by oxygen. Initially the attack can occur all around the crystallite at a number of different locations within the crystalline domain.

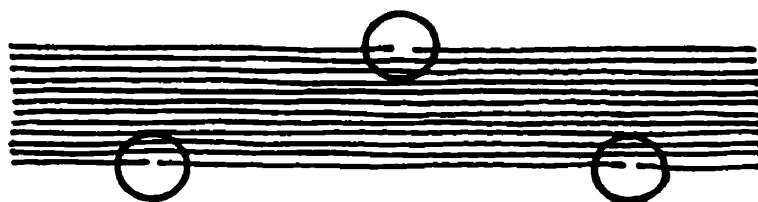


**Figure 5.16d** Attack on the crystalline domain.

Attack of this nature results in the cellulose chain gradually being “peeled” away from the crystallite. This occurs because the intramolecular hydrogen bonding that is responsible for keeping the chains together is weakened by oxygen interference.<sup>48,74</sup> The crystallite at this point can be thought of as having fine “hairs” developing around it. Chain “peeling” reduces the length of these “hairs”. Further attack of the glycosidic linkage can also occur at exposed crystalline cellulose. The oxygen can then have an influence at the two positions shown in Figure 5.16e.

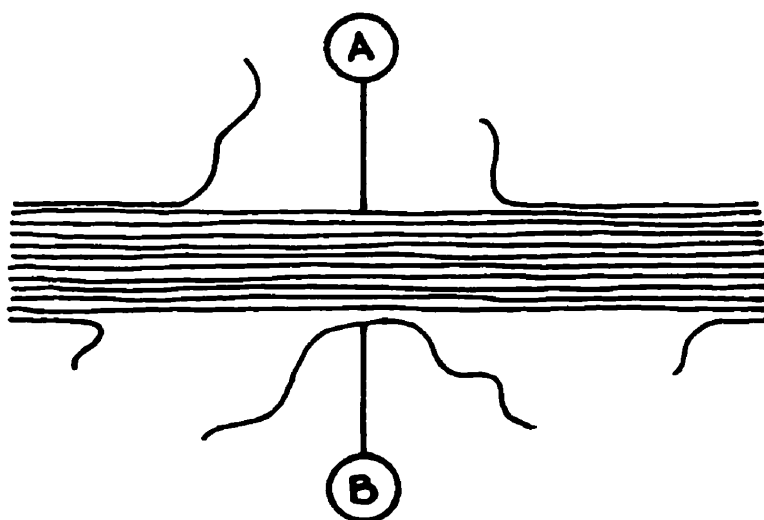


**Figure 5.16e** Attack at two positions on exposed crystalline material of cellulose.

Attack at position A can occur if enough of the severed chain is peeled away to expose fresh crystalline cellulose. If enough new crystalline material is exposed to oxygen then further attack continues on the crystallite. The attack of the crystallite eventually arrives at a point where there is too much amorphous material surrounding the crystallite.





**Figure 5.16f** Amorphous regions developing from oxygen attacking the outer portions of the crystalline domain.

The crystalline material becomes virtually protected by the surrounding amorphous regions which are more readily susceptible to further oxygen attack. When enough of the amorphous material around the crystallite has been removed by chain cleavage and “peeling” reactions, then the oxygen can continue to penetrate the crystalline material within.

Molecules of cellulose at position B in Figure 5.16e shows that there is only a small amount of cellulose anchoring the chain to the crystallite. If the intramolecular hydrogen bonding is not strong enough or if further attack at the anchor point occurs, the cellulose molecules could possibly detach themselves from the crystallite. The resulting chain is thus considered amorphous if it is large enough to cause x-ray diffraction, interference with an infrared beam, or alter the overall molecular mobility of the surrounding area to be probed by solid state NMR spectroscopy.

In summary, if attack occurs only at position 1 in the amorphous region (Figure 5.16a) then the overall relative degree of crystallinity increases. If attack at position 2 in the crystalline region is predominant and follows the pattern of position B (Figure 5.16e) then the overall relative degree of crystallinity decreases. If however, attack only at position 2 occurs then the crystallinity initially decreases towards an equilibrium point until further attack can take place on the crystallite. As noted earlier, each of these attack mechanisms are examined independently to understand the logic of oxygen attack. However in reality, all of these attacks by oxygen may occur simultaneously. Statistically, however, one mode of attack may predominate the other.

The changes in the relative degree of crystallinity during pulp bleaching can be explained by the various attack sites of oxygen on cellulose because all the attack mechanisms can occur concomitantly. Since the changes in the relative degree of crystallinity was observed to occur in three distinct stages by all three instrumental techniques, this theory appears to be consistent in explaining the observed phenomena.

In stage 1. (for example from 0 to 10 minutes in Figure 4.2) attack of the amorphous domains of cellulose is more favourable than attack of the crystalline domains. This does not imply that there is no attack in the crystalline domains. Since the crystallites may be surrounded by some amorphous material, the path of the oxygen reaching the crystalline material is impeded. It is also harder to attack the crystalline material due to the tight packing and strong hydrogen bonding that holds the cellulose molecules together in a crystallite. This favoured attack of oxygen on the loosely held amorphous material causes a rapid increase in the relative degree of crystallinity initially at the start of oxidation.

In stage 2. (for example from 10 to 15 minutes in Figure 4.2) a decrease in the relative degree of crystallinity is observed. Attack of the crystalline domain becomes more dominant in this stage. Since the oxygen begins to attack the crystalline domain resulting in areas of amorphous material developing (as shown in Figures 5.16e and 5.16f) there is a dominance of amorphous material over crystalline material. This increase results in a decrease in the relative degree of crystallinity.

In stage 3, (for example from 15 minutes onwards in Figure 4.2) the crystallites are overcome with surrounding amorphous "hair" because of the predominant crystalline to amorphous attack that takes place in stage 2. After stage 2, further oxygen attack on the crystallite is not possible until some of the surrounding amorphous material is cleared away to expose new crystalline material. In so doing a limited amount of attack is possible on the crystalline material because any cleaved amorphous material results in more amorphous material being available for further attack. Since the amorphous material is more susceptible to attack than the tightly held crystalline domain, the overall relative degree of crystallinity increases but not as quickly as in stage 1. In stage 3, time

is spent converting crystalline material to amorphous domains during oxidation whereas in stage 1. the oxygen is readily attacking the available amorphous material.

### **5.6.1 Explanation for the Differences Between Q-90 and Cotton Cellulose**

In addition to the common distinct stages of changes in the relative degree of crystallinity observed by each instrumental technique, there was a notable difference at which time stage 3 commenced for Q-90 pulp and cotton cellulose. The transition between stage 2 and stage 3 was marked by a minimum in the relative degree of crystallinity. In the case of Q-90, the minimum occurred at 15 minutes while for cotton cellulose, it occurred at 30 minutes. The theory proposed above can also explain these differences.

The cotton cellulose is known to be more densely packed than the Q-90 cellulose.<sup>97</sup> Thus attack of the crystallites is more difficult for cotton cellulose. It is harder to disrupt the intramolecular hydrogen bonding that holds the crystallites together in a denser structure. Attack on the crystallite in the case of cotton cellulose results in shorter "hairs" of amorphous material radiating out than in the case of Q-90. In light of this, stage 1 for cotton cellulose is prolonged so the minimum occurs later.

Timpa and Wanjura have shown that the width of the crystallite is also important in oxygen attack. The crystallite width in cotton is larger than in Q-90.<sup>171</sup> This results in a larger surface to volume ratio of the crystallite for cotton than for Q-90. Oxygen attack in cotton is not as evident as in Q-90 because of the proportion of surface attack on the crystallite to crystallite size itself. For a change in the relative degree of crystallinity to be compared at par, either more attack must take place within a given time or the same amount of attack for a longer time. The latter is most likely the case for these results since the oxygen attack rate remains the same. As noted in the solid state NMR spectroscopic data, Q-90 and cotton cellulose achieved a comparable relative degree of crystallinity with time. Hence, it is reasonable to conclude that the amorphous domains of cotton cellulose took longer to degrade than Q-90 before the crystalline regions were further attacked.

## Chapter 6

### Results & Discussion – Part III

#### Cellulose Depolymerisation and Oxidation

---

Evaluation of the x-ray diffraction, FTIR spectroscopy and solid state NMR spectroscopy results concludes that these techniques are valid to examine changes in cellulose crystallinity. All three techniques provided reproducible and consistent results. In order to understand why the relative degree of crystallinity changes occurred for each of the four cellulose samples using the three instrumental techniques a comparison of the techniques for each sample and a comparison of the samples using each technique were presented. A theory was also proposed to explain the trends observed in the relative degree of crystallinity changes with time.

However, in oxidising cellulose in the kettle reactor, degradation of the cellulose chains also occur. Degradation may occur when the oxygen attacks the cellulose chain causing cleavage. The degradation can be monitored by viscosity measurements. Degradation may also occur on the cellulose chain that does not result in a cleavage such as oxidation of select carbons to carboxylic acids. The change in carboxylic acid content of the oxidised cellulose can be measured using conductometric titration. Both viscosity and conductometric titration results are presented in this chapter along with some relationships that can be derived in comparing the information from the two techniques.

##### 6.1 Viscosity and Chain Scission

Viscosity may follow the degradation of high molecular weight carbohydrates such as cellulose.<sup>136,137</sup> The change in pulp strength for the four cellulose types studied here can be examined by measuring their viscosities at various times during oxidation. Cellulose degradation can also be expressed by the average number of glycosidic linkage scissions in a cellulose chain. The chain scission number is calculated by first converting the viscosity value to an average degree of polymerisation (DP) using the following equation.<sup>172</sup>

$$DP = [961.38 \log (\text{viscosity})] - 245.3 \quad (6.1)$$

where viscosity is expressed in units of pascal seconds (mPa x s). The average degree of polymerisation is then converted to a chain scission number (CS) using the following equation.<sup>172</sup>

$$CS = [(1/DP) - (1/DP_0)] DP_0 \quad (6.2)$$

where DP is the degree of polymerisation for the sample after treatment and DP<sub>0</sub> is the degree of polymerisation of the original sample before treatment. The chain scission number is a measure of the average number of glycosidic bonds that are cleaved per cellulose chain during a reaction.

The viscosity values and the chain scission numbers were determined for the four cellulose samples (Q-90, hemicellulose reduced, cotton cellulose and Avicel). The cellulose samples subjected to pressurised oxygen in the kettle reactor were examined. For each cellulose sample, at least two duplicate measurements were performed to obtain viscosity.

#### **6.1.1 Q-90 Pulp**

Figure 6.1 shows the relationship of the viscosity and chain scission number as a function of oxidation time for the Q-90 pulp.

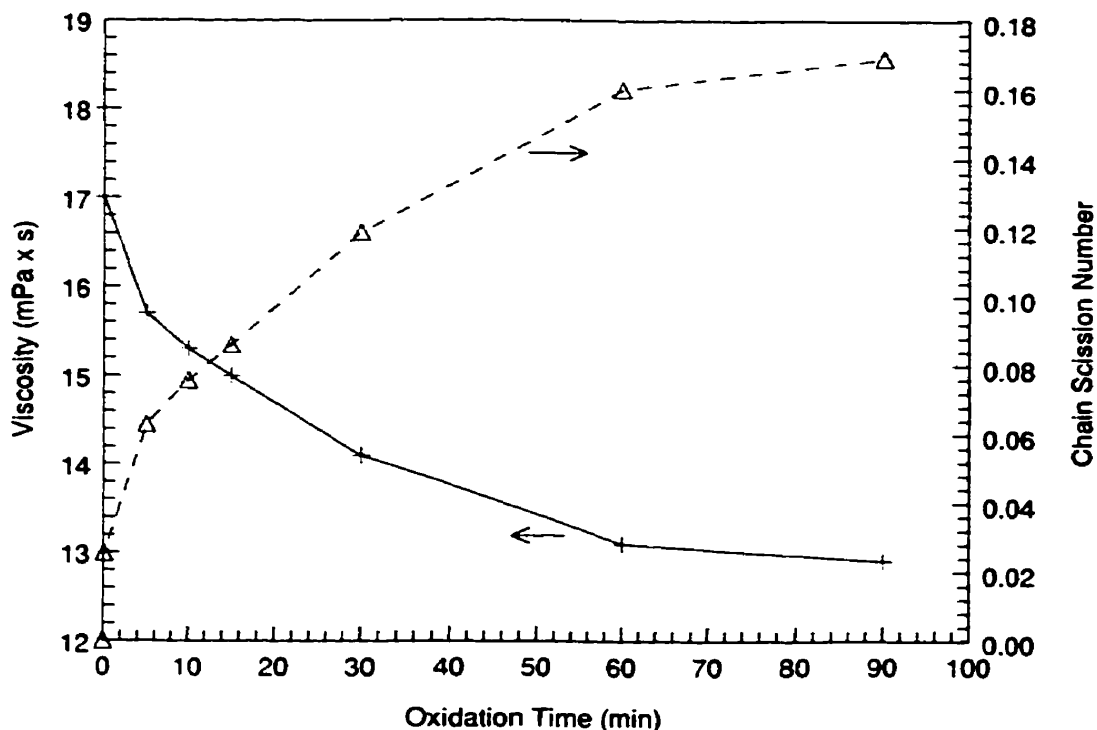


**Figure 6.1** Q-90 data for the viscosity (-+-) and chain scission number (-Δ-) as a function of oxidation time.

Figure 6.1 shows viscosity decreasing gradually with time. This indicates that cellulose degradation of the Q-90 pulp is increasing with time as oxidation progresses. Analogously there is an increase in the number of chain scissions with time. After 5 minutes  $6.3 \times 10^{-3}$  scissions per cellulose chain take place. By 90 minutes of oxidation time, the number of scissions per cellulose chain has increased almost three fold to  $1.7 \times 10^{-2}$ .

### 6.1.2 Hemicellulose Reduced Pulp

For the hemicellulose reduced sample, the same analyses were conducted obtaining similar data to that of the Q-90 pulp. There is a decrease in viscosity and an increase in chain scission number with time. The plot for the hemicellulose reduced samples is presented in Figure 6.2.

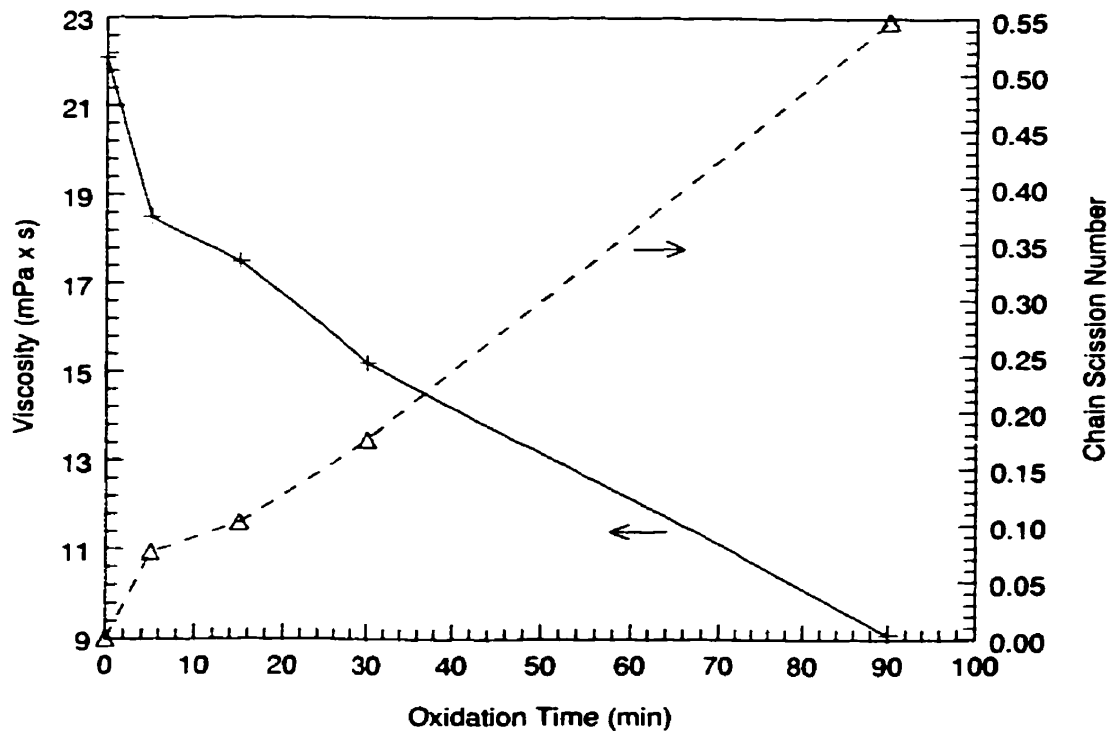


**Figure 6.2** Hemicellulose reduced pulp data for viscosity (-+-) and chain scission number (-Δ-) as a function of oxidation time.

A feature in Figure 6.2 for hemicellulose reduced pulp, that is not evident in Figure 6.1 for Q-90, is the notable change in slope that is apparent in three time stages. It appears that the rate of cellulose degradation changes with each time range. This can be paralleled to the three distinct changes in slope representing the relative degree of crystallinity measurements versus time as seen in Figure 5.1. The first stage in Figure 5.1 occurs from 0 to 10 minutes, the second from 10 to 15 minutes and the final stage from 15 minutes onwards. In Figure 6.2 the same three stages are evident.

### 6.1.3 Cotton Cellulose

The cotton cellulose viscosity and chain scission numbers have been plotted against oxidation time in Figure 6.3.

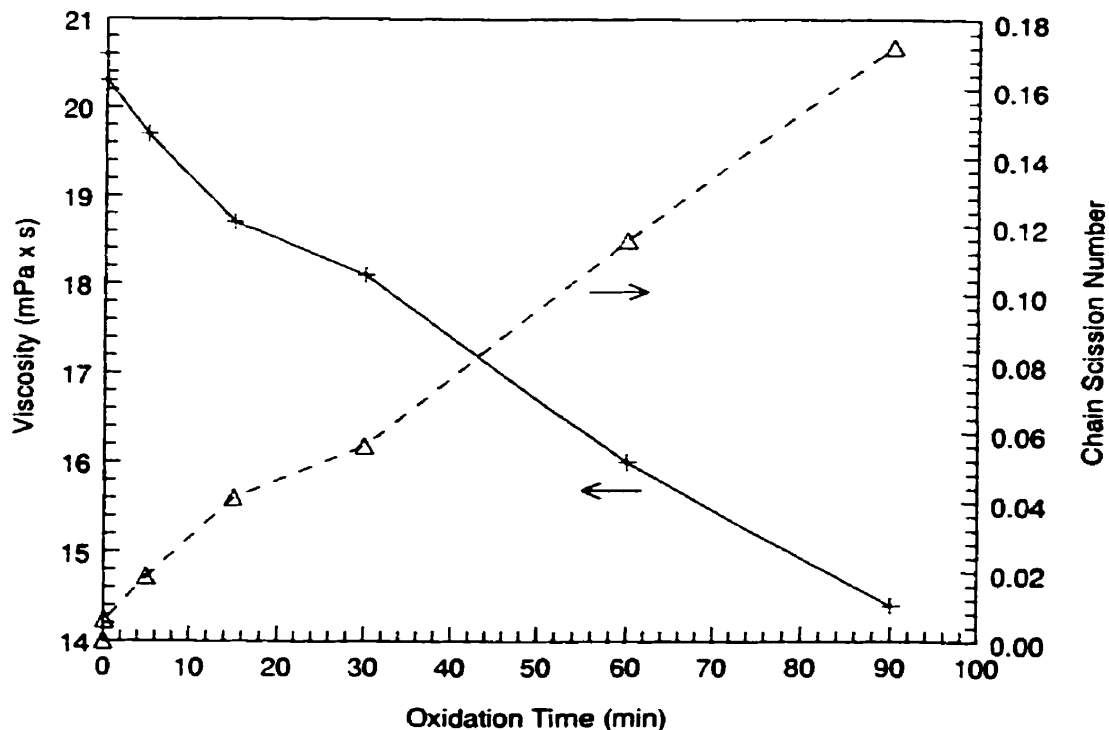


**Figure 6.3** Cotton cellulose data for viscosity (-+-) and chain scission number (-Δ-) as a function of oxidation time.

The degradation of the cellulose is again evident. There is a decrease in the viscosity number with time indicating a reduction in the cellulose fibres. The chain scission numbers conversely increase with oxidation times. This increase in the chain scission number shows that there is more cleavage of the cellulose chains as the oxidation time increases. Once again the degradation of the cotton cellulose in three stages is apparent.

#### 6.1.4 Avicel

The viscosity and chain scission numbers for the Avicel samples were also plotted as a function of oxidation time. As expected, there was no significant change evident in viscosity or chain scission number with time. Avicel is comprised of very short molecular chains of cellulose that have very little amorphous character.<sup>120</sup> All the oxygen attack should then occur by the chain “peeling” reaction.<sup>77</sup> Both the viscosity and the chain scission number curves appeared as flat lines parallel to the x-axis. This is in agreement with Figures 5.9 and 5.10 and the explanations given regarding Avicel in section 5.3.



### 6.1.5 Degree of Polymerisation

The degree of polymerisation is a measure of the number of glucose units that are linked together in an average cellulose chain.<sup>61</sup> This value can provide important information as to the change in cellulose length as oxidation progresses. The degree of polymerisation is calculated from the viscosity values using equation 6.1 outlined earlier. Table 6.1 lists the initial and final degree of polymerisation for each of the four cellulose samples studied.

Cellulose	Initial DP <sup>1</sup>	Final DP <sup>2</sup>	DP Change
Q-90	961.2	822.2	-139.0
Hemicellulose Reduced	1046.9	676.5	-370.4
Cotton	1017.5	868.1	-149.4
Avicel	56.4	50.3	-6.1

<sup>1</sup> Initial values are taken from the samples that were not oxidised.

<sup>2</sup> Final values taken for Q-90, hemicellulose reduced and cotton are after 90 minutes of oxidation, and for Avicel are after 60 minutes of oxidation.

**Table 6.1** Degree of polymerisation data for the cellulose samples used.

The cellulose sample showing the greatest reduction in the degree of polymerisation is the hemicellulose reduced pulp. To obtain this particular cellulose, the original Q-90 cellulose underwent a procedure in which more than half of the original hemicellulose present was removed.<sup>147</sup> With much less hemicellulose present, oxygen attack of the cellulose is less impeded and therefore predominant. In looking at the change in the degree of polymerisation for the Q-90 and cotton cellulose samples that still possess some hemicellulose it is apparent that the reduction is not as significant as when the hemicellulose is removed.

### 6.2 Conductometric Titration

Conductometric titration is used to measure the total amount of carboxylic acids present in a cellulose sample.<sup>146</sup> Analysing the carboxylic acid content of a particular cellulose at various oxidation times shows the amount of oxidation that has taken place.

This technique, however, cannot distinguish between oxidation that takes place on the cellulose and that which takes place on the hemicellulose.<sup>145</sup> If hemicellulose is present in the sample then it can also be oxidised to yield an increase in the carboxylic acid content. An increase in carboxylic acid indicates an increased amount of oxidation.

The four samples of cellulose (Q-90, hemicellulose reduced, cotton cellulose and Avicel) were all subjected to conductometric titration and the results of these measurements are discussed in the following sections. Due to the large time requirement involved in obtaining these results, conductometric measurements were conducted only in duplicate for each data point. The agreement between the values of the duplicate measurements alone was reassuring.

### 6.2.1 Q-90 Pulp

The carboxylic acid content as a function of oxidation time for the Q-90 cellulose samples is shown in Figure 6.4. The samples that were placed in the kettle reactor with pressurised oxygen, and with pressurised nitrogen and autoclaved nitrogen are plotted.

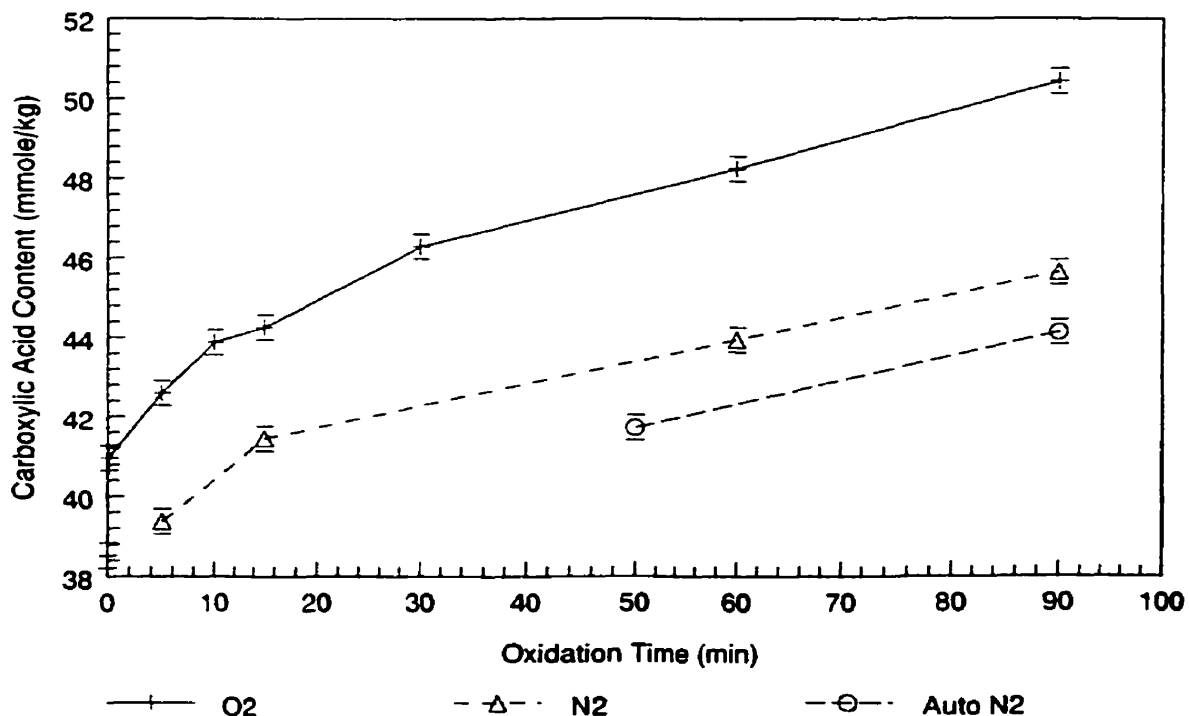


**Figure 6.4** Conductometric titration data for Q-90 showing the carboxylic acid content as a function of oxidation time.

The curves of pressurised nitrogen and autoclaved nitrogen if extrapolated to the origin overlap with the oxygen pressurised control sample (having a carboxylic acid content of 38.3 mmole/kg). The curve for the oxygen treated sample shows the most significant changes in the amount of carboxylic acid present. This is because the Q-90 pulp has the most amount of oxygen readily available for reaction to occur. As anticipated for the samples that were subjected to pressurised nitrogen, the amounts of carboxylic acid content are much lower. The autoclaved nitrogen sample prior to being placed in the kettle reactor with pressurised nitrogen shows the least amount of change as would be anticipated from the amount of oxygen available for oxidation to occur. Nitrogen and autoclaved nitrogen samples were tested to examine how the oxygen initially present within the cellulose samples, contribute to cellulose degradation.

A closer look at the curve for the oxygen samples reveals that it can be divided up into three distinct stages. The first stage which occurs from 0 to 10 minutes has a rapid increase in the amount of carboxylic acids being generated. The second stage from 10 to 15 minutes shows an increase as well but not as significant. The third stage from 15 minutes onward shows a steady increase. These results have a close resemblance to the data that were presented for the relative degree of crystallinity determinations. The stages occur at the same time intervals as before and so the observation appears to be consistent.

### **6.2.2 Hemicellulose reduced Pulp**

The carboxylic acid content as a function of time for the hemicellulose reduced samples was also plotted. The data is seen in Figure 6.5.

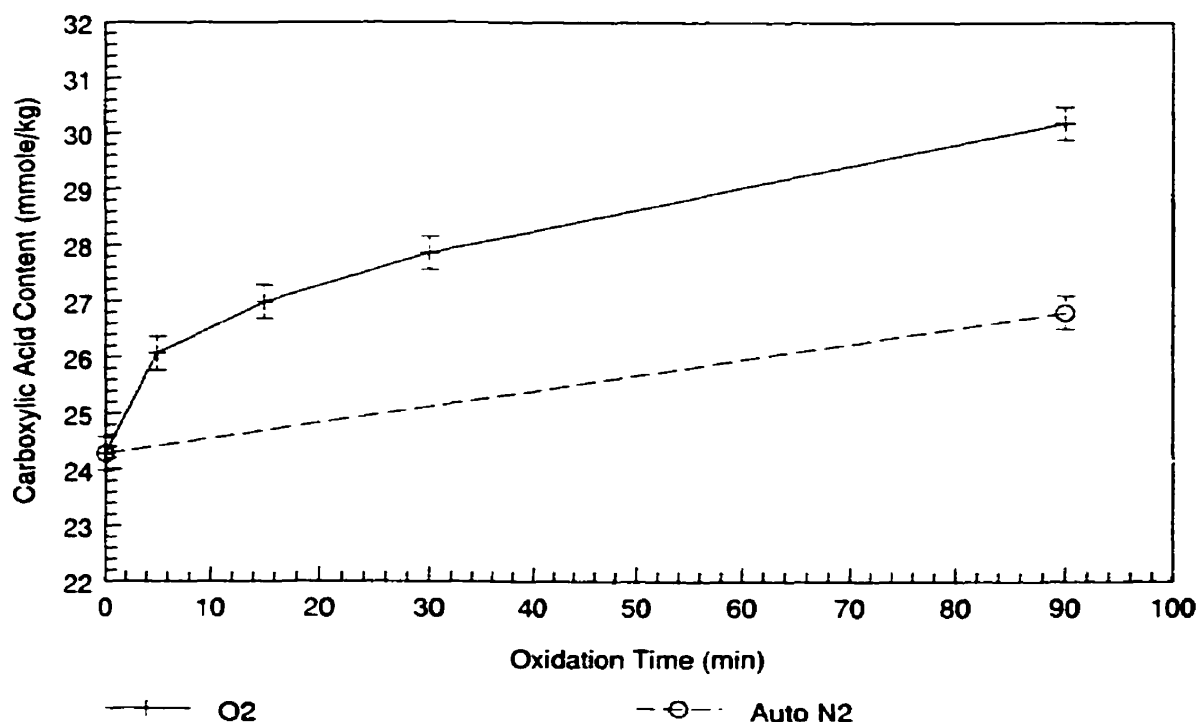


**Figure 6.5** Conductometric titration data for hemicellulose reduced pulp showing the carboxylic acid content as a function of oxidation time.

The oxygen curve appears to show more significant changes in the amount of carboxylic acids present than the autoclaved nitrogen curve. The overall magnitude of the values obtained for hemicellulose is lower than that for the Q-90 samples. This is because more than half the hemicellulose was removed. The hemicellulose component is more easily oxidised than the cellulose because of its irregular molecular structure.<sup>12</sup> The reduced amount of hemicellulose present translates into a reduction in carboxylic acids. This is evident by comparing the oxygen treated samples shown in Figures 6.4 and 6.5.

The three distinct stages of oxidation are not so evident from Figure 6.5 because there was no 10 minute sample performed for this analysis. It is assumed that if the 10 minute sample was present it would have a carboxylic acid value greater than the 15 minute sample.

### 6.2.3 Cotton Cellulose

Figure 6.6 is a plot of the carboxylic acid content versus the oxidation time for the cotton cellulose samples.

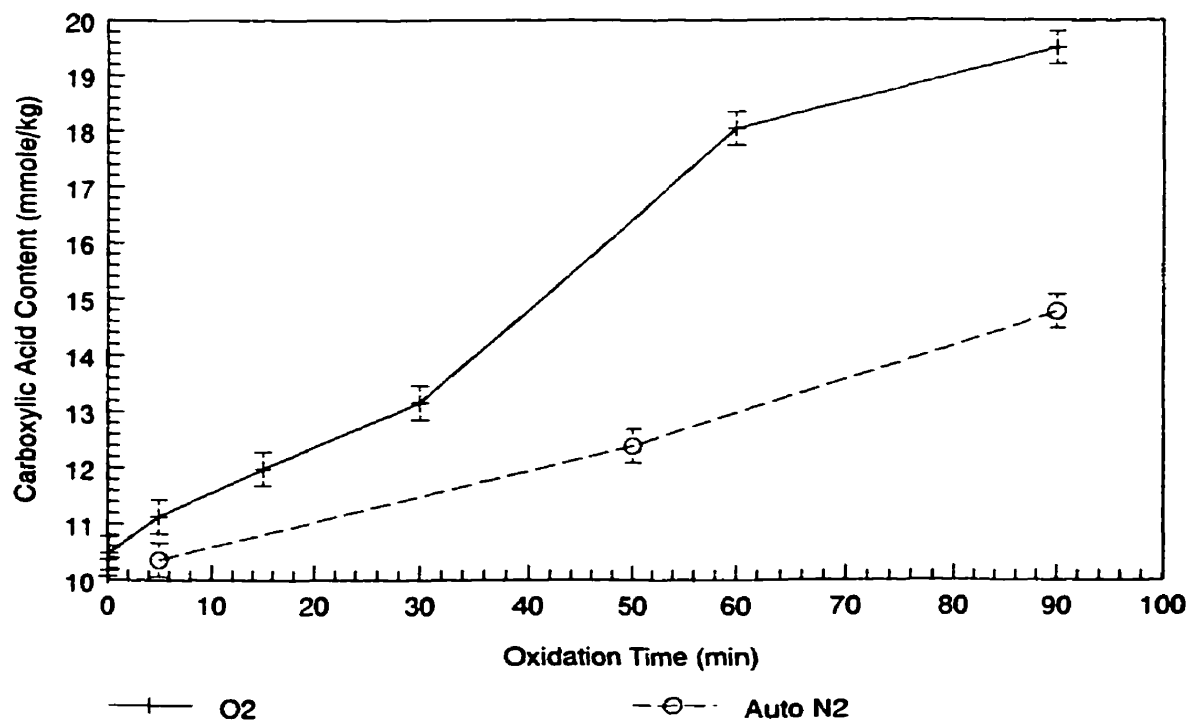


**Figure 6.6** Conductometric titration data for cotton cellulose showing the carboxylic acid content as a function of oxidation time.

The three stages of oxidation that were apparent in the relative degree of crystallinity measurements for cotton are also present in this graph. These stages however differ from the Q-90 stages in the same way that they differed in the crystallinity analysis. Thus the same conclusions that were provided in the theory outlined in section 5.4.1 holds true.

#### 6.2.4 Avicel

For all Avicel samples, the carboxylic acid content was about 10.5 mmole/kg. There was no change in content evident from the start to 60 minutes of oxidation. The data confirms that the attack of oxygen on the Avicel sample involves the reducing end groups in a chain “peeling” reaction. If this is the case, then whenever the oxygen attacks the reducing end group of the cellulose chain a single glucose molecule is cleaved.<sup>87</sup> This allows another reducing end group to be oxidised and have another carboxylic acid. The net result is that there is no change in the overall amount of carboxylic acids present with oxidation.

### 6.3 Comparison of Viscosity and Conductometric Titration Measurements

If the viscosity measurements are compared with the data obtained from the conductometric titrations, interesting conclusions and confirmations can be derived. Some of these comparisons are illustrated in the following sections. First a comparison of the carboxylic acid content and the degree of polymerisation is discussed followed by a look at how the chain scission number varies with the carboxylic acid content.

#### 6.3.1 Carboxylic Acid Content & Degree of Polymerisation

Figure 6.7 shows a plot of the carboxylic acid content as a function of the degree of polymerisation for the Q-90 cellulose samples that were oxidised in the kettle reactor with pressurised oxygen.

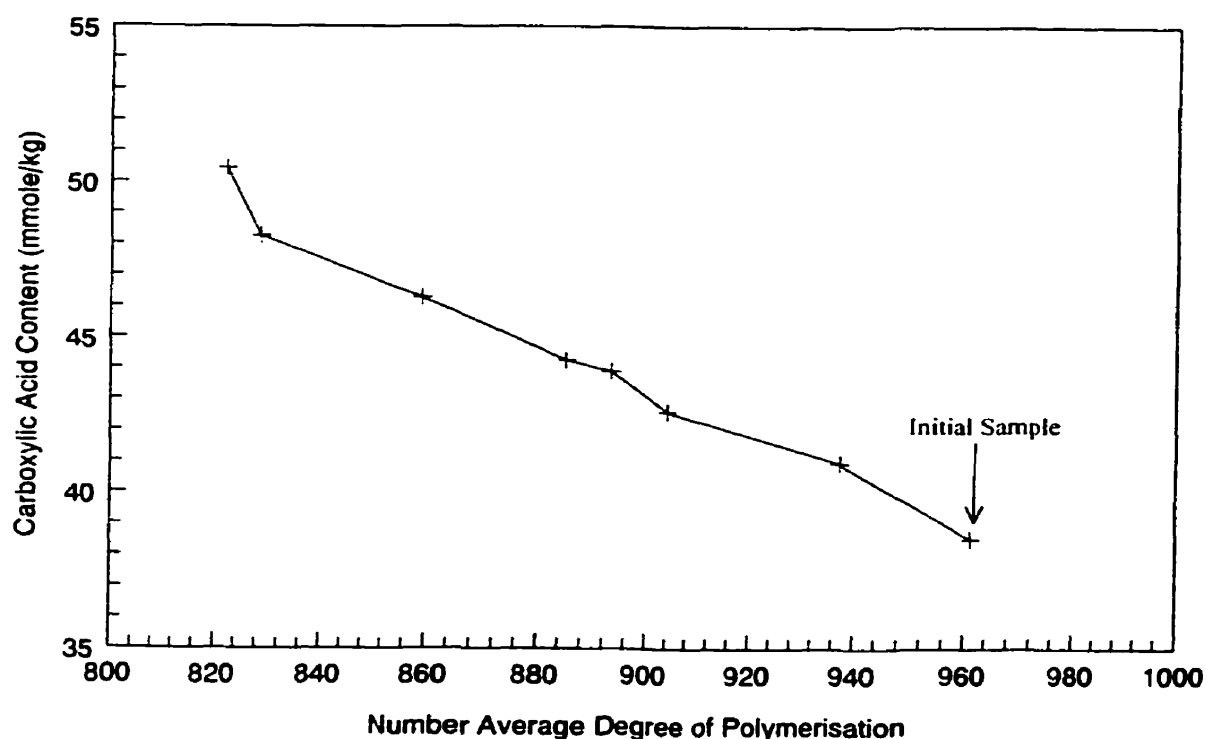


**Figure 6.7** Q-90 data showing the relationship of carboxylic acid content as a function of the degree of polymerisation.

Initially the carboxylic acid content is about 38 mmole/kg and has a degree of polymerisation of about 960. This means that even before any oxidation can take place there is already a significant amount of carboxylic acids present. As oxidation takes place, the amount of carboxylic acids increases while the degree of polymerisation

decreases. This concludes that oxidation takes place on the cellulose chain with resulting cleavage of the chain and decrease in polymer chain length. The cleavage that occurs has to be more than just chain "peeling" otherwise there would not be an increase in the carboxylic acid content.

The oxidation of the sample which increases the carboxylic acid content can be attributed to either or both the oxidation of the cellulose chain with or without cleavage, or from the hemicellulose present. When the same graph was plotted for the hemicellulose reduced sample the rise in the carboxylic acid content that occurred was not as significant as the rise in Figure 6.7. This indicates that some of the oxidation that increases the amount of carboxylic acids is definitely caused by the hemicellulose present within the cellulose fibres. Similar data are seen for the cotton cellulose samples. The plot of the Avicel samples show no significant changes as would be expected.

### 6.3.2 Chain Scission & Carboxylic Acid Content

A comparison of the chain scission number and carboxylic acid content also presents interesting conclusions. Plots of this nature were performed and the slope of the resulting curves obtained for the four cellulose samples studied appear in table 6.2.

Cellulose Type	Slope
Q-90	64.0
Hemicellulose Reduced	9.5
Cotton	58.7
Avicel	1.1

**Table 6.2** Slope values for the various cellulose samples calculated from a plot of the chain scission number versus carboxylic acid content.

The units for the slope are expressed in the number of scissions per cellulose chain over the amount of carboxylic acids in mmole/kg. All the values for the slope are above unity which indicates that there are more carboxylic acids being generated per cellulose chain than there are cleavages on that same chain. This could be due to two factors.

The first being that oxidation is taking place at various sites on the cellulose chain but no cleavage results. Some of these sites may include the reducing end group, the C3 and C6 carbons. The second factor is that the oxidation increases the carboxylic acid content due partly to the hemicellulose contribution. When the slopes of the Q-90 and hemicellulose reduced samples are compared, there is a big difference. When most of the hemicellulose is removed from the sample, there is a reduction in the number of carboxylic acids generated for every chain cleavage. This means that in the Q-90 data, the hemicellulose plays a significant role in contribution of carboxylic acid content. For the hemicellulose reduced sample, the slope is still not unity which can be concluded that oxidation of the cellulose takes place at sites on the cellulose chain other than those sites involved in chain cleavage.

#### **6.4 Summary**

In oxidising the various cellulose samples, degradation of the cellulose chains occurred. When the oxygen attacked the cellulose chains, causing chain cleavage, the degradation was monitored by viscosity measurements. It was shown that the viscosity of each of the four samples, with the exception of Avicel, increased with oxidation time. This results in a decrease of the average degree of polymerisation with time under oxidative conditions. Oxygen also attacked the cellulose chains and did not result in a cleavage. This results in oxidation of select carbons to carboxylic acids. These changes in carboxylic acid content were measured using conductometric titrations. As oxidation time progressed for each of the four cellulose samples chosen, so did the total amount of carboxylic acid present. A relationship between carboxylic acid content and degree of polymerisation has been obtained. In addition, the number of scissions in a cellulose chain (chain scission number) was compared to the carboxylic acid content. From these comparisons, a relationship was developed between viscosity measurements and conductometric titrations.



## Chapter 7

### Conclusions

---

To gain an understanding of the physicochemical properties of cellulose as it underwent the oxygen delignification process various analyses were performed. The relative degree of crystallinity was measured as a function of time for a number of different types of cellulose. The cellulose samples chosen were a fully bleached softwood pulp (Q-90), a hemicellulose free pulp derived from Q-90, a cotton cellulose and a microcrystalline cellulose (Avicel). Each sample after being oxidised for varying times were then characterised by three instrumental techniques, x-ray diffraction, Fourier transform infrared (FTIR) spectroscopy and  $^{13}\text{C}$  solid state nuclear magnetic resonance (NMR) spectroscopy.

The three methods of determining the relative degree of crystallinity on Q-90 pulp have been presented for which results showed an initial decrease in the relative degree of crystallinity towards an oxidation time of approximately 15 minutes. This pattern was typical for all oxygen treated Q-90 samples. Repeat experiments were conducted to ascertain the significance of this decrease in the relative degree of crystallinity. The reproduction of the sample preparation for oxidation and the repeated analyses for each instrumental technique generated similar results for the relative degree of crystallinity as a function of oxidation time. Evaluation of the x-ray diffraction, FTIR spectroscopy and solid state NMR spectroscopy results concludes that these techniques are valid to examine changes in cellulose crystallinity. All three techniques provided reproducible and consistent results.

For each of the three techniques the data of the hemicellulose reduced samples mimicked those of the original Q-90 sample results. It was apparent that the cellulose was changed from cellulose I to II due to mercerisation when removing the hemicellulose from the Q-90 pulp, however, this did not skew the results significantly. From the data presented it is clear that the minimum in the relative degree of crystallinity occurring at

15 minutes in the Q-90 samples is still prevalent in the hemicellulose reduced samples. Hence, hemicellulose does not appear to contribute to this phenomenon.

To better understand what may be taking place as oxygen attacks cellulose, another cellulose model was chosen. Cotton cellulose with about the same degree of polymerisation as the Q-90 sample was used. The data obtained by x-ray diffraction, FTIR spectroscopy and solid state NMR spectroscopy showed a consistent trend for oxygen pressurised samples. An increase in the relative degree of crystallinity followed by a decrease towards 30 minutes and another increase. The changes from decreasing relative degree of crystallinity to increasing relative degree of crystallinity occurred consistently at the 30 minute measurement point and the profiles for the relative degree of crystallinity versus oxidation times using each technique were remarkably similar. When these oxygen curves were compared with the curves obtained with the Q-90 and hemicellulose free samples it is evident that the minimum in relative degree of crystallinity moves from 15 minutes (for Q-90 and hemicellulose free pulp) to 30 minutes.

Since the data for the Q-90 and cotton cellulose samples are reproducible but vary in the time where a marked change in relative degree of crystallinity occurs in the profile, another type of cellulose called Avicel was chosen. By using the techniques of x-ray diffraction, FTIR spectroscopy and solid state NMR spectroscopy to analyse various oxidised Avicel samples, it was found that there was no change in the relative degree of crystallinity with time. It can be hypothesised that the oxygen reaction with cellulose takes place through a chain "peeling" process due to the fact that there is very little amorphous material for the oxygen to attack. This was evident in the data as the relative degree of crystallinity showed no change as time progressed.

In order to understand why the relative degree of crystallinity changes occurred for each of the four cellulose samples using the three instrumental techniques a comparison of the techniques for each sample and a comparison of the samples using each technique were presented. A theory is also proposed to explain the trends observed in the relative degree of crystallinity changes with time.

In oxidising the various cellulose samples, degradation of the cellulose chains occurred. When the oxygen attacked the cellulose chains, causing chain cleavage, the degradation was monitored by viscosity measurements. It was shown that the viscosity of each of the four samples, with the exception of Avicel, decreased with oxidation time. This results in a decrease of the average degree of polymerisation with time under oxidative conditions. Oxygen also attacked the cellulose chains and did not result in a cleavage. This results in oxidation of select carbons to carboxylic acids. These changes in carboxylic acid content were measured using conductometric titrations. As oxidation time progressed for each of the four cellulose samples chosen, so did the total amount of carboxylic acid present. A relationship between carboxylic acid content and degree of polymerisation has been obtained. In addition, the number of scissions in a cellulose chain (chain scission number) was compared to the carboxylic acid content. From these comparisons, a relationship was developed between viscosity measurements and conductometric titrations.

## Chapter 8

### Recommendations for Future Work

---

The knowledge gained so far by the analysis of the physicochemical properties of cellulose as it undergoes the oxygen delignification process has been very valuable. It has been shown that there are three distinct stages in the plot of the relative degree of crystallinity versus oxidation time for various celluloses. This may provide the pulp and paper industry with an insight into obtaining stronger paper by modifying the oxygen delignification process. However, the data obtained in this thesis is preliminary and so further investigation into a better understanding is required before suggestions to practical applications can be made.

Oxidation times chosen in this work revealed that there was a local maximum value at 10 minutes and a minimum value at 15 minutes for the Q-90 cellulose. The maximum and minimum values can be precisely obtained if this work is repeated using shorter time intervals. Repeating the measurements at perhaps, half minute oxidation time intervals, between 5 and 30 minutes and then analysing the results with one of the three instrumental techniques explored in this work would provide the necessary information. In a similar way the cotton cellulose can be analysed for a maximum and minimum value by careful investigation of the oxidation times that lie between 15 and 60 minutes.

Alternatively, the contribution of transition metal ions on the relative degree of crystallinity and on the degradation of the cellulose can be investigated by adding known amounts of transition metals to the cellulose. These new samples can then be oxidised and analysed to investigate the influence of the metal ion contribution. At the same time various protectors can be added in the reactor to examine if they can reduce or eliminate the degradation effects of the transition metal ions. The contribution of lignin can also be studied in a similar manner by oxidising the cellulose in the reactor in the presence of lignin and various lignin model compounds.

Other types of cellulose, that have not been studied in this thesis should also be examined. Bacterial and algae celluloses have large uniform crystal lattices. It would be

interesting to see how they would be modified under the oxidation conditions used in this work. Also from a more practical perspective, the oxidation of cellulose from a hardwood can be examined. Hardwood cellulose differs from that of softwood chosen for investigation in this thesis.

Other instrumental techniques, like near infrared spectroscopy and water retention, can be examined using one of the cellulose samples chosen in this study to see how accurately the changes in the degree of crystallinity can be monitored. Using one of these other techniques can provide another valid and viable way of examining changes in cellulose crystallinity.

The effect of the degree of polymerisation on the oxidation and relative degree of crystallinity would prove to be another interesting study. By varying the degree of crystallinity for one of the cellulose samples chosen in this thesis and examining it in the same way, a comparison can be made. This may provide useful information in understanding the cleavage reactions that take place on the cellulose during oxidation. The degree of polymerisation can also be investigated using gel permeation chromatography. In doing this, the values for the degree of polymerisation obtained by viscosity measurements can be compared and evaluated.

In this work the carboxylic acid content was monitored as a function of oxidation time. This however, does not reflect on the total oxidation that takes place on the cellulose fibres. If however, a method to determine the carbonyl content can be developed, then this information along with the carboxylic acid content information can be summed to give a value that can be equated with the total oxidation that takes place on the cellulose fibres.

Weight loss as a function of oxidation time was not recorded in the present study. Further examination of weight loss measurements would be necessary to see if the amorphous material is in fact being degraded prior to crystalline material. The theory proposed herein suggests that once the crystalline regions are attacked, then new amorphous regions are formed that subsequently preclude attack on the remaining crystallites. However, from a kinetic point of view the attack on the crystallites could be a rate determining step. Thus the amorphous material surrounding the crystallite could be degraded much faster than it can develop. In light of this, further kinetic studies be performed to validate the theory.

## Chapter 9

### References

---

- 1 Dence C. W., and Reeve D. W., *Pulp Bleaching: Principles and Practice*, Tappi Press, Atlanta, 1996.
- 2 Rydholm S. A., *Pulping Processes*, Interscience Publishers, New York, 1965.
- 3 Singh R. P., *The Bleaching of Pulp (third edition)*, Tappi Press, Atlanta, 1979.
- 4 Pryke D. C., and Reeve D., *A Survey of Chlorine Dioxide Delignification Practices in Canada*, Tappi Journal, **80(5)**, 153, 1997.
- 5 Brelid H., Friberg T., and Simonson R., *TCF Bleaching of Softwood Kraft Pulp. Part 3. Ion Exchange of Softwood Kraft Pulp Prior to Oxygen Delignification*, Nordic Pulp and Paper Research Journal, **12(2)**, 80, 1997.
- 6 Roberts J. C., *Paper Chemistry (second edition)*, Blackie Academic & Professional, London, 1996.
- 7 Young R. A., and Akhtar M., *Environmentally Friendly Technologies for the Pulp and Paper Industry*, John Wiley and Sons Inc., New York, 1998.
- 8 Cardona D., Chirat C., and Lachenal D., *Nondegrading Oxygen Bleaching*, International Pulp Bleaching Conference, 1998.
- 9 Biermann C. J., *Essentials of Pulping and Papermaking*, Academic Press, New York, 1993.
- 10 Carter D., Johnson T., McKenzie D., and Idner K., *Oxygen Delignification - A Study of Performance Parameters*, Pulping Conference, 469, 1996.
- 11 Sarkanen K. V., Kakehi K., Murphy R. A., and White H., *Studies on Oxidative Delignification Mechanisms. Part I. Oxidation of Vanillin with Chlorine Dioxide*, Tappi, **45(1)**, 24, 1962.
- 12 Casey J. P., *Pulp and Paper Chemistry and Chemical Technology (third edition), Volume I*, John Wiley and Sons Inc., New York, 1980.
- 13 Kocurek M. J., *Handbook for Pulp and Paper Technologists*, Tappi Press, Atlanta, 1982.

- 14 Rapson W. H., Anderson C. B., and King G. F., *Carbonyl Groups in Cellulose and Color Reversion. Part II. Hypochlorite Bleaching and Color Reversion*, Tappi, **41(8)**, 422, 1958.
- 15 Histed J. A., and Nicolle F. M. A., *Water Reuse and Recycle in CDEHDED Bleach Sequence*, Tappi, **59(3)**, 75, 1976.
- 16 Axegaard P., and Tormund D., *Kinetics and Stoichiometry of Hypochlorite Bleaching - A Comparison with Chlorine Dioxide*, Svensk Papperstidn, **88(3)**, R36, 1985.
- 17 Vice K., Trepte R., Stuart P., and Johnson T., *The Cluster Rule - The Road to Promulgation*, Tappi Journal, **80(12)**, 34, 1997.
- 18 Gillespie R. J., Humphreys D. A., Baird N. C., and Robinson E. A., *Chemistry (second edition)*, Allyn and Bacon, Massachusetts, 1989.
- 19 Pryke D. C., Winter P., Bouree G. R., and Mickowski C., *The Impact of Chlorine Dioxide Delignification on Pulp Manufacture and Effluent Characteristics*, Pulp and Paper Canada, **95(6)**, T230, 1994.
- 20 Masschelein W. J., *Chlorine Dioxide*, Ann Arbor Science Publishers Inc., Michigan, 1979.
- 21 Earl P. F., *The Fundamental of Chlorine Dioxide (ECF) Bleaching*, Tappi Pulping Conference Proceedings, 129, 1998.
- 22 Presley J. R., *Bleach Plant Faces New Environmental Hurdle in Adsorbable Organic Halides*, Pulp and Paper, **64(7)**, 252, 1990.
- 23 Reeve D. W., and Earl, P. F., *Chlorinated Organic Matter in Bleached Chemical Pulp Production. Part 1. Environmental Impact and Regulation of Effluent*, Pulp and Paper Canada, **90(4)**, 65, 1989.
- 24 Brannland R., and Fossum G., *How to cope with TOCl*, Tappi Pulping Conference Proceedings, 243, 1987.
- 25 McDonough T. J., *Oxygen Bleaching Processes*, Tappi Journal, **69(6)**, 46, 1986.
- 26 Johnson A. P., *Oxygen Delignification Systems Flourish as Mills Push for Lower Kappa Levels*, Pulp and Paper, **67(3)**, 103, 1993.

- 27 Sjostrom E., *Behaviour of Pulp Polysaccharides During Oxygen Alkali Delignification*, Chemistry of Delignification with Oxygen, Ozone and Peroxide, Uni Publishers Co. Ltd., Tokyo, 61, 1980.
- 28 van Lierop B., Liebergott N., and Faubert M. G., *Using Oxygen and Peroxide to Bleach Kraft Pulps*, CPPA Annual Technical Meeting, Montreal, **Volume B**, 81, 1993.
- 29 Lapiere L., Bouchard J., Berry R. M., and Van Lierop B., *Chelation Prior to Hydrogen Peroxide Bleaching of Kraft Pulps: an Overview*, Journal of Pulp and Paper Science, **21(8)**, J268, 1995.
- 30 Owins R. W., Strunk W. G., and Meng T. Y., *Bleaching with Hydrogen Peroxide in High Density Storage*, Pulp and Paper Canada, **86(9)**, 79, 1985.
- 31 Basta J., Holtinger L., Hermansson W., and Lundgren P., *Metal Management in TCF/ECF Bleaching. Part 1. TCF Bleaching*, Proceedings from the International Pulp Bleaching Conference, Vancouver, 29, 1994.
- 32 Fuhrmann A., Malinen R., Rautonen R., Hausalo T., and Sagfors P.-E., *Influence of Ozonation Parameters on Delignification and Cellulose Degradation*, Eight International Symposium on Wood and Pulping Chemistry - Oral Presentation Preceedings, **1**, 337, 1995.
- 33 Brodin A., Gierer J., and Zhang Y., *On the Selectivity of Ozone Delignification of Softwood Kraft Pulps*, Wood Science and Technology, **27(2)**, 115, 1993.
- 34 Rice R. C., and Netzer A., *Handbook of Ozone Technology and Application*, Volume I, Ann Arbor Science Publishers, Ann Arbor, 1982.
- 35 Homer G., Muguet M., Epiney M., and Johnson S., *Oxygen, Ozone, and Chlorine Dioxide*, CPPA Annual Technical Meeting, Montreal, A297, 1996.
- 36 Lindholm C-A., *Effect of Pulp Consistency and pH in Ozone Bleaching. Part 6. Strength Properties*, Nordic Pulp and Paper Research Journal, **5(1)**, 22, 1990.
- 37 Timell T. E., *Microbial and Enzymatic Degradation of Wood and Wood Components*, Springer-Verlag, Heidelberg, 1990.
- 38 Tench L., and Harper S., *Oxygen Bleaching Practices and Benefits: an Overview*, Tappi Journal, **70(11)**, 55, 1987.
- 39 Delpech F., and Robert A., *Relative Considerations of the Delignification of Plants by Oxygen in an Alkaline Environment*, Cellulose Chemistry and Technology, **27(3)**, 287, 1993.



- 40 *Glossary of Bleaching Terms.*, Canadian Pulp and Paper Association - Technical Section. Montreal. 1996.
- 41 Yasumoto M., Matsumoto Y., and Ishizu A., *The Role of Peroxide Species in Carbohydrate Degradation During Oxygen Bleaching. Part I. Factors Influencing the Reaction Selectivity Between Carbohydrate and Lignin Model Compounds*, *Journal of Wood Chemistry and Technology*, **16(1)**, 95, 1996.
- 42 Abrahamsson K., Lowendahl L., and Samuelson O., *Pretreatment of Kraft Pulp with Nitrogen Dioxide Before Oxygen Bleaching*, *Svensk Papperstidn*, **84(18)**, R152. 1981.
- 43 Samuelson O., and Sjoberg L., *Alkaline Delignification of Kraft Pulps Pretreated with Nitrogen Dioxide*, *Pulp and Paper Science*, **9(1)**, TR21. 1983.
- 44 Fossum G., and Marklund A., *Pretreatment of Kraft Pulp is the Key to Ease Final Bleaching*, Tappi International Pulp Bleaching Conference, Atlanta, 253, 1988.
- 45 Gierer J., Reitberger T., and Yang E., *Formation and Involvement of Hydroxyl Radicals in Oxygen Bleaching*, Oral Presentation Proceedings of the ACM Workshop on Role Based Access Control, New York, **1**, R2-1, 1997.
- 46 Bouchard J., Abatzoglou N., Chornet E., and Overend R. P., *Characterization of Depolymerized Cellulosic Residues. Part I. Residues obtained by Acid Hydrolysis Processes*, *Wood Science and Technology*, **23**, 343, 1989.
- 47 Iribarne J., and Schroeder L. R., *High Pressure Oxygen Delignification of Kraft Pulps. Part I. Kinetics*, Pulping Conference, 125, 1995.
- 48 Sjostrom E., *Wood Chemistry - Fundamentals and Applications (second edition)*, Academic Press, New York, 1993.
- 49 Brown G., *Effects of Metal Ions on Oxygen Delignification of Kraft Pulp*, *Paper Age*, **112(10)**, 18, 1996.
- 50 Bouchard J., Nugent H. M., and Berry R. M., *A Comparison Between Acid Treatment and Chelation Prior to Hydrogen Peroxide Bleaching of Kraft Pulps*, *Journal of Pulp and Paper Science*, **21(6)**, J203, 1995.
- 51 Dafaye J., and Gadelle A., *Protection Mechanism by Magnesium Salts Against Cellulose Degradation During Alkaline-Oxygen Delignification*, International Pulp Bleaching Conference, 43, 1973.

- 52 Robert A., Rerolle P., Viallet A., and Martin-Borret O., *Oxygen Treatment of Pulps to Further Subsequent Bleaching*, ATIP Review, **18(4)**, 151, 1964.
- 53 Samuelson O., and Ojteg U., *Behaviour of Calcium, Magnesium and Manganese Compounds During Oxygen Bleaching of Kraft Pulps*, Journal of Wood Chemistry and Technology, **15(3)**, 303, 1995.
- 54 Yokoyama T., Matsumoto Y., and Meshitsuka G., *The Role of Peroxide Species in Carbohydrate Degradation During Oxygen Bleaching. Part III. Effect of Metal Ions on the Reaction Selectivity Between Lignin and Carbohydrate Model Compounds*, Journal of Pulp and Paper Science, **25(2)**, J42, 1999.
- 55 Samuelson O., and Ojteg U., *Influence of Manganese and Magnesium on Oxygen Bleaching in Carbonate Media after a Nitrogen Dioxide Pretreatment*, Holzforschung, **50(4)**, 379, 1996.
- 56 Mackay K. M., and Mackay R. A., *Introduction to Modern Inorganic Chemistry (fourth edition)*, Prentice Hall, Englewood Cliffs, 1989.
- 57 Cotton F. A., and Wilkinson G., *Advanced Inorganic Chemistry (fifth edition)*., John Wiley and Sons, New York, 1988.
- 58 Gratzl J. S., *Chemical Principles of Pulp Bleaching with Oxygen, Hydrogen Peroxide and Ozone - a short review*, Papier, **46(10A)**, VI, 1992.
- 59 Singh A., *Phenoxy- and Oxy-radicals and Their Role in Oxygen Delignification*, International Oxygen Delignification Conference Proceedings, 111, 1987.
- 60 Roberts J. C., *The Chemistry of Paper*. The Royal Society of Chemistry, Cambridge, 1996.
- 61 Fengel D., and Wegener G., *Wood: Chemistry, Ultrastructure, Reactions*, Walter de Gruyter, New York, 1984.
- 62 Gellerstedt G., Gustafsson K., and Lindfors E-L., *Structural Changes in Lignin During Oxygen Bleaching*, Nordic Pulp and Paper Research Journal, **1(3)**, 14, 1986.
- 63 Gellerstedt G., and Lindfors E-L., *Hydrophilic Groups in Lignin After Oxygen Bleaching*., Tappi Journal, **70(6)**, 119, 1987.
- 64 Asgari F., and Argyropoulos D. S., *Fundamentals of Oxygen Delignification. Part II. Functional Group Formation/Elimination in Residual Kraft Lignin*, Canadian Journal of Chemistry, **76**, 1606, 1998.

- 65 Lai Y.-Z., Funaoka M., and Chen H.-T., *Oxygen Bleaching of Kraft Pulp. Part I. Role of Condensed Units*, *Holzforschung*, **48(4)**, 355, 1994.
- 66 Gierer J., *Basic Principals of Bleaching. Part I. Cationic and Radical Processes*, *Holzforschung*, **44(5)**, 387, 1990.
- 67 Gierer J., *The Reactions of Lignins with Oxygen Containing Species*, Seventh International Symposium on Wood and Pulping Chemistry Proceedings, **Volume 1**, Beijing, 301, 1993.
- 68 Hagstrom-Nasi C., and Sjostrom E., *Alkaline Oxygen Oxidation of Dioxane Lignin and Cresol in Aqueous Ethanol*, *Journal of Wood Chemistry and Technology*, **8(3)**, 299, 1988.
- 69 Gellerstedt G., and Lindfors E.-L., *On the Structure and Reactivity of Residual Lignin in Kraft Pulp Fibers*, International Pulp Bleaching Conference Notes, Stockholm, 73, 1991.
- 70 Arthur J. C., *Cellulose Chemistry and Technology*, American Chemical Society, Washington, 1977.
- 71 Marchessault R. H., and Sudararajan P. R., *Cellulose, The Polysaccharides*, **2**, 11, 1983.
- 72 Stevens M. P., *Polymer Chemistry - An Introduction (second edition)*, Oxford University Press, Oxford, 1990.
- 73 Nevell T. P., and Zeronian S. H., *Cellulose Chemistry and its Applications*, John Wiley and Sons, New York, 1985.
- 74 Agarwal N., and Gustafson R., *Effect of Carbohydrate Degradation on Zero-span Tensile Strength*, *Tappi Journal*, **78(1)**, 97, 1995.
- 75 Abrahamsson K., and Samuelson O., *Oxygen Alkali Cooking of Wood Meal. Part III. Influence of Oxygen Pressure, Carbon Dioxide and Metal Compounds*, *Svensk Papperstidning*, **13**, 480, 1973.
- 76 Theander O., *Carbohydrate Reactions in Oxygen Alkali Delignification Processes, Chemistry of Delignification with Oxygen, Ozone and Peroxide*, Uni Publishers Co. Ltd., Tokyo, 43, 1980.
- 77 Olm L., and Teder A., *The Kinetics of Oxygen Bleaching*, *Tappi*, **62(12)**, 43, 1979.
- 78 Gratzl J. S., *Reactions of Polysaccharides and Lignins in Bleaching with Oxygen and Related Species*, Oxygen Delignification Symposium Notes, 1, 1990.

- 79 Crescenzi V., Belardinelli M., and Rinaldi C., *Polysaccharides Depolymerization via Hydroxyl Radicals Attack in Dilute Aqueous Solution*, Journal of Carbohydrate Chemistry, **16(4&5)**, 561, 1997.
- 80 Nunn J. R., and van der Linde M. J., *The Protective Action of Magnesium in Oxygen Bleaching of Pulp. Part 1. The Complexing of Methyl-alpha-D-Glucopyranoside with Magnesium Ions*, Chemistry of Delignification with Oxygen, Ozone and Peroxide, Uni Publishers Co. Ltd., Tokyo, 79, 1980.
- 81 Samuelson O., and Stolpe L., *Degradation of Carbohydrates During Oxygen Bleaching. Part 1. Cellobiitol as a Model Substance*, Svensk Papperstidning, **20**, 662, 1969.
- 82 Ericsson B., Lingren B. O., and Theander O., *Factors Influencing the Carbohydrate Degradation Under Oxygen-Alkali Bleaching*, Svensk Papperstidn., **74**, 757, 1971.
- 83 Minor J., and Sanyer S., *Oxygen/Alkali Oxidation of Cellulose and Model Alcohols and the Inhibition by Iodide*, Journal of Polymer Science - Part C, **36**, 73, 1971.
- 84 Hearne D. O., Thompson N. S., and Schroeder L. R., *Degradation of Methyl beta-D-ribofuranoside and Methyl beta-D-xylofuranoside by Oxygen in Aqueous Sodium Hydroxide Solution*, Journal of Wood Chemistry and Technology, **11(3)**, 307, 1991.
- 85 Minor J., and Sanyer S., *Carbohydrate Stabilization with Iodide in Oxygen Bleaching of Kraft Pulps*, Tappi Journal, **57(2)**, 109, 1974.
- 86 Masura V., *Delignification and Degradation of Kraft Pulp During Oxygen Bleaching*, Cellulose Chemistry and Technology, **27**, 201, 1993.
- 87 Gustavsson R., and Swan B., *Evaluation of the Degradation of Cellulose and Delignification During Oxygen Bleaching*, Tappi, **58(3)**, 120, 1975.
- 88 Dahlman O., Morck R., Larsson P. T., Lindquist A., and Rydlund A., *Modification of the Hemicellulose Composition During TCF Bleaching of Kraft Pulps*, Ninth International Symposium on Wood and Pulp Chemistry, Oral Presentations, M1-1, 1997.
- 89 Isogai A., Ishizu A., and Nakano J., *Residual Lignin in Unbleached Kraft Pulp. Part II. Analysis of Unbleached Kraft Pulp by New Permethylation Method*, Journal of Wood Chemistry and Technology, **7(4)**, 463, 1987.

- 90 Isogai A., Ishizu A., and Nakano J., *Residual Lignin and Hemicellulose in Wood Cellulose. Analysis Using New Permethylation Method*. *Holzforschung*, **43(5)**, 333, 1989.
- 91 Stamm A. J., *Wood and Cellulose Science*. The Ronald Press Co., New York., 1964.
- 92 Ferrus R., and Pages P., *Water Retention Value and Degree of Crystallinity By Infrared Absorption Spectroscopy in Caustic Soda Treated Cotton*, *Cellulose Chemistry and Technology*, **11**, 633, 1977.
- 93 Howsmon J. A., *Water Sorption and the Poly-phase Structure of Cellulose Fibers*, *Textile Research Journal*, **March**, 152, 1949.
- 94 Basch A., Wasserman T., and Lewin M., *Near-Infrared Spectrum of Cellulose: A New Method for Obtaining Crystallinity Ratios*. *Journal of Polymer Science: Polymer Chemistry Edition*, **12**, 1143, 1974.
- 95 Smart L., and Moore E., *Solid State Chemistry*, Chapman and Hall, London, 1992.
- 96 Halliday D., and Resnick R., *Fundamentals of Physics (third edition)*, John Wiley and Sons, New York, 1988.
- 97 Atalla R. H., *The Structures of Cellulose - Characterization of the Solid States*, American Chemical Society, Washington, 1987.
- 98 Meyer K. H., and Misch L., *The Constitution of the Crystalline Part of Cellulose. Part VI. The Positions of the Atoms in the New Space Model of Cellulose*, *Helv. Chim. Acta*, **20**, 232, 1937.
- 99 Ishikawa A., Okano T., and Sugiyama J., *Fine Structure and Tensile Properties of Ramie Fibres in the Crystalline Form of Cellulose I, II, III, and IV*, *Polymer*, **38(2)**, 463, 1997.
- 100 Kroonbatenburg L. M. J., and Kroon J., *The Crystal and Molecular Structures of Cellulose I and II*, *Glycoconjugate Journal*, **14(5)**, 677, 1997.
- 101 Atalla R. H., Gast J. C., Sindorf D. W., Bartuska V. J., and Maciel G. E., *<sup>13</sup>C NMR Spectra of Cellulose Polymorphs*, *Journal of the American Chemical Society*, **102(9)**, 3249, 1980.
- 102 Gardner K. H., and Blackwell J., *Structure of Native Cellulose*, *Biopolymers*, **13**, 1975, 1974.

- 103 Evans R., Newman R. H., Roick U. C., Suckling I. D., and Wallis A. F. A., *Changes in Cellulose Crystallinity During Kraft Pulping. Comparison of Infrared, X-ray Diffraction and Solid State NMR Results*, *Holzforschung*, **49(6)**, 498, 1995.
- 104 Newman R. H., and Hemmingson J. A., *Determination of the Degree of Cellulose Crystallinity in Wood by Carbon-13 Nuclear Magnetic Resonance Spectroscopy*, *Holzforschung*, **44(5)**, 351, 1990.
- 105 Billmeyer F. W., *Textbook of Polymer Science (second edition)*, John Wiley and Sons, New York, 1971.
- 106 O'Connor R. T., DuPre E. F., and Mitcham D., *Applications of Infrared Absorption Spectroscopy to Investigations of Cotton and Modified Cottons. Part I. Physical and Crystalline Modifications and Oxidation*, *Textile Research Journal*, **28**, 382, 1958.
- 107 Michell A. J., *Infra-red Spectroscopy Transformed - New Applications in Wood and Pulping Chemistry*, *Appita Journal*, **41(5)**, 375, 1988.
- 108 Hortling B., Tamminen T., and Kentta E., *Determination of Carboxyl and Non-Conjugated Carbonyl Groups in Dissolved and Residual Lignins by IR Spectroscopy*, *Holzforschung*, **51(5)**, 405, 1997.
- 109 Michell A. J., *Note on a Technique for Obtaining Infrared Spectra of Treated Wood Surfaces*, *Wood and Fiber Science*, **20(2)**, 272, 1988.
- 110 Pekarovicova A., Venditti R. A., Cao H., Lou Y. M., and Jean Y. C., *Cellulose Free Volume Characterization Using Positron Annihilation Lifetime Spectroscopy*, *Journal of Pulp and Paper Science*, **23(3)**, J101, 1997.
- 111 Schultz T. P., and Glasser W. G., *Quantitative Structural Analysis of Lignin by Diffuse Reflectance Fourier Transform Infrared Spectrometry*, *Holzforschung*, **40(Supplement)**, 37, 1986.
- 112 Schultz T. P., Templeton M. C., and McGinnis G. D., *Rapid Determination of Lignocellulose by Diffuse Reflectance Fourier Transform Infrared Spectroscopy*, *Analytical Chemistry*, **57**, 2867, 1985.
- 113 Atalla R. H., and VanderHart D. L., *Studies on the Structure of Cellulose Using Raman Spectroscopy and Solid State <sup>13</sup>C NMR*, *Proceedings of the Tenth Cellulose Conference*, 169, 1988.

- 114 Andrew E. R., Bradbury A., and Eades R. G., *Removal of Dipolar Broadening of Nuclear Magic Resonance Spectra of Solids by Specimen Rotation*, *Nature*, **183**, 1802, 1959.
- 115 Hartman S., and Hahn E. L., *Nuclear Double Resonance Spectroscopy*, *Bulletin of the American Physics Society*, **5**, 498, 1959.
- 116 Fyfe C. A., Stephenson P. J., Veregin R. P., Hamer G. K., and Marchessault R. H., *Insights into the Lattice Structure of Cellulose II From the High Resolution CP/MAS Solid State  $^{13}\text{C}$  NMR Spectrum of Cellotetrose*, *Journal of Carbohydrate Chemistry*, **3(4)**, 663, 1984.
- 117 Fyfe C. A., Dudley R. L. Stephenson P. J., Deslandes Y., Hamer G. K., and Marchessault R. H., *Application of High-Resolution Solid-State NMR with Cross-Polarization / Magic-Angle Spinning (CP/MAS) Techniques to Cellulose Chemistry*, *Journal of Macromolecular Science - Part C*, **C23(2)**, 187, 1983.
- 118 Hirai A., Horii F., and Kitamaru R., *CP / MAS  $^{13}\text{C}$  NMR Study of Never-Dried Cotton Fibers*, *Journal of Polymer Science: Part C: Polymer Letters*, **28**, 357, 1990.
- 119 Pfeffer P. E., *High Resolution Solid State  $^{13}\text{C}$  NMR and its Applications in Carbohydrate Chemistry*, *Journal of Carbohydrate Chemistry*, **3(4)**, 613, 1984.
- 120 Hirai A., Horii F., and Kitamaru R., *Carbon-13 Spin-Lattice Relaxation Behaviour of the Crystalline and Noncrystalline Components of Native and Regenerated Celluloses*, *Cellulose Chemistry and Technology*, **24**, 703, 1990.
- 121 Argyropoulos D. S., and Morin F. G., *Probing the Macromolecular Structure of Wood and Pulps with Proton Spin-Lattice Relaxation Time Measurements in the Solid State*, *Wood Science and Technology*, **29**, 19, 1995.
- 122 Kosikova B., Hricovini M., and Simonutti R.,  *$^{13}\text{C}$  NMR Study of Solid State Reaction of Cellulose with Lignin Monomers*, *Holzforschung*, **50(4)**, 335, 1996.
- 123 Willis J. M., and Herring F. G., *Effect of Water in the  $^{13}\text{C}$  CP/MAS NMR Spectrum of White Spruce Wood*, *Macromolecules*, **20**, 1554, 1987.
- 124 Ahvazi B., and Argyropoulos D. S., *Proton Spin-Lattice Relaxation Time Measurements of Solid Wood and its Constituents as Function of pH*, *Wood Science and Technology*, **33**, 1999.
- 125 Argyropoulos S. S., Morin F. G., and Lapcik L., *Magnetic Field and Temperature Effects on the Solid State Proton Spin-Lattice Relaxation Time Measurements of Wood and Pulps*, *Holzforschung*, **49(2)**, 115, 1995.

- 126 Ni J., and Frazier C. E., *Molecular Correlation to Macroscopic Wood Performance using CP/MAS NMR*, *Holzforschung*, **50(4)**, 327, 1996.
- 127 Newman R. H., *Carbon-13 Nuclear Magnetic Resonance Studies of Molecular Motion in Wood and Paper*, Fourth International Symposium on Wood and Pulping Chemistry, Paris, 195, 1987.
- 128 Sarkanen K. V., and Ludwig C. H., *Lignins: Occurrence, Formation, Structure and Reactions*, Wiley-Interscience, New York, 1971.
- 129 Wickholm K., Larsson P. T., and Iversen T., *Assignment of Non-Crystalline Forms in Cellulose I by CP/MAS <sup>13</sup>C NMR Spectroscopy*, *Carbohydrate Research*, **312**, 123, 1998.
- 130 Newman R. H., Hemmingson J. A., and Suckling I. D., *Carbon-13 Nuclear Magnetic Resonance Studies of Kraft Pulping*, *Holzforschung*, **47(3)**, 234, 1993.
- 131 Newman R. H., *Evidence for Assignment of <sup>13</sup>C NMR Signals to Cellulose Crystallite Surfaces in Wood, Pulp and Isolated Celluloses*, *Holzforschung*, **52(2)**, 157, 1998.
- 132 Earl W. L., and VanderHart D. L., *High Resolution, Magic Angle Sample Spinning <sup>13</sup>C NMR of Solid Cellulose I*, *Journal of the American Chemical Society*, **102(9)**, 3251, 1980.
- 133 Zhbankov R. G., Ioelovich Y. M., Treimanis A., Lippmaa E. T., Teeaar R., Kaputskii F. N., Grinshpan D. D., and Lushchik L. G., *Determination of the Degree of Crystallinity of Cellulose by High Resolution Solid State Carbon-13 NMR*, *Khim. Drev*, **4**, 3, 1986.
- 134 Teeaar R., Serimaa R., and Paakkari T., *Crystallinity of Cellulose as Determined by CP/MAS NMR and XRD Methods*, *Polymer Bulletin*, **17**, 231, 1987.
- 135 Sterk H., Sattler W., Janosi A., Paul D., and Esterbauer H., *<sup>13</sup>C NMR Spectroscopy to Determine the Degree of Crystallinity of Cellulose*, *Das Papier*, **41**, 664, 1987.
- 136 Vidal P. F., Basora N., Overend R. P., and Chomet E., *A Pseudouniversal Calibration Procedure for the Molecular Weight Determination of Cellulose*, *Journal of Applied Polymer Science*, **42**, 1659, 1991.
- 137 Lind J., and Merenyi G., *Hydroxyl Radical Induced Viscosity Loss in Cellulose Fibres*, *Journal of Wood Chemistry and Technology*, **17(1&2)**, 111, 1997.



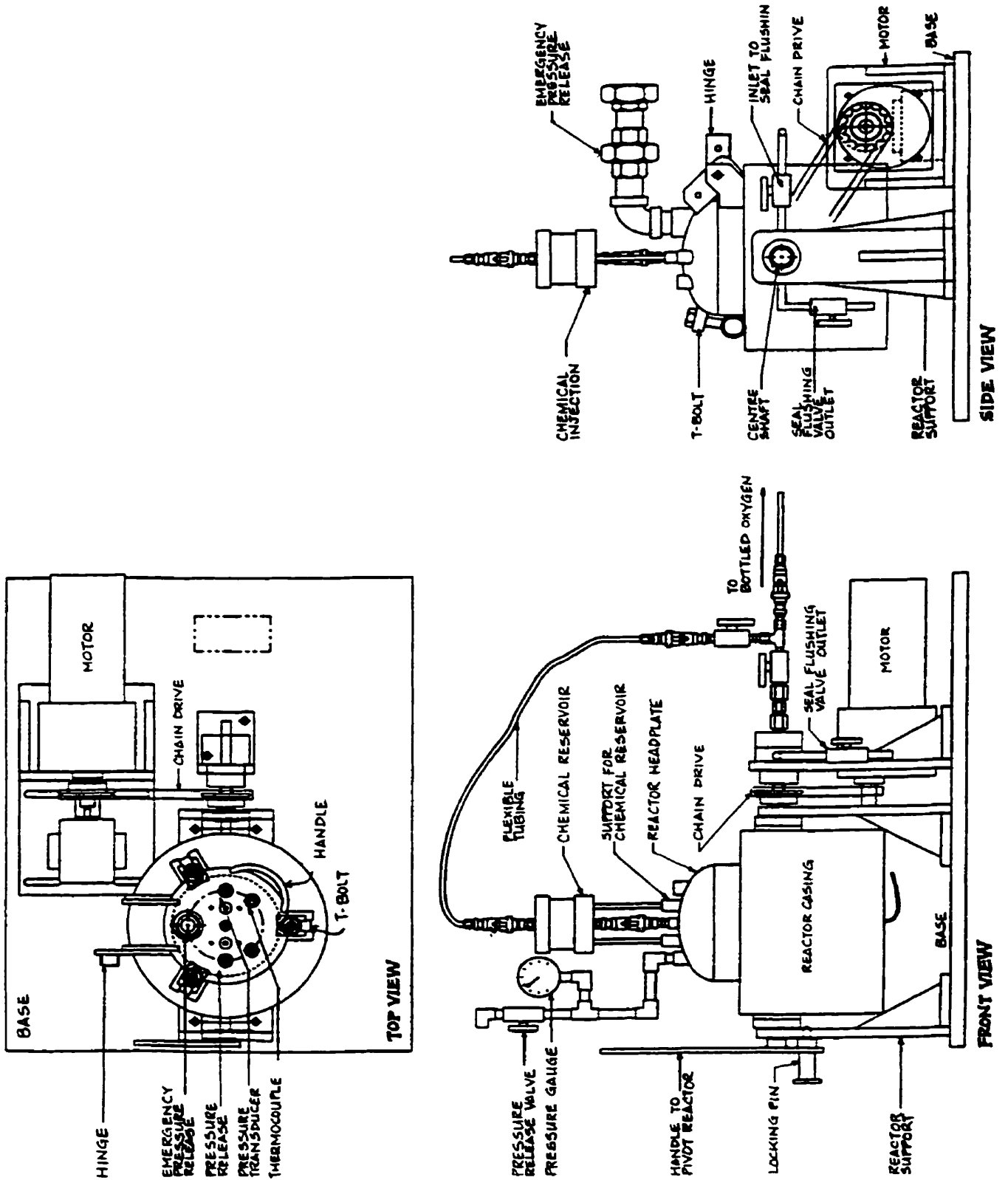
- 138 Bouchard J., Overend R. P., and Chornet E., *Mechanism of Dilute Acid Hydrolysis of Cellulose Accounting for its Degradation in the Solid State*, Journal of Wood Chemistry and Technology, **12(3)**, 335, 1992.
- 139 Bouchard J., Lacelle S., Chornet E., Vidal P. F., and Overend R. P., *Mechanism of Depolymerization of Cellulose by Ethylene Glycol Solvolysis*, Holzforschung, **47(4)**, 291, 1993.
- 140 Westermark U., and Gustafsson K., *Molecular Size Distribution of Wood Polymers in Birch Kraft Pulps*, Holzforschung, **48 (Supplement)**, 146, 1994.
- 141 Lapierre L., and Bouchard J., *Molecular Weight Determination of Softwood Kraft Cellulose: Effects of Carbanilation Solvent, Hemicelluloses and Lignin*, PPR 1256, 1996.
- 142 Silva A. A., and Laver M. L., *Molecular Weight Characterization of Wood Pulp Cellulose - Dissolution and Size Exclusion Chromatographic Analysis*, Tappi Journal, **80(6)**, 173, 1997.
- 143 Donnan F. G., and Harris A. B., *Osmotic Pressure and Conditions of Aqueous Solutions of Congo Red and Reversible Membrane Equilibrium*, Journal of the Chemical Society, **99**, 1554, 1911.
- 144 Katz S., Beatson R. P., and Scallan A. M., *The Determination of Strong and Weak Acidic Groups in Sulfite Pulps*, Svensk Papperstidn, **87(6)**, R48, 1984.
- 145 Grignon J., and Scallan A. M., *Effect of pH and Neutral Salts Upon the Swelling of Cellulose Gels*, Journal of Applied Polymer Science, **25**, 2829, 1980.
- 146 Scallan A. M., *The Effect of Acidic Groups on the Swelling of Pulps: a Review*, Tappi Journal, **65(11)**, 73, 1983.
- 147 Beelik A., Conca R. J., Hamilton J. K., and Partlow E. V., *Selective Extraction of Hemicelluloses From Softwoods*, Tappi, **50(2)**, 78, 1967.
- 148 *The Measurement of Proton-Enhanced Carbon-13 T<sub>1</sub> Values by a Method which Suppresses Artifacts*, (Communications), Journal of Magnetic Resonance, **30**, 613, 1978.
- 149 Chen J. N., Yan S. Q., and Ruan J. Y., *A Study on the Preparation, Structure, and Properties of Microcrystalline Cellulose*, Journal of Macromolecular Science - Pure & Applied Chemistry, **A33(12)**, 1851, 1996.
- 150 Geil P. H., Baer E., and Wada Y., *The Solid State of Polymers*, Dekker, New York, 1974.

- 151 Dimmel D. R., *Bleaching Reactions of Amorphous and Crystalline Cellulose*, International Pulp Bleaching Conference - Posters, 107, 1994.
- 152 Roffael E., and Schaller K., *Effect of Heat Treatment on Cellulose*, Holz Roh-Werst., **29(7)**, 275, 1971.
- 153 Hernadi S., *Thermal Ageing in Oxygen of Paper Made From Cellulose at Different Degrees of Beating*, Svensk Papperstid. **79(13)**, 418, 1976.
- 154 Hernadi S., *Decomposition of Cellulose Under the Combined Effect of Thermal-Hydrolytic and Thermal-Oxidative Processes*, Cellulose Chemistry and Technology, **11(2)**, 131, 1977.
- 155 Heiner A. P., and Teleman O., *Structural Reporter Parameters for the Characterisation of Crystalline Cellulose*, Pure and Applied Chemistry, **68(11)**, 2187, 1996.
- 156 Hsu C. L., and Hsieh J. S., *Oxygen Bleaching Kinetics at Ultra Low Consistency*, Tappi Journal. **70(12)**, 107, 1987.
- 157 Ziderman I. I., and Perel J., *Decreased Crystallinity of Hydrocellulose I During Alkali Catalyzed Depolymerization*, Journal of Macromolecular Science - Physics, **B24(1-4)**, 181, 1985.
- 158 Sindorf D. W., Bartuska V. J., and Maciel G. E., *Characterization of Silica-Attached Systems by Silicaon-29 and Carbon-13 Cross-Polarization and Magic-Angle Spinning Nuclear Magnetic Resonance*, Journal of the American Chemical Society, **102**, 3249, 1980.
- 159 Maciel G. E., Kolodziejcki W. L., Bertran M. S., and Dale B. E., *Carbon-13 NMR and Order in Cellulose*, Macromolecules, **15**, 686, 1982.
- 160 Earl W. L., and VanderHart D. L., *Observations by High-Resolution Carbon-13 Nuclear Magnetic Resonance of Cellulose I related to Morphology and Crystal Structure*, Macromolecules, **14**, 570, 1981.
- 161 Akitsu H., Gril J., Morooka T., and Norimoto M., *Dynamic Mechanical Properties of Chemically Modified Wood*, Chemical Modification of Lignocellulosic Proceedings, Rotorua, New Zealand, 7-8, 130, 1992.
- 162 Lindgren J. J., Bjorkman A., Salem L., and Solijamo K., *Chemically Modified Wood: Solid-State-Cross-Polarization-Magic-Angle-Spinning NMR Spectroscopy*, ACS Symposium Series, **489(21)**, 320, 1992.

- 163 Fengel D., Jakob H., and Strobel C., *Influence of the Alkali Concentration on the Formation of Cellulose II*, *Holzforschung*, **49(6)**, 505, 1995.
- 164 Fengel D., *Isolation, Characterization and Structure of Polysaccharides*, *Papier*, **37(12)**, 567, 1983.
- 165 Petitpas T., Oberlin M., and Mering J., *Confirmation of P. H. Hermans Hypothesis: on Cellulose II Chains*, *Journal of Polymer Science – Part C*, **2**, 423, 1963.
- 166 Takai M., and Colvin J. R., *Mechanism of Transition Between Cellulose I and Cellulose II During Mercerization*, *Journal of Polymer Science – Chem. Ed.*, **16**, 1335, 1978.
- 167 Lewin M and Pearce E. M., *Handbook of Fiber Chemistry (second edition)*, Marcel Dekker Inc., New York, 1998.
- 168 Roberts E. M., Saxena I. M., and Brown R. M., *Cellulose and Wood – Chemistry and Technology*, Schuerch, New York, 1989.
- 169 Kuga S., Takagi S., and Brown R. M., *Native Folded-Chain Cellulose II*, *Polymer*, **34(15)**, 3293, 1993.
- 170 Lewin M., and Sello S. B., *Handbook of Fiber Science and Technology (volume 1 – part A)*, Marcel Dekker, New York, 1983.
- 171 Timpa J. D., and Wanjura D. F., *Environmental Stress Responses in Molecular Parameters of Cotton Cellulose*, *Proceedings of the Tenth Cellulose Conference*, 1145, 1988.
- 172 Bouchard J., Morelli E., and Berry R., *Gas-Phase Addition of Methanol or Acetic Acid with Ozone in High Consistency Ozone Bleaching of Softwood Kraft Pulp*, PPR 1305, 1997.

# Appendix I

## Schematic of the Kettle Reactor



## Appendix II

### Metal Ion Analysis Results

Sample	Oxidation Time (min)	Before Metal Ion Removal (mg/kg)			After Metal Ion Removal (mg/kg)		
		Fe	Mn	Cu	Fe	Mn	Cu
Q-90	Control	22.20	1.10	7.07	17.50	< DL	2.20
	0	22.00	4.00	4.70	13.10	< DL	< DL
	5	15.50	4.50	18.60	10.80	< DL	< DL
	10	19.30	4.40	3.70	12.70	< DL	1.90
	15	15.10	3.90	3.30	5.50	< DL	< DL
	30	17.00	3.70	3.90	13.30	< DL	< DL
	60	18.80	2.70	4.60	14.60	< DL	< DL
	90	13.10	3.60	4.50	5.50	< DL	< DL
Duplicate Q-90	5	54.40	3.75	2.90	14.80	< DL	1.20
	5	10.90	3.00	2.80	2.50	< DL	1.10
	10	11.40	3.55	3.00	4.25	< DL	1.00
	10	11.00	3.25	2.00	5.31	< DL	0.90
	15	9.79	4.19	2.40	7.39	< DL	0.90
	15	13.10	3.10	8.31	5.59	< DL	0.90
	30	34.70	3.84	3.29	15.40	< DL	1.80
	30	7.37	4.33	2.20	3.95	< DL	0.80
Hemicellulose Free	Control	17.80	1.30	1.70	6.90	< DL	< DL
	5	9.90	1.50	1.30	5.30	< DL	< DL
	15	9.70	1.20	1.70	7.40	< DL	1.10
	30	11.50	1.40	1.30	3.60	< DL	< DL
	90	18.00	1.40	2.60	2.60	< DL	1.00
Cotton	Control	6.03	< DL	2.85	5.85	< DL	1.80
	0	10.80	< DL	3.17	3.40	< DL	0.80
	5	6.61	< DL	3.63	3.60	< DL	1.00
	15	12.30	0.80	2.69	6.61	< DL	2.10
	30	4.29	< DL	3.90	4.20	< DL	1.20
	55	7.15	0.30	3.67	2.40	< DL	0.90
	60	7.13	< DL	3.11	6.87	< DL	1.40
	90	23.80	0.50	2.81	5.98	< DL	0.80
	95	8.75	0.30	4.19	6.38	< DL	1.50
	Avicel	Control	4.92	< DL	0.90	4.48	< DL
0		3.93	< DL	0.90	1.90	< DL	0.60
60		4.02	< DL	1.50	1.10	< DL	0.90
Ion Detection Limits (DL)		1.00	0.20	0.40	1.00	0.20	0.40